Reference

REPORT NO. DOT - TSC - OST - 71 - 4

A THEORY OF AIRCRAFT COLLISION-AVOIDANCE SYSTEM DESIGN AND EVALUATION

EDMUND J. KOENKE
TRANSPORTATION SYSTEMS CENTER
55 BROADWAY
CAMBRIDGE, MA. 02142

MAY 1971
TECHNICAL REPORT

Prepared for
OFFICE OF THE SECRETARY OF TRANSPORTATION
WASHINGTON, D.C. 20590

1. Report No. DOT-TSC-OST-71-4	2. Government Accession No.	3. Recipient's Catalog No.
4. Title and Subtitle A THEORY OF AIRCRAFT COLLISION AVOIDANCE SYSTEM DESIGN AND EVALUATION*		5. Report Date MARCH, 1971
		6. Performing Organization Code PG
7. Author(s) Edmund J. Koenke		8. Performing Organization Report No. DOT-TSC-OST-71-4
9. Performing Organization Name and Address Transportation Systems Center 55 Broadway Cambridge, Ma. 02142		10. Work Unit No.
		11. Contract or Grant No.
12. Sponsoring Agency Name and Address Department of Transportation		13. Type of Report and Period Covered Technical Report
		14. Sponsoring Agency Code G3000

15. Supplementary Notes *Submitted in partial fulfillment of the requirements for the degree of Doctor of Science, at the Massachusetts Institute of Technology, March 1971

16. Abstract

The problem of aircraft anti-collision system design and evaluation is discussed in this work. Two evaluation criteria, *conflict ratio* and *probability of missed critical alarm* are formulated and are found to be independent of both traffic density and traffic model. These parameters depend only on system alarm thresholds, critical miss distances and relative position prediction uncertainty. This results in a simple method for system evaluation and examination of new anti-collision concepts. A closed-form method for estimating system alarm rate is also developed based on both a new traffic model and empirical data. Anti-collision systems are numerically compared by use of the criteria developed in this thesis. In the terminal area it is found that the *conflict ratio* ranges from about 900 for a simple PWI device to about 25 for a full state collision avoidance system. The difference in the en-route environment is found to be less severe. The design of a low conflict ratio collision avoidance system is also discussed in this thesis and both an algorithm and display are developed.

17. Key Words
Anti-collision system
Collision avoidance
Air traffic models
Collision detection and avoidance
Traffic model formulations (air)

18. Distribution Statement
Unclassified-Unlimited

19. Security Classif. (of this report)	20. Security Classif. (of this page)	21. No. of Pages	22. Price
Unclassified	Unclassified	184	

TABLE OF CONTENTS

LIST OF ILLUSTRATIONS

LIST OF ILLUSTRATIONS (cont.)

LIST OF TABLES

LIST OF TABLES (cont.)

NOMENCLATURE

A_i	Constants
a_i	Constants
a	Acceleration
B_i	Constants
B	Weighting Matrix
b_i	Weighting coefficients
C_i	Constants
C_i^j	Transformation Matrix, i frame to j frame
CR	Conflict Ratio
D	Deviation of the normal
$D(\bar{x},t)$	Density distribution
d	Radius of spherical collision volume
E	Expectation operator
E_i	Error Coefficient Matrix
$F(R_0)$	Traffic Factor for terminal radius R_0
h	Altitude
$\dot{h}$	Altitude rate
I	Identity Matrix
I_ν	modified Bessel function of order ν
i	index
j	index
K	Number of lanes
K_g	Gain Matrix
K_i	Constants

K_μ	Model Constant
k	Index
L	Latitude
l	Longitude
M	Number of aircraft in M^{th} group
M_g	Gain Matrix
m	Miss-distance
N	Number of aircraft in N^{th} group
N_c	Expected number of collisions
N_h	Number of hourly terminal operations
n	Index
$\bar{n}$	Unit normal vector
P	Position covariance matrix
P_c	Collision Probability
P_f	Probability of false alarm
$P_{f/c}$	Conditional probability of false alarm
$P_{m/c}$	Conditional probability of missed alarm
$P_{M,N}$	Probability of collision between M and N groups of aircraft
P_r	Probability
p_i	Differentiation wrt i^{th} frame
Q	Velocity covariance matrix
$Q_{M,N}$	Probability of no collision between M and N groups of aircraft
R	Percent of time for conflict resolution
R_0	Radius of terminal airspace

r_0	Distance between centers of circular flight paths
$\bar{r}_i^n$	Position vector of the i^{th} aircraft in the n frame
r_u	Distance of aircraft 1 to collision
r_v	Distance of aircraft 2 to collision
S(t)	Sensitivity coefficient matrix
S_c	Collision Surface
T_e	Escape Time
T_p	Process Time
T_r	Reaction Time
$\bar{T}_E$	Mean-Time-To-Encounter
t	Time
u	Unit step function
U(x,t)	Position probability density distribution
V	Volume
V_c	Collision volume
$V_{a/s}$	Volume of airspace
V_i	Protected volume of i^{th} aircraft
$\tilde{V}_n$	Average speed of the n^{th} group of aircraft
v_n	Normal component of relative velocity vector
$\bar{v}_i$	Velocity vector of the i^{th} aircraft
W(x,y,z)	Probability density distribution
$\bar{w}$	Relative velocity vector
x,y,z	Coordinate axes
$\bar{x}_i$	State vector
Z_i	Square of range measurement

α	Angle between the relative position and relative velocity vectors
β	Relative bearing angle
$\dot{\beta}$	Rate of change of the line of sight
γ	Angle between the relative position and aircraft velocity vectors
δ	Angle between the relative position and relative velocity vectors
Δh	Altitude difference
ε_L	Lateral threshold
ε_v	Vertical threshold
ξ	Dummy variable
η	Relative bearing angle
λ	Collision frequency
$\Lambda_{M,N}$	Collision frequency between M and N aircraft groups
μ	Encounter frequency
μ_c	Critical encounter frequency
μ_f	False alarm rate
μ_s	System encounter frequency
Π	Product operator
$\bar{\rho}$	Relative range vector
ρ_ε	Critical threshold radius
ρ_T	General threshold radius
ρ	Range
$\dot{\rho}$	Range rate
$\ddot{\rho}$	Range acceleration
σ	Dummy variable
σ_i	Uncertainty of the i^{th} measurement

Σ	Summation operator
τ	Time to closest approach
τ_c	Time to collision
τ_L	Linear time to collision
τ_M	Minimum time to collision
τ_W	System warning time
ϕ	Elevation angle
Φ	Integral of the error function
$\Phi(t,t_o)$	State transition matrix
ψ	Relative heading
ψ_i	Azimuth of the i^{th} aircraft
ω	Angular velocity
ω_{ij}	Angular velocity of the j frame relative to the i frame
Ω_{ij}^{k}	Skew symmetric matrix of $\bar{\omega}_{ij}$ in the k frame

CHAPTER 1

INTRODUCTION AND SUMMARY

1.1 Problem Statement and Historical Background

Methods of avoiding mid-air collisions have received considerable attention during recent years. The initial efforts date back to the mid-air collision over the Grand Canyon in 1956. The research in this area was further spurred on by the collision of two airliners over New York City in December of 1960. The amount of work performed in collision avoidance is illustrated by the fact that since 1955, over 1000 papers have been published in this research area (1)*. In view of the vast amount of literature available in this research area, it is of interest to briefly review the progress to date. In summarizing the status of prior work, three prime study areas will be discussed:

Collision Detection and Avoidance

Traffic Model Formulation

System Design and Evaluation

Collision Detection and Avoidance

The fundamentals of collision detection and avoidance are discussed in the literature (2) through (10). Typically, these referenced works treat the problem of the collision of two aircraft flying with constant velocity. This problem is known as the rectilinear collision problem. Russell(2) performed an error

---

*Numbers in parenthesis refer to numbered references in the bibliography.

analysis for typical collision avoidance systems designed with rectilinear theory in 1959. McKown, Morrel and Holt,(4,5,7) discuss rectilinear collision criteria, and Morrel's work published in 1956 appears to be one of the first treatments of this subject. Computer studies of the rectilinear collision phenomenon were performed by Joy(6) in 1964 and by Catalano and McKown(8) in 1963. In the same year, LaRochelle(10) published a study of the feasibility of collision avoidance systems. In this work, system functions and rectilinear collision criteria, specifically the TAU criterion, are discussed. Thus, as illustrated by the above work, a thorough treatment of the rectilinear collision phenomenon is available in the literature. A treatment of curvilinear collision detection is presented by Crafton(3). This work was reported in 1959 and utilizes series expansion methods for analysis purposes. An alternate closed-form solution to this problem is presented in Chapter 4 of this thesis.

Traffic Model Formulation

Typical statistical treatments of the problem of the collision of two aircraft are presented in (11) through (18). These referenced works deal primarily with the formulation of a model for predicting the frequency of collision of aircraft in a specific environment and assume that the problem of simultaneous multiple collisions is negligible. Some of this work deals with a presentation of collision and near-miss statistics. Examples of this are the work by Tibbs(11) published in 1963, by the Department of Transportation(15) in 1968 and by the National

Transportation Safety Board(14) in 1967. The work published by the Department of Transportation(15) is most useful and was invaluable in this thesis research.

Many closed-form (i.e., algebraic) traffic models are also available in the literature. The gas model which assumes totally random motion of aircraft is frequently used in many system studies and has been applied to the collision avoidance problem as recently as 1969 in both the Alexander Report(36) as well as by Flanagan and Willis(16) and the Department of Transportation NMAC report(15). Another model, based on the ordered motion of aircraft in lanes was developed by Marks(12) in 1963 and applied to separation standard studies. In 1962, Bellantoni(17) developed a generalized model describing the probability of collision between two aircraft. The gas model, and the models developed by the Royal Aircraft Establishment(12) were shown to be subsets of this more general model. The Bellantoni model is extended to the case for N aircraft in this thesis and is also the basis for the Hub Model developed in Chapter 3 of this work. Arcon Corporation(43) developed a number of traffic models, also in closed form, to represent various airway structures.

Numerical simulation models have also been developed. Typical of these is the model developed by Britt and Schrader(19) in 1969. The result of applying this model to various systems is used for the validation of the closed form solutions obtained in this thesis.

System Design and Evaluation

Much work has been done in anti-collision system design and is typically represented in the literature by references (20) through (30). Systems which detect the presence of aircraft within a certain range of another aircraft are referred to as *pilot warning indicators* (PWI). Studies of these systems have been performed by Catalano and McKown(8), and by vanSaun(20). Work is currently being performed by the Department of Transportation in this area. A concept using xenon flashers and IR detectors is being investigated.

Another type of anti-collision system is the *collision avoidance system* (CAS). This system detects intruder aircraft, evaluates the threat, and commands evasive action. Work on the design and flight test of a system of this type which utilizes a time-frequency technique* to obtain range and range-rate is being conducted by McDonnell-Douglas, Bendix, and Sierra-Wilcox. Flight tests of these systems were made and evaluated by Martin Marietta(42). Nagy(23) presents an operational analysis of the time-frequency concept.

Other collision avoidance system concepts are currently being studied by RCA (the SECANT System) and by Honeywell (an Army Helicopter Application)(40). Evaluation of a CAS based on

---

*A method for estimating range by measuring the time difference between two high-precision, synchronized clocks. Range rate is estimated by comparing the measured clock frequency to a standard value.

range bouncing methods is performed by Dinerman(30) who showed that this method does not have much promise.

Analyses of collision avoidance systems are reported in the literature by Jenkins(22), Russell(27), Frye and Killham(29,37), and by Willis(34).

Evaluations of collision avoidance systems are reported by National Company, Inc.(25), Martin Marietta Co.(42), and Sperry Gyroscope Co.(8). All of these evaluations are based either on flight test data or on simulation, but no closed-form method of anti-collision system evaluation appears to be available in the literature.

In summarizing the prior work performed in collision avoidance, a number of points should be noted:

(1) A thorough treatment of the rectilinear collision detection and avoidance problem is available in the literature.

(2) A number of traffic models for the prediction of mid-air collisions have been formulated.

(3) A number of anti-collision devices and systems have been designed, fabricated and even flight tested.

(4) Numerical methods of system evaluation based upon computer simulations have been developed and applied to a number of system design concepts.

Problem Statement

The problem which is addressed in this research work is that of formulating a closed form method of system evaluation which

can be used both for the comparative evaluation of anti-collision systems and for the formulation and examination of new anti-collision system design concepts.

The development of this method will provide insight for the system design process which numerical evaluation methods do not reveal. Further, by using data first available in 1969(15,36) concerning the frequency of near-mid-air collisions (NMAC's), comparison of traffic models with data will also be made. Finally, a system design based on the results of the above analyses will be developed and discussed.

1.2 Approach to the Problem

To begin this research work, it is important to state that the prime objective of an anti-collision system is to prevent mid-air collisions. A broad functional categorization of anti-collision systems is possible by considering the functions of both the pilot and the system. Further, a specific method of aircraft control for collision avoidance is suggested by this functional approach.

Given both the system categorization and control structure, it is necessary to formulate some method for evaluation of these categories. Evaluation criteria which give a measure of system efficiency and of system safety are thus developed. Formulation of these criteria leads to an investigation of the phenomena of collision and near-miss both from the statistical and deterministic points of view. Numerical evaluation of the broad system

categories utilizing the evaluation criteria and available data will then be performed. Finally, a system design based upon the insight provided by the analytical evaluation method will be presented as an example to illustrate the utility of the solution to the problem.

1.3 Thesis Organization and Summary

In Chapter 2, anti-collision systems are categorized as *pilot warning indicators*, *collision detection systems*, or *collision avoidance systems*. A control structure employing three levels is then suggested. A first level of control restricts potential aircraft maneuvers to standard maneuvers. The second level of control prohibits maneuvers which would result in an actual mid-air incident if they were executed. The third level of control commands positive evasive action in order to avoid an existing collision threat.

A variety of system evaluation parameters are investigated, resulting in the formulation of a measure of system efficiency called *Conflict Ratio*. Another parameter, named the *Probability of Missed Critical Alarm*, is formulated and provides a measure of system safety. These parameters are functions of system encounter frequency, the uncertainty in predicted relative position of the conflicting aircraft, the system alarm thresholds, and the minimum allowable separation (critical miss distance) between the conflicting aircraft. System evaluation using these parameters can be performed without statistical traffic models or traffic

density information; however, as shown in the following paragraph, statistical models are introduced for the evaluation of other system parameters such as system encounter frequency.

In Chapter 3, a statistical analysis of the collision phenomenon is performed to derive a method for the calculation of system encounter frequency. A typical traffic model is examined and compared to existing near-miss data(15) to validate its use for the computation of encounter frequency. This comparison shows the necessity for the formulation of a new traffic model designated as the hub model, which is then shown to compare favorably with empirical data. The problem of quantifying the probability of simultaneous multiple threats is also investigated in this chapter to determine whether consideration of this possibility should be included in a system design. The results of this quantification indicate that the probability of occurrence of this event is less than 1×10^{-6} per approach in New York during 1968.

Chapter 4 is a deterministic investigation of the collision phenomenon made to develop methods for determining system alarm thresholds and the critical miss distance.

The bases for choosing system alarm thresholds are to allow for relative position prediction errors and to provide sufficient time to perform an evasive maneuver. Chapter 4 presents the equations of relative motion, suggests collision criteria, and discusses relative position prediction, measurements, data and error propagation. These analyses give the ability to evaluate

both the system alarm thresholds and the relative position prediction uncertainty. Coupled with the statistical results, this permits a closed-form formulation of both *conflict ratio* and *probability* of *missed critical alarm*.

In Chapter 5, a numerical evaluation of the major anti-collision system categories is carried out for both terminal area and en-route environments. A variety of system design options are then discussed, leading to the presentation of a system design which has a low value of *conflict ratio* and *probability* of *missed critical alarm*. This is a cooperative system which requires a complete estimate of the relative position and velocity vectors between the conflicting aircraft. It utilizes curvilinear collision detection and avoidance as well as the three levels of control previously discussed. An aircraft display concept is also presented to illustrate the feasibility of the proposed collision avoidance system design concept.

The major conclusions of this research work and recommendations for future work are presented in Chapter 6.

CHAPTER 2

ANTI-COLLISION SYSTEM EVALUATION TECHNIQUES

2.1 Introduction

Before attempting to discuss the evaluation of anti-collision systems, it is helpful to precisely define a collision avoidance system.

A collision avoidance system is one which *detects* the presence of other aircraft, *evaluates* collision threat, *indicates* proper evasive maneuvers, and then *confirms* that proper evasive action has been taken.

Many types of anti-collision devices, methods and systems are currently being studied, designed, fabricated, and even flight tested. These devices have one item in common, i.e., they attempt to reduce the probability of aircraft collision. Other than that, they vary widely and include functional, design, computational, and implementation differences. Some of the more basic of these devices simply perform the detection function, others rely on linear assumptions for threat evaluation, and still others require a complete measurement of state and a ground installation to accomplish the task of collision avoidance.

A complete evaluation of every specific system and/or system concept is considered beyond the scope of this work but the more important considerations of the basic types of anti-collision systems, design concepts, control techniques, computational algorithms, and implementation methods are considered. These

considerations provide the capability of performing the trade-offs required in choosing a specific system design approach to satisfy a given collision-avoidance specification and, even more basically, will provide the technical data necessary to formulate the specification itself.

2.2 Anti-Collision System Categories

Based on the definition of a collision-avoidance system, the following classification of anti-collision devices is postulated:

Pilot Warning (Indicator) Systems (PWI)

Collision Detection Systems (CDS)

Collision Avoidance Systems (CAS)

The system types referred to as PWI and CAS are frequently mentioned in the literature but the category of CDS is introduced by the author for clarity.

A system which detects the presence of intruder aircraft is broadly defined as a *pilot warning system*. In addition to detection, it may also give a crude indication of the intruder's position either by a bearing indication, a bearing-elevation measurement or even possibly a range or range-altitude indication. Xenon flashers and IR sensors are currently being flight tested to determine to what extent this type of system accomplishes the detection and location function. In a PWI system, the functions of threat evaluation, avoidance maneuver determination and monitoring are left to the pilot.

A system which detects the presence of other aircraft and also evaluates a collision threat is defined as a Collision Detection System. This system, like the PWI system, leaves the choice of avoidance maneuvers to the pilot but relieves him of the task of collision detection. This is a considerable improvement over PWI. One major drawback for both CDS and PWI is the possible choice of the wrong avoidance maneuver, (e.g., allowing both aircraft to maneuver can have the effect of either accelerating or delaying the time of collision but not of eliminating the threat). Holt(37) and vanSaun(20) point out that "Hazard evaluation and maneuver selection can be impossible when closing rates reduce the time to perform these functions below the required minimum. Finally, escape maneuvers can be compensating, causing aircraft to be directed toward each other in an apparent controlled collision, much like the occasional collision each of us has had with an approaching pedestrian."

The final system category is that of collision avoidance. In this system, the functions of intruder detection, threat evaluation, maneuver indication and monitoring are performed automatically. A typical system of this type is the McDonnell Douglas "EROS" system which is based on a time-frequency technique for the measurement of range and range-rate. Collision detection and threat evaluation are accomplished by use of the TAU criterion which estimates the time-to-collision by computing the ratio of range to range rate. A range threshold is also used for

safety purposes. Vertical avoidance maneuvers are then calculated automatically and displayed to the pilot.

Figure 2.1 is an illustration of the basic anti-collision system categories defined above. Also illustrated are the associated anti-collision functions which are performed either by the pilot or automatically by the system hardware.

SYSTEM FUNCTION / CATEGORY	INTRUDER DETECTION	THREAT EVALUATION	AVOIDANCE COMMAND	MANEUVER MONITOR	MANEUVER EXECUTE
PWI	S	P	P	P	P
CDS	S	S	P	P	P
CAS	S	S	S	S	S/P

S = System
P = Pilot

Figure 2.1.- Anti-collision system categories and functions.

2.3 Anti-Collision System Control Structure

Examination of the basic functions of an anti-collision system, and in particular the threat evaluation and avoidance command functions, leads to the establishment of a basic control structure for collision avoidance.

In order to discuss the threat evaluation function, one must first define a threat. As is suggested by (34), there are two types of threats:

Actual Threats,

Potential Threats.

An actual threat is defined as that which exists when both aircraft are on flight paths which will cause a violation of

specified separation criteria if no maneuvers are made to alter the current state. A potential threat is defined as that which exists when both aircraft are on flight paths which do not constitute an actual threat but, because of geometry and maneuverability, are capable of causing an actual threat if one or both aircraft make an improper maneuver.

In designing collision avoidance systems, protection from both actual and potential threats must be provided since ignoring potential threats can result in the creation of an actual threat with insufficient time for avoidance.

The protection against an actual threat consists of both prevention by means of negative commands and resolution of existing conflicts by positive commands. Negative commands are used to prevent potential threats from becoming actual threats. This is accomplished by issuing commands to prohibit the dangerous maneuvers.

As mentioned above, a potential threat is a situation which under certain maneuver combinations could result in an actual threat. An infinite number of future positions are possible for both aircraft if one allows all combinations and values of turn rate and climb-dive rate. Thus, prediction of potential threats could be quite tedious and time consuming. If however one adopts the philosophy that various degrees of control are required to eliminate collisions, this problem can be simplified considerably. For example, if maneuvers are limited to standard maneuvers within a control region then the calculations for potential

threat evaluation are very straight-forward. Thus, three levels of control are postulated namely:

Level 1- Limit aircraft to their existing state or to standard maneuvers to change state

Level 2- Limit maneuvers by prohibiting those which are dangerous

Level 3- Command definite maneuvers for avoidance of an actual threat

The various degrees of control imposed on the pilot within the control region of another aircraft is not too high a price to pay to avoid a collision particularly since it will potentially allow closer spacing of aircraft in the terminal area. This could also result in easing the current crowding of terminal airspace and allow a higher departure and arrival rate.

If in addition to the above control structure and the associated regions of control one also considers the intruder detection function, a monitor region must also be established in which aircraft are acquired and monitored to determine when and if they enter the control region.

Figure 2.2 illustrates the control structure defined above as well as the basic monitor, control, and safety regions of the aircraft. The safety region or the protected volume is chosen on the basis of both the separation criteria and the system prediction uncertainty. It should also be pointed out that all anti-collision systems do not have every level of control or every region illustrated. For example, a PWI may only use the monitor

and control region for intruder detection purposes and the pilot will have to establish his own positive and negative command regions based on the information available to him.

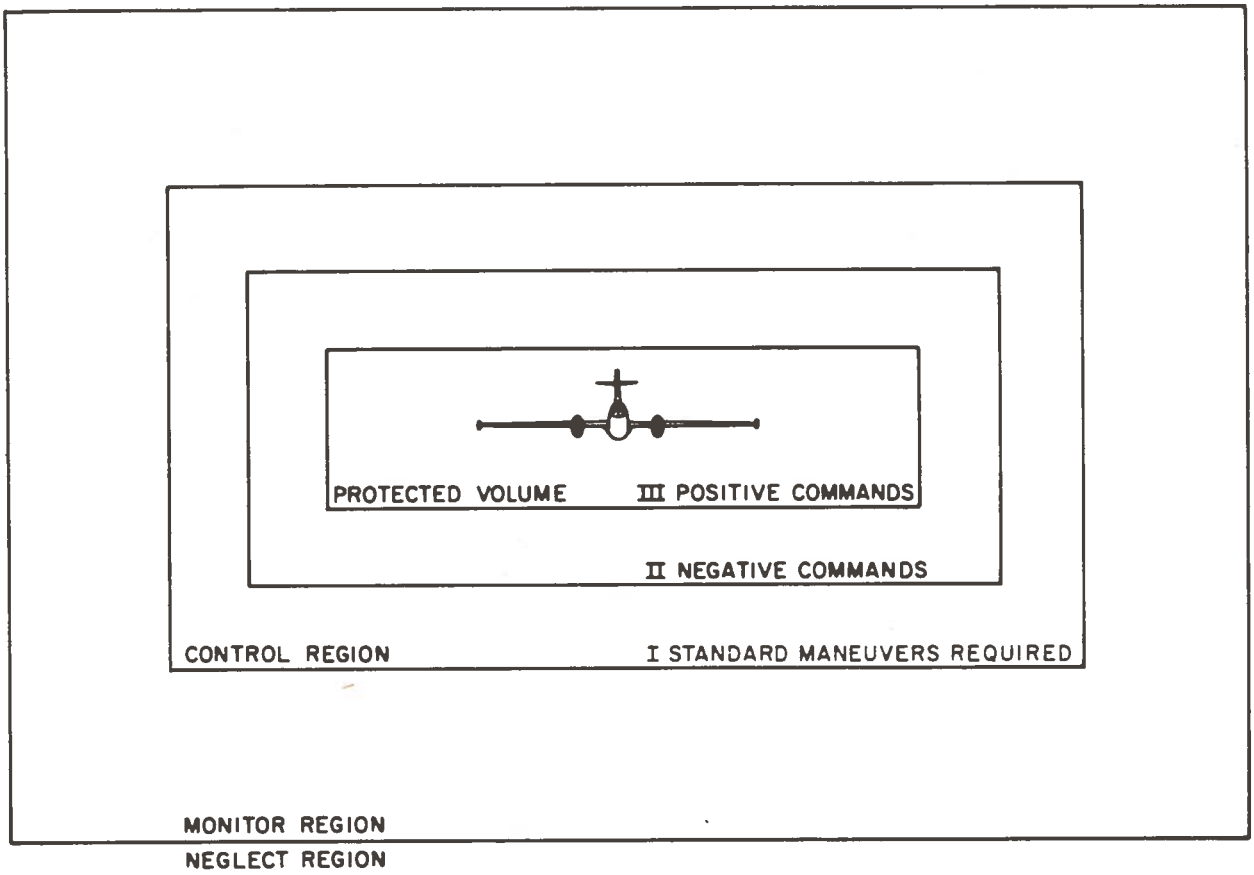

Figure 2.2.- Anti-collision system control structure.

A detailed treatment of the methods for computing the dimensions of these regions as well as an algorithm for implementation of these concepts will be presented in Chapters 4 and 5 of this research.

2.4 System Evaluation Parameters

In addition to system types and control methods, both technical and economic factors must be considered in the evaluation of anti-collision systems. Political considerations will not be included in this work.

One prime factor which must be discussed is cost. Cost is defined to include, but is not limited to, items such as size, power, weight and dollars. This is an important consideration simply because of the economics involved. Obviously, a small general aviation (GA) aircraft could not transport a large computer or a heavy system and furthermore, unless the dollar cost is low, the GA owners could not afford to purchase the system. At most, it is expected that a GA aircraft could carry a special purpose transceiver, computer and display.

Dollar costs for currently available systems range from about $400.00 for a PWI using transponder signals to about $40,000.00 for an airline version of a CAS. Two economically and technically promising solutions to the hardware problem for a full state CAS were recently reported by Litchford in Aeronautics and Astronautics(39), and by Klass in Aviation Week(40).

Parameters such as size, weight, power and dollars must be considered for a specific system evaluation but are difficult to estimate without a specific system definition. However, the type of equipment required for various system design options can be determined. Cost can then be established simply by considering the required equipment complement, equipment specifications and purchase price.

Cooperative airborne system concepts ranging from PWI to total state CAS and their associated equipment complements are presented in Table 2.1. In this table, the bearing only or bearing-elevation systems are primarily considered for PWI application. Range, range/altitude, range/range-rate, and complete data set concepts are being considered for either the collision detection or the collision avoidance application.

In Table 2.1, aircraft instruments include an altimeter, air-speed indicator and compass. Each of these equipments must interface with the communications equipment and computer where indicated. Communications equipment consists of a transponder of the type described in (39) or a transmitter/receiver. Xenon flashers and IR sensors are also being considered as both location and communication devices for PWI application. The computer can range from a small special purpose type for CDS to a large general or special purpose type for CAS. For ground based systems, computers of the type anticipated for automated ground control could be used. In fact, the collision avoidance function could be included in the computer sizing studies being performed for third and fourth generation air traffic control systems.

An airborne display for a CAS is discussed in Chapter 5 of this work. Displays for PWI and CDS would be less complicated and could range from a visual or audio signal for a PWI all the way to the CAS display illustrated in Chapter 5.

The area-navigator for the airborne concept could consist of inertial navigators which cost on the order of $100,000.00 to the

TABLE 2.1.- REQUIRED EQUIPMENT COMPLEMENT FOR VARIOUS AIRBORNE SYSTEM TYPES (COOPERATIVE SYSTEMS)

SYSTEM TYPE	Aircraft Instruments	Area Navigator	Communications	Computer	Display	Comments
Range Only	None	None	Transponder	None	Light	PWI
Range/ Range-Rate	None	None	Transponder	SP	Light	CDS
Range/Altitude	Altimeter	None	Transponder	SP	Light	Code Wheel on Altimeter
Range/ Altitude Range-Rate	Altimeter	None	Transponder	SP or GP	Light or Direction	PWI, CDS or CAS application
Bearing Only	None	Optional	Transmitter & Directional Receiver	SP	Direction	PWI application
Bearing/ Elevation	None	Optional	Transmitter & Directional Receiver	SP	Direction	PWI
Range Vector/ Velocity Vector	Altimeter air-speed Compass	Required	Transmitter Receiver	GP/SP	Avoidance Command	CAS

SP = Special Purpose
GP = General Purpose

less costly radio navigation systems. A combined low-cost-inertial/radio navigator could also be used. Radio navigators such as VOR/DME, Loran, Omega, Decca and navigation satellite systems are all potential candidates. Low cost area navigation may possibly be achieved by the methods recently reported in (39). Ground based area navigation would consist basically of radar techniques, but even with ground tracking for horizontal position location, on-board instrument information providing altitude, air-speed and heading is desirable. This need arises from the time lags introduced into the system by the estimation of velocity information from low-frequency position information. The type of equipment required for a full-state collision avoidance system (as designed by this author) is presented in Table 2.2.

With this information, it is possible for the system design engineer to estimate the system cost factor associated with a specific system design. This cost factor will not be estimated in this research since the choice of specific hardware for a particular system design is considered outside the scope of this work.

Before attempting a numerical evaluation of systems, carefully defined criteria must be chosen. A number of evaluation criteria are defined below:

System Encounter Frequency. The number of actual encounters per unit time that a particular system would experience in a given airspace.

TABLE 2.2.- EQUIPMENT COMPLEMENT FOR FULL STATE CAS DESIGN OPTIONS

Design Option	Equipment Location	Area Navigator	Aircraft Instruments	Communications	Computer	Display
AIRBORNE	AC-ML	X	X	X	X	X
	GA	X	X	X	X	X
	GND					
GROUND	AC-ML	optional	X	X		X
	GA	optional	X	X		X
	GND	X		X	X	X
MIXED	AC-ML	X	X	X	X	X
	GA	optional	X	X		X
	GND	X		X	X	X

AC = Air Carrier Aircraft

ML = Military Aircraft

GA = General Aviation Aircraft

GND = Ground Station

X denotes that the indicated equipment is required in the indicated location

Blank denotes no equipment requirement

Critical Encounter Frequency. The number of aircraft passages per unit time that are closer than a critical miss distance in a given airspace.

Mean-Time-To-Encounter. The reciprocal of the encounter frequency.

Conflict Ratio. The ratio of system encounter frequency to critical encounter frequency. A perfect system would have a conflict ratio of 1.

False Alarm Rate. The difference between the system encounter frequency in a given environment and the critical encounter frequency for the same environment.

Next, it is necessary to determine methods for computing the parameters, and then interpreting the results of the numerical evaluation. Computation of certain of these parameters can be accomplished by simulation as illustrated in (19). This method however is quite tedious, time consuming and expensive since extensive data collection, processing and computer simulation is required to obtain similar results for different terminals and alternate collision criteria. An alternative analytical method of computing these parameters is desired.

Two specific parameters for numerical comparison of anti-collision systems are chosen in this research. The first of these parameters is *conflict ratio* defined above. This parameter is chosen because it gives a measure of the collision avoidance action required by the pilot and possesses certain special properties which will be shown in the next chapter of this work.

The second parameter chosen for numerical comparison of systems is the *probability of missed critical alarm*. A missed critical alarm is defined to occur when a system fails to predict with sufficient warning a passage of two aircraft closer than a pre-specified distance (critical miss distance). This parameter is chosen because it gives a measure of system safety.

These parameters can be used for system evaluation by deriving formulae which permit numerical computation as a function of various system properties. From the definition of conflict ratio, it is seen that one must be able to estimate both the system encounter frequency and the critical encounter frequency. A statistical method of computing these parameters is presented as Chapter 3.

CHAPTER 3

STATISTICAL FORMULATION OF EVALUATION CRITERIA

3.1 Introduction

This chapter is devoted to the formulation and validation of a probabilistic and statistical theory of collision. From this theory, formulae for the computation of the system evaluation criteria, *conflict ratio* and *probability of missed critical alarm*, can be derived.

A number of other questions concerning system design and evaluation can also be answered by statistical treatment. For example, the number of aircraft to be handled simultaneously by a system, the measurement accuracy of a system, the prediction of system effectiveness as a function of aircraft density, and the prediction of mid-air incidents as a function of aircraft density are typical questions which can be answered with an adequate statistical theory.

The analysis presented in this work is based on the development of a general collision probability theory. Simulation and empirical data are used to validate traffic models and to quantify the results of these analyses. This work is then followed by a specific derivation of system evaluation criteria and the establishment of a number of intrinsic properties of these criteria.

3.2 Collision Probability Theory

This section addresses the problem of determining the probability of collision between two aircraft. A number of definitions are presented first, for clarity. In the statistical study performed in this chapter, it is convenient to introduce a definition of collision. This does not mean that aircraft actually collide.

Protected Volume. That space about an aircraft which is to be kept free from the protected airspace of intruder aircraft.

Collision Surface and Volume. A collision surface, S_c, is the locus of points of the center of the protected volume of one aircraft generated by translating without rotation the protected volume of one aircraft about the protected volume of another aircraft (see Figure 3.1) such that both protected volumes always have at least one point in common. Note that the orientation of these volumes may change relative to each other as a function of time, thus varying the collision surface as a function of time. A collision volume V_c, is that volume bounded by the collision surface.

Collision. A collision is defined to occur when the relative position vector $\bar{\rho}$ is contained within the collision volume or when its tip lies on the collision surface (see Figure 3.1).

With these definitions, the probability of at least one collision between two aircraft in a time ($t_0 \leq t \leq t_1$) can be formulated. The frequency with which the relative position vector

enters the collision volume V_c is defined as the collision frequency. Let $\bar{n}$ be the inward normal to the collision surface S_c and $\bar{w}$ be the relative velocity vector between the two aircraft (see Figure 3.1).

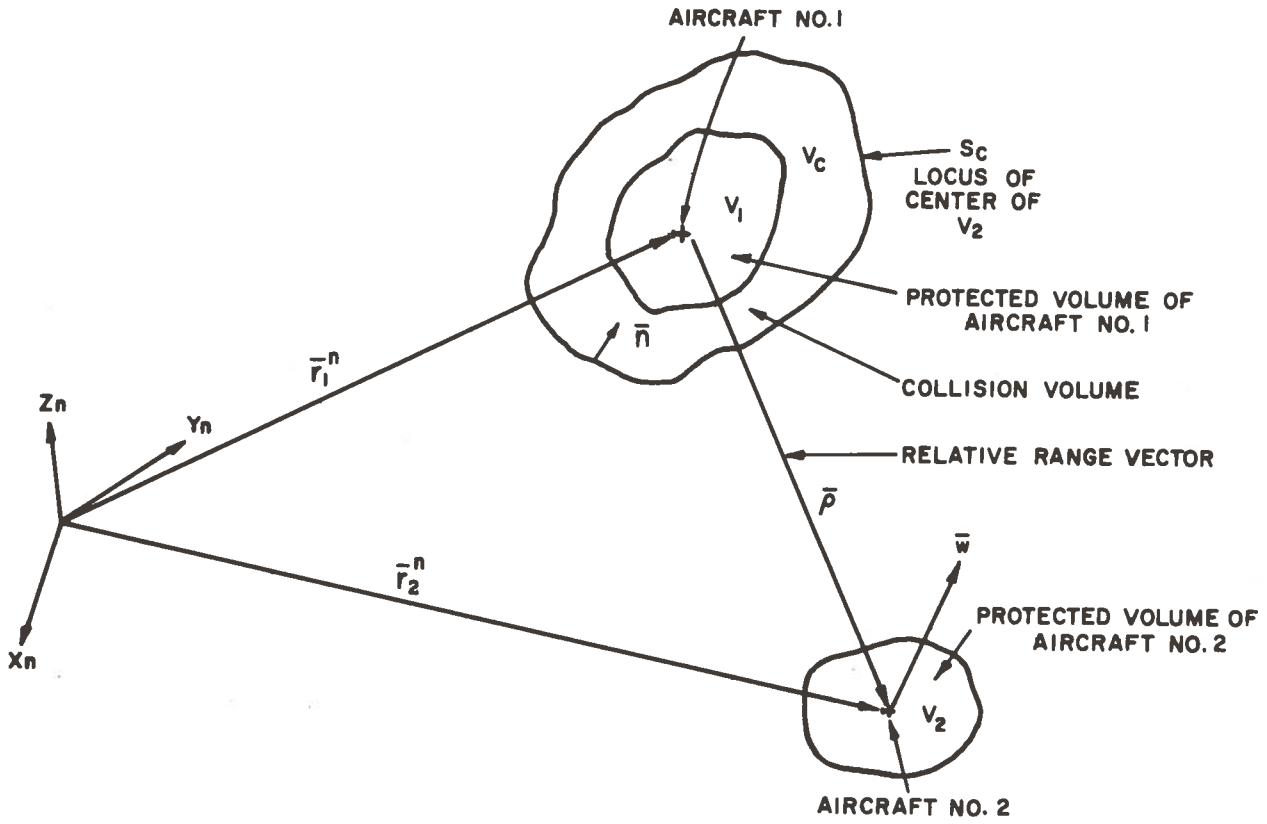

Figure 3.1.- Collision volume geometry.

The frequency with which $\bar{\rho}$ enters the volume V_c is given by the divergence theorem

$$\lambda = \frac{1}{V_c} \int_{V_c} dw\ \bar{w}\ dV = \frac{1}{V_c} \int_{S_c} \bar{w} \cdot \bar{n}\ dS \qquad (3.1)$$

Now, assuming that $\bar{w}$ is a random variable, the ensemble average of λ is given by

$$\tilde{\lambda} = \int_{\substack{\text{Vel} \\ \text{Space}}} d(\bar{w})\ f(\bar{w},t)\lambda \tag{3.2}$$

where f is the probability density distribution of $\bar{w}$.

Suppose that the joint probability density distribution of $\bar{\rho}$ and $\bar{w}$ is known to be $W(\bar{\rho},\bar{w},t)$. In this case, it is

$$f(\bar{w},t) = \int_{V_c} d(\bar{\rho})\ W(\bar{\rho},\bar{w},t)$$

which can be approximated by $f(\bar{w},t) \approx W(\bar{o},\bar{w},t)\ V_c$ since V_c is small compared to the airspace volume $(V_{a/s})$.

NOTE

This is a critical assumption to this formulation, and if violated, the following model is invalid.

By substitution one obtains the relation

$$\tilde{\lambda} = \int_{\substack{\text{Vel} \\ \text{Space}}} d(\bar{v})\ W(\bar{o},\bar{w},t)\ V_c \cdot \frac{1}{V_c} \int_{S_c} \bar{w}\cdot\bar{n}dS_c \tag{3.3}$$

Noting that

$$\int_{S_c} \bar{w}\cdot\bar{n}dS_c = w\delta S_c$$

where δS_c is the area of the projection of the collision surface on a plane perpendicular to the velocity vector, one can write the general relation for the collision frequency as

$$\tilde{\lambda} = \int_{\substack{\text{Vel} \\ \text{Space}}} d(\bar{w})\ W(\bar{o},\bar{w},t)\ w\delta S_c \qquad (3.4)$$

It should be pointed out that in general, δS_c will vary with time.

This result is in agreement with that obtained in (17) and in (17) it is shown that with proper assumptions, (3.4) reduces to the familiar result obtained in the kinetic theory of gases i.e.

$$\tilde{\lambda} = \frac{4}{3}\pi d^2\ v/V_{a/s}$$

where d is the diameter of a gas molecule, v is its speed and $V_{a/s}$ is the volume of the space considered. This is the expression frequently used in the literature to approximate the collision frequency between aircraft but as will be pointed out in Chapter 5, this can lead to large prediction errors. A more realistic example of the application of the general relation (3.4) for collision frequency is presented as Example III-1 and deals with the problem of two aircraft flying nominal flight paths. From this example, the probability of collision for a specific route structure and navigational accuracy can be determined.

The example is applicable to separation standard studies, area navigation system specifications, and holding pattern analyses.

Example III-1. Collision Frequency for Two Aircraft on Nominal Flight Paths

Suppose that two aircraft each have a spherical protection volume of radius r_1 and r_2 respectively. The collision surface in this case is a sphere of radius $r = r_1 + r_2$ so that the projection on any plane will be the area of a circle $\delta S = \pi r^2$ and is constant in time. Next, assume that the relative position and velocity distributions are independent so that

$$W(\bar{\rho},\bar{w},t) = W_\rho(\bar{\rho},t)\ W_w(\bar{w},t)$$

and under these assumptions, the collision frequency is

$$\tilde{\lambda} = \pi r^2\ W_\rho(0,t) \int_{\text{Vel Sp.}} w\ W_w\ (\bar{w},t)\ d(\bar{w})$$

Now, assume gaussian distributions for the relative position and velocity errors so that

$$W_\rho(\bar{\rho},t) = \frac{1}{(2\pi)^{3/2}\ |P|^{1/2}}\ e^{-\frac{1}{2}(\bar{\rho}-\tilde{\bar{\rho}})^T\ P^{-1}\ (\bar{\rho}-\tilde{\bar{\rho}})}$$

where

$$P = E[(\bar{\rho}-\tilde{\bar{\rho}})\ (\bar{\rho}-\tilde{\bar{\rho}})^T]$$

and

$$\tilde{\bar{\rho}} = E(\bar{\rho}) \quad ; \quad E = \text{expectation operator}$$

Similarly, for the velocity distribution assume

$$W_w(\bar{w},t) = \frac{1}{(2\pi)^{3/2}|Q|^{1/2}} e^{-\frac{1}{2}(\bar{w}-\tilde{\bar{w}})^T Q^{-1}(\bar{w}-\tilde{\bar{w}})}$$

By substitution of these distributions into the equation for the collision frequency, one obtains

$$\tilde{\lambda} = \frac{\pi r^2 e^{-\frac{1}{2}\tilde{\rho}^T P^{-1}\tilde{\rho}}}{(2\pi)^3|P|^{1/2}|Q|^{1/2}} \int_{-\infty}^{\infty}\int_{-\infty}^{\infty}\cdots\int_{-\infty}^{\infty} we^{-\frac{1}{2}(\bar{w}-\tilde{\bar{w}})^T Q^{-1}(\bar{w}-\tilde{\bar{w}})} dw_x dw_y dw_z$$

where

$$w = (w_x^2 + w_y^2 + w_z^2)$$

Note that if the position and velocity covariance matricies of aircrafts 1 and 2 are given by P_1, V_1; P_2, V_2 respectively, the position and velocity covariance matricies P and V are given by

$$P = P_1 + P_2$$

$$V = V_1 + V_2$$

since

$$\bar{\rho} = \bar{r}_2 - \bar{r}_1 \; ; \quad \bar{w} = \bar{v}_2 - \bar{v}_1$$

By substituting

$$\bar{u} = (\bar{w} - \tilde{\bar{w}})$$

the collision frequency can be written in the form

$$\tilde{\lambda} = \frac{\pi r^2 e^{-\frac{1}{2}\tilde{\rho}^T P^{-1}\tilde{\rho}}}{(2\pi)^3 |P|^{1/2} |Q|^{1/2}} \iiint_{-\infty}^{\infty} (|\bar{u}+\tilde{\bar{w}}|) e^{-\frac{1}{2}\bar{u}^T Q^{-1}\bar{u}} du_x du_y du_z$$

Applying the Schwarz inequality

$$|\bar{u} \cdot \bar{w}| \leq |\bar{u}||\bar{w}|$$

is obtained, so that

$$|\bar{u} + \tilde{\bar{w}}| \leq |\bar{u}| + |\tilde{\bar{w}}|$$

and

$$\tilde{\lambda} \leq \frac{\pi r^2 e^{-\frac{1}{2}\tilde{\rho}^T P^{-1}\tilde{\rho}}}{(2\pi)^3 |P|^{1/2} |Q|^{1/2}} \left[\iiint_{-\infty}^{\infty} (|\bar{u}| + |\tilde{\bar{w}}|) e^{-\frac{1}{2}\bar{u}^T Q^{-1}\bar{u}} du_x du_y du_z \right]$$

For small errors $\bar{u} \approx \tilde{\bar{w}}$, no gross error should occur from using this approximation. Further, the approximation is conservative, and results in

$$\tilde{\lambda} \leq \frac{\pi r^2 e^{-\frac{1}{2}\tilde{\rho}^T P^{-1}\tilde{\rho}}}{(2\pi)^3 |P|^{1/2} |Q|^{1/2}} \left[\iiint_{-\infty}^{\infty} (\bar{u}^T \bar{u}) e^{-\frac{1}{2}\bar{u}^T Q^{-1}\bar{u}} du_x du_y du_z \right.$$

$$\left. + |\tilde{\bar{w}}| \iiint_{-\infty}^{\infty} e^{-\frac{1}{2}\bar{u}^T Q^{-1}\bar{u}} du_x du_y du_z \right]$$

By integrating, this expression becomes

$$\tilde{\lambda} \leq \frac{\pi r^2 e^{-\frac{1}{2}\tilde{\rho}^T P^{-1}\tilde{\rho}}}{(2\pi)^3 |P|^{1/2} |Q|^{1/2}} \left[\sqrt{2}\ (2\pi)^{3/2} \sigma_v^4 \frac{\Gamma(2)}{\Gamma(3/2)} + (2\pi)^{3/2} \sigma_v^3 |\tilde{\bar{w}}| \right]$$

Where

$$|Q|^{1/2} = \sigma_v^3 \ ; \quad \Gamma(2) = 1 \ ; \quad \Gamma(3/2) = \frac{1}{2}\pi^{1/2}$$

The collision frequency is given by

$$\boxed{\tilde{\lambda} \approx \frac{r^2 e^{-\frac{1}{2}\tilde{\rho}^T P^{-1}\tilde{\rho}}}{|P|^{1/2}} \left[\frac{\sigma_v}{\pi} + \frac{|\tilde{\bar{w}}|}{2(2\pi)^{1/2}} \right]}$$

Where, in general P, $\tilde{\rho}$, $\tilde{\bar{w}}$, and σ are functions of time.

The above expression for collision frequency represents many interesting cases which are presented below.

CASE I. Zero Relative Velocity

This case represents parallel velocity vectors which are equal in magnitude and for this case the collision frequency is

$$\tilde{\lambda} = \frac{r^2 e^{-\frac{1}{2}\tilde{\rho}^T P^{-1}\tilde{\rho}}}{|P|^{1/2}} \cdot \frac{\sigma_v}{\pi}$$

Also, for a circular holding pattern (i.e. circular paths at different altitudes) use a position vector given by

$$\tilde{\rho} + \begin{Bmatrix} o \\ o \\ \Delta h \end{Bmatrix}$$

CASE II. Constant Relative Velocity

In this case, the expression for the collision frequency is

$$\tilde{\lambda} \leq \frac{r^2 e^{-\frac{1}{2}\tilde{\tilde{\rho}}^T P^{-1} \tilde{\tilde{\rho}}}}{|P|^{1/2}} \left(\frac{\sigma_v}{\pi} + \frac{\tilde{w}}{2(2\pi)^{1/2}} \right)$$

Many special situations are handled by this assumption and are illustrated below.

(a) Head-On Situation

$$\tilde{\tilde{\rho}} = \begin{Bmatrix} \rho_o - \tilde{w}t \\ S \\ \Delta h \end{Bmatrix} ; \qquad \tilde{w} = \text{const}$$

S = Lateral separation

(b) Concentric Circles, Co-altitude

$$\tilde{\tilde{\rho}} = \begin{Bmatrix} \tilde{\rho} \sin \omega t \\ \tilde{\rho} \cos \omega t \\ 0 \end{Bmatrix}; \qquad \tilde{w} = \tilde{\rho}\omega$$

ω = angular velocity

With this formulation, an avoidance guidance scheme can be evaluated since the values of $\sigma_v, |P|$ can be considered as the accuracy with which commands are followed and the quantities $\tilde{\tilde{\rho}}$ and $\tilde{\tilde{v}}$ can be considered as the relative position and velocity commands of the scheme. Another application of this result is the evaluation of area-navigation systems. For this application consider that the covariance matrix is simply calculated from the relation

$$P_i(t) = \Phi_i(t,t_o)\ E_i\ \Phi_i^T(t,t_o) \quad ; \qquad i = 1,2$$

where E_i is the covariance matrix of the system errors and Φ_i is the state transition matrix of the i^{th} aircraft. The combined covariance matrix, considering both aircraft systems is

$$P = \Phi_1\ E_1\ \Phi_1{}^T + \Phi_2\ E_2\ \Phi_2{}^T$$

If $\bar{\rho}$ and $\bar{w}$ are correlated or if Q is not equidirectional, numerical integration may be necessary.

Extension to N aircraft

Next, by a consideration of the probability of collision, a generalization of collision frequency to N aircraft is possible. This can be accomplished by the following considerations. If $\tilde{\lambda}$ is the collision frequency, $P(t,t + \Delta t) \approx \tilde{\lambda}\Delta t$ is the probability of one or more collisions in time $(t,t + \Delta t)$. Let $Q(t_o,t + \Delta t)$ be the probability of no collision in $(t_o,t + \Delta t)$ so that $Q(t_o,t)$ is the probability of no collision in (t_o,t). Assume the added time Δt is independent from the total time (t_o,t) without collision so that

$$Q(t_o,t + \Delta t) = Q(t_o,t)\ Q(t,t + \Delta t)$$

also,

$$\Delta Q = Q(t_o,t + \Delta t) - Q(t_o,t)$$

and,

$$\Delta Q = Q(t_o,t)\ [Q(t,t + \Delta t) - 1]$$

but

and therefore

$$\lim_{\Delta t \to 0} \frac{\Delta Q}{Q} = -\tilde{\lambda}\Delta t$$

which yields the solution

$$\left.\begin{aligned} Q(t_o,t) &= e^{-\tilde{\lambda}(t-t_o)} \\ P(t_o,t) &= 1-e^{-\tilde{\lambda}(t-t_o)} \end{aligned}\right\} \qquad (3.5)$$

where P is the probability of at least one collision among two aircraft in a time (t_o,t) assuming constant collision frequency. To find the probability of one aircraft colliding at least once with one of N-1 other aircraft consider that by assuming independence of occurences, one obtains

$$P_{1,N}(t,t+\Delta t) = P_{1,2}+P_{1,3}+ \cdots +P_{1,N} \; ; \quad P_{1,1} = 0$$

so that

$$P_{1,N}(t,t+\Delta t) \approx (\lambda_{1,2}+\lambda_{1,3}+ \cdots +\lambda_{1,N})\ \Delta t$$

and

$$P_{1,N}(t,t+\Delta t) \approx \Lambda_{1,N}\ \Delta t$$

where

$$\Lambda_{1,N} = \sum_{i=2}^{N} \lambda_{1,i} \qquad (3.6)$$

For constant $\lambda_{1,i}$ one obtains the probability of collision from

$$P_{1,N}(t_o,t) = 1-e^{-\Lambda_{1,N}(t-t_o)}$$

and in the event of time varying collision frequencies one has the relation

$$P_{1,N}(t_o,t) = 1-e^{-\int_{t_o}^{t} \Lambda_{1N}(\tau)d\tau} \qquad (3.7)$$

For N = 2, this reduces to the formula for two aircraft as one would expect. i.e.

$$P_{1,2} = 1-e^{-\lambda_{1,2}(t-t_o)}$$

This probability is useful for the design of an on-board collision avoidance system since concern is for only one aircraft with respect to N - 1 others in this type of design. If however, there is concern also for ground-based collision avoidance or traffic control systems, then the probability of collision among all N aircraft must be determined. Since the collision of an aircraft with itself is impossible, the probability of no collision among N aircraft in (t_o,t) is given by

$$Q_{N,N} = \left\{ \prod_{i=1}^{N} \prod_{j=1}^{N} q_{i,j} \right\}^{1/2} \quad ; \; i \neq j$$

where

$$q_{i,j} = e^{-\int_{t_o}^{t} \lambda_{i,j}(\tau)d\tau}$$

and

$$\lambda_{ij} = \int_{\substack{\text{Vel}\\ \text{Space}}} d(\bar{w})\,[W(0,\bar{w},t)w\delta s]_{i,j}$$

Thus,

$$Q_{N,N} = e^{-\frac{1}{2}\int_{t_o}^{t} \sum_{i=1}^{N} \sum_{j=1}^{N} \lambda_{ij}(\tau)d\tau} \qquad i\neq j$$

Define the total collision frequency

$$\Lambda_{N,N} = \frac{1}{2} \sum_{i=1}^{N} \sum_{j=1}^{N} \lambda_{ij}(t)\,(1-\delta_{ij}) \tag{3.8}$$

where

$$\delta_{ij} = \begin{cases} 0 & i\neq j \\ 1 & i=j \end{cases}$$

so that the probabilities of interest are given by

$$Q_{N,N} = e^{-\int_{t_o}^{t} \Lambda_{N,N}(\tau)d\tau} \tag{3.9}$$

$$P_{N,N} = 1 - e^{-\int_{t_o}^{t} \Lambda_{N,N}(\tau)d\tau} \tag{3.10}$$

3.3 Generalized Traffic Model

One purpose of a traffic model is to predict midair conflicts under assumed conditions of density, velocity, lane structure and the like. To perform this prediction, (3.8) could be evaluated directly to determine collision frequency but if the number of aircraft is large, this becomes a rather lengthy computation. For example, if 1000 aircraft are involved, 1,000,000 values of λ_{ij} must be computed before the overall collision frequency can be computed. As a result, some approximation to equation (3.8) is desired. This approximation technique is presented as Appendix A with two examples which illustrate the application of this result. The equations derived for making this approximation to the collision frequency among a single group of aircraft or between two groups of aircraft are given by

$$\left.\begin{aligned} \Lambda_{N,N} &= \frac{N(N-1)}{2} E_{NN}(\lambda_{ij}) \\ \text{and} \\ \Lambda_{M,N} &= MN\, E_{MN}(\lambda_{ij}) \end{aligned}\right\} \tag{3.11}$$

where

$$E_{KN}(\lambda_{ij}) = \int d(\tilde{\tilde{x}}_i) \int d(\tilde{\tilde{x}}_j)\ U_N(\tilde{\tilde{x}}_i)\ U_K(\tilde{\tilde{x}}_j)\ \lambda_{ij}(\tilde{\tilde{x}}_i, \tilde{\tilde{x}}_j) \qquad (3.12)$$

The expression $E_{KN}(\lambda_{ij})$ is a constant with respect to the numbers of aircraft M and N but may depend on time as might M and N themselves. Also, the expression $U(\tilde{\tilde{x}}_i)$ is the probability density distribution of nominal position and velocity for a large number of aircraft (see Appendix A). From (3.11) it can be stated that

$$\left.\begin{aligned} \Lambda_{NN} &= N(N-1)\ K_{NN} \\ \text{and that} \\ \Lambda_{MN} &= MN\ K_{MN} \end{aligned}\right\} \qquad (3.13)$$

It must be emphasized that this result is independent of the probability distributions chosen. Only the value of the slope (K) depends on the distributions used. If N and M are constant, the number of collisions for a given time T is approximated by

$$\left.\begin{aligned} N_c &= K_1 N^2 \ ; \quad K_1 = K_{NN} T \\ \text{for a large single group of aircraft and by} \\ N_c &= K_2 N^2 \ ; \quad K_2 = K_{MN} T \end{aligned}\right\} \qquad (3.14)$$

for two groups of aircraft.

All of the work which has been done to empirically validate the N^2 or NM relationship in reference (36) applies. To assume

that because this relationship is verified, the assumptions of (36) concerning uniform distributions are valid, is incorrect, since it has been shown that the relationship (3.13) is independent of the distributions. It is also apparent that, unless the vehicle states are explicit functions of the density, the square relationship with density cannot be altered by adjusting the nominal paths. The slope of the relation however is a function of these nominals and can be adjusted by manipulation of the flight paths and thus the distributions.

The main objective in formulating the analytical model is to find that set of distributions which gives a high correlation with the empirically derived N^2 slope relationship determined in reference (36). This constitutes a true validation of the postulated model. Since empirical data can be used for prediction of collisions or near-misses as a function of density, this model is useful primarily for computation of both the critical encounter frequency and the system encounter frequency.

A brief review of the work which was accomplished in Appendix C-3 of reference (36) is useful here to illustrate by example the importance of the distributions used. First, the quadratic relationships were established using a theory analogous to that employed in the kinetic theory of gases (see Example III-1). Second, a number of plots of near-misses between air carriers, general aviation, and military aircraft were made using reference (15). The number of near-misses were plotted vs. traffic factor for a number of airports. Finally, a least squares fit

of a straight line to this data was made and then the correlation coefficients and confidence levels were calculated.

Results show that a high degree of correlation (89.98%) between data and curve fit exist which verifies the linear relationship between the number of near-misses and the traffic factor. In order to understand how this relates to the number of aircraft and thus the density, it is necessary to understand what is meant by the traffic factor.

Traffic Factor

The traffic factor is used to obtain an estimate of the numbers of aircraft N and M. The data available do not give the number of aircraft directly but rather the number of annual operations N_0 and M_0 of the groups N and M respectively. An operation consists of a landing or takeoff. The average hourly rate at which operations occur is given by

$$N_h = N_o/365T$$

where T is the number of hours per day over which the traffic is assumed to be constant. A value of T = 12 hours was used in (36).

The number of aircraft of group N that will be in the terminal area at any instant is given by

$$N = N_h \, R_o/\tilde{V}_N$$

where R_o is the radius of the terminal area, $\tilde{V}_N$ is the average speed of group N, and N_h is the number of operations per hour. A further refinement is introduced to take into account the different characteristics of local and itinerate traffic. It is

assumed that all air carrier (AC) traffic is itinerate while general aviation (GA) and military traffic (ML) include both local and itinerate flights. GA local traffic may however use an airport other than the prime airport of consideration and these flights are not included in the computation of traffic factor. The traffic factor for AC and GA is given by

$$F(30) = AC(30)\ [GA_L(0) + GA_I(30)]$$

where $AC(30)$ is the number of annual AC operations at the given airport, $GA_L(0)$ is the number of local GA annual operations at the given airport and $GA_I(30)$ is the sum of all GA itinerate operations within a 30 mile radius of the airport.

Let the AC aircraft be denoted as group N and the GA aircraft be group M. The average number of aircraft of group N in the terminal area at any instant is given by

$$N = \frac{AC(30)}{365T} \cdot R_o/\tilde{V}_{AC}$$

and for group M by

$$M = [GA_L(0) + GA_I(30)]\ R_o/\tilde{V}_{GA}$$

Thus, the traffic factor is linearly related to the product of the groups of aircraft by

$$F(30) = \left(\frac{365}{R_o}\right)^2 T^2\ \tilde{V}_{AC}\ \tilde{V}_{GA}\ MN \qquad (3.15)$$

The results of (36) apply equally as well to the number of aircraft as they do to the traffic factor.

Suppose that it is desired to estimate the number of near-misses between GA and AC aircraft in a one year period. Assume for purposes of example that the kinetic theory of gases model is used to make this prediction. The collision frequency between these two groups is given by

$$\Lambda_{MN} = \frac{4}{3} \pi d^2 \frac{\tilde{V}_{MN}}{V_{a/s}} \tag{3.16}$$

so that the expected number of incidents in one year is

$$N_c = \Lambda_{MN} \cdot 365T \tag{3.17}$$

under the assumptions of the gas model. The volume of the airspace is found from

$$V_{a/s} = \pi R_o^2 h \tag{3.18}$$

where h is the altitude of the airspace. Choosing the following values of the parameters

d = 500 ft.

h = 10,000 ft.

v = 200 knots

T = 12 hrs.

F = 6.5×10^{11} (New York Area; 1968)

the estimated number of near-misses using the gas model is 4,100, which is far in excess of the actual 42 incidents reported in the data (36). This result dramatically illustrates the dependence of the slope on the distributions and, because of this dependence,

the remainder of this work is directed at establishing a method of computing the slope analytically.

3.4 The "HUB" Traffic Model

Based upon Appendix C-5 of reference (36), the following traffic models will be proposed to replace previously formulated models. These models will be referred to as "Hub Models." Two Hub Models are formulated: the first is a navigational hub; the second is an airport hub. These two differ primarily in the consideration of the nominal altitude and velocity profiles. Straight and level flight is assumed for the navigational hub while approach and departure flight paths are assumed for the airport hub.

The Navigational Hub

For this type of model, the following assumptions are made. Assume that the airspace of the hub is cylindrical with radius R_0 and altitude h_0. Further, assume that there are K lanes with nominal azimuths α_k and altitudes h_k. Assume also that there are M_k aircraft in lane L_k and that the positions of the aircraft in lane are uniformly distributed along the radius, but have nominal altitude h_k and azimuth α_k. Next, assume that in a given lane all aircraft have the same heading and the same average speed. Figure 3.2 illustrates the geometry of this model.

From geometry, it is readily established that

$$\tilde{\bar{r}}_i = \tilde{\bar{\rho}}_i + \tilde{\bar{h}}_i$$

$$\tilde{\bar{\rho}}_i = \rho_i \begin{Bmatrix} \cos \alpha_k \\ \sin \alpha_k \\ 0 \end{Bmatrix}$$

$$\tilde{\bar{h}}_i = h_k \begin{Bmatrix} 0 \\ 0 \\ 1 \end{Bmatrix}$$

and that

$$\tilde{\bar{v}}_i = v_k \begin{Bmatrix} \cos \theta_k \\ \sin \theta_k \\ 0 \end{Bmatrix}$$

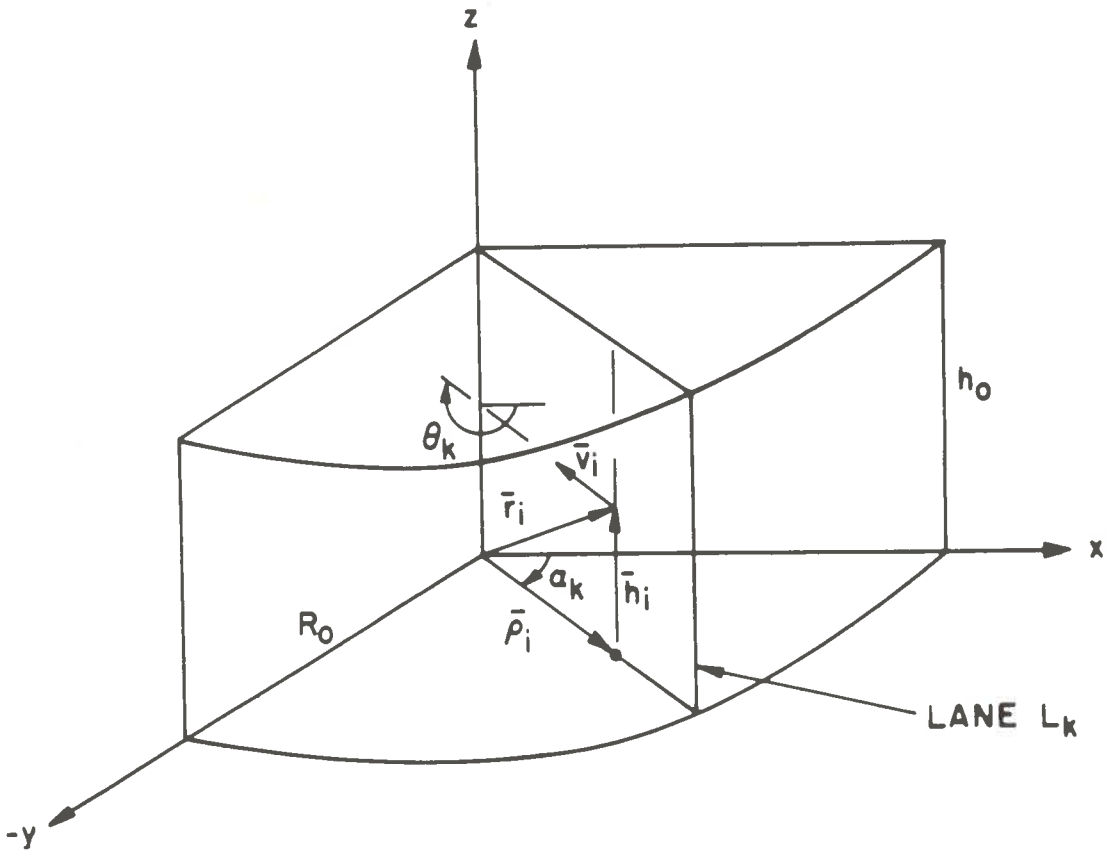

Figure 3.2.- Hub model geometry

Note that the average altitude and speed of the i^{th} aircraft has been chosen to be equal to the nominal altitude and speed of the k^{th} lane. The total number of aircraft in the hub is given by

$$N = \sum_{k=1}^{K} M_k$$

Treating each lane as a special group, and utilizing the results of Appendix A, the collision frequency

$$\Lambda = \sum_{k=1}^{K} \sum_{\ell=1}^{K} \Lambda_{M_k M_\ell}$$

This includes collisions within the same lane as well as between lanes. The probability density distribution within a lane (note the uniform assumption) is given by

$$U(\tilde{\bar{x}}_i) = 1/R_0$$

where R_0 is the lane length. Again appealing to the results of Appendix A, one obtains the collision frequency between the lanes as

$$\left.\begin{aligned} \Lambda_{M_k M_\ell} &= M_k M_\ell \, E(\lambda_{ij}) \quad ; \quad k \neq \ell \\ \text{and the in-lane frequency as} & \\ \Lambda_{M_k M_k} &= \frac{M_k (M_{k-1})}{2} E(\lambda_{ij}) \quad ; \quad k = \ell \end{aligned}\right\} \qquad (3.19)$$

where

$$E(\lambda_{ij}) = \int d(\tilde{\bar{x}}_i) \int d(\tilde{\bar{x}}_j) U_{M_k}(\tilde{\bar{x}}_i) U_{M_\ell}(\tilde{\bar{x}}_j) \lambda_{ij}(\tilde{\bar{x}}_i, \tilde{\bar{x}}_j)$$

Next, recall from Example III-1 that for two aircraft flying nominal flight paths that

$$\lambda_{ij} = \frac{d^2}{|P|^{1/2}} \left(\frac{\sigma_v}{\pi} + \frac{|\tilde{\bar{v}}_i - \tilde{\bar{v}}_j|}{2(2\pi)^{1/2}} \right) e^{-\frac{1}{2}(\tilde{\bar{r}}_i - \tilde{\bar{r}}_j)^T P^{-1} (\tilde{\bar{r}}_i - \tilde{\bar{r}}_j)}$$

and assume that

$$P = \begin{bmatrix} \sigma_r^2 & & 0 \\ & \sigma_r^2 & \\ 0 & & \sigma_h^2 \end{bmatrix}$$

Appropriate substitution and integration yields

$$\left.\begin{aligned} E(\lambda_{ij}) &= \frac{\pi}{2} \cdot \frac{d^2}{R_o^2 \sigma_h} \left\{ \frac{\sigma_v}{\pi} + \frac{[v_k^2 + v_\ell^2 - 2v_k v_\ell \cos(\theta_k - \theta_\ell)]}{2(2\pi)^{1/2}} \right\} \\ &\quad \frac{e^{-\frac{1}{2}(h_k - h_\ell)/\sigma_h^2}}{\sin(\alpha_k - \alpha_\ell)} \quad ; \; k \neq \ell \\ E(\lambda_{ij}) &= \frac{1}{\sqrt{2\pi}} \cdot \frac{d^2 \sigma_v}{R_o \sigma_r \sigma_h} \quad ; \; k = \ell \end{aligned}\right\} \qquad (3.20)$$

where

$$|P|^{1/2} = \sigma_r^2 \, \sigma_h$$

From (3.19), and (3.20) the collision frequency between lanes is given by

$$\Lambda_{k\ell} = \sum_{k=1}^{K} \sum_{\ell=1}^{K} M_k M_\ell \, E(\lambda_{ij})(1-\delta_{k\ell}) \quad ; \; k \neq \ell \tag{3.21}$$

and the in-lane frequency by

$$\Lambda_{kk} = \frac{1}{\sqrt{2\pi}} \frac{d^2 \sigma_v}{R_o \sigma_r \sigma_h} \sum_{k=1}^{K} \frac{M_k (M_{k-1})}{2} \tag{3.22}$$

where K is the number of lanes and M_k the average number of aircraft per lane.

The Airport Hub

From the data given in references (15) and (36) 55 percent of the critical incidents which occurred in the terminal area occurred in an overtaking situation, in-lane. Furthermore, the prime cause of these incidents was one aircraft "cutting-out" another aircraft in the pattern. As a result of this information, and under the assumption that the collision frequencies are proportional to the percentages, it suffices to use the result of the Navigational Hub in-lane collision frequency Λ_{kk} and to increase this by a factor of 1.82 (100%/55%) to account for the remaining head-on (2%) and crossing (43%) incidents. This results in the following expression for collision frequency in an airport hub

$$\Lambda = 0.725 \, \frac{M(M-1)}{2} \, K \, d^2 \sigma_v / R_o \sigma_r \sigma_h \tag{3.23}$$

where σ_h is the altitude uncertainty between aircraft, σ_r is the lateral position uncertainty between aircraft and σ_v is the uncertainty in the relative speed.

A further refinement of this model is obtained from the following considerations. In reference (15), hazardous near-misses are classified as either critical or potential. Critical is defined as a situation where collision avoidance was due to chance rather than action on the part of the pilot. A potential incident is defined as an incident which might have resulted in a collision if no action had been taken by either pilot. All hazardous incidents occurred with aircraft passage less than 500 ft except when closure rates were greater than 400 knots.

From these definitions of incident type, it appears that in a potential situation, the aircraft were seen and avoided;while in the critical situation, it was too late to execute an avoidance maneuver even if the intruder were seen. It is also reported in (15) that 28.1 percent of the hazardous incidents were classified as critical and of these, 128 occurred en-route and 189 in the terminal area. Also, 719 of the total 1128 incidents occurred in the terminal airspace.

These data are presented in table 3.1, and can be interpreted to mean that the pilots' ability to "spot" aircraft reduces the total number of predicted critical NMACs by a factor of 3.2. Accounting for this factor in equation (3.23) yields the following expression for predicting the frequency of critical incidents in the terminal area

$$\Lambda_{critical} = 0.226 \frac{M(M-1)}{2} K d^2 \sigma_v / R_0 \sigma_r \sigma_h \qquad (3.24)$$

TABLE 3.1.- NEAR-MISS DATA

Type	Terminal	En-Route	Totals
Critical	189	128	317
Potential	530	281	811
Totals	719	409	1128

To validate this model, return to the statistics for the New York area during 1968. A total of 42 critical incidents were reported during that year for that area. In the Alexander Report(36), it is estimated that 4 times this amount or 168 actual critical incidents occurred.

For the New York area, there are approximately 20 identifiable lanes and, based on the traffic factor, an average of 60 aircraft are estimated to be airborne at any one time. It is assumed that there are an average of three aircraft per lane, that the protected volume is 500 ft., that the radius of the hub is 30 nm, (consistent with F(30)) and also (for purposes of illustration) that the uncertainties are

$$\sigma_w = 1 \text{ knot} \quad ; \quad \sigma_h = 500 \text{ ft.} \quad ; \quad \sigma_\rho = 1 \text{ nm.}$$

With these assumptions an estimate of the number of critical incidents, from equations (3.20) and (3.21), equal to 167 is obtained as compared to the 168 estimated from empirical data in the Alexander report(36).

It must be emphasized that the fundamental result of this model validation is that correct order of magnitude estimates of mid-air incidents can be obtained.

Further verification of the hub model is obtained by considering that the predicted number of NMACs as well as being a function of N^2 in the model, is also a function of the protection radius d^2. From (15), there were 719 NMACs $\leq$ 500 ft in the terminal areas while the number less than 250 ft was 161. The estimated number of NMACs less than 250 ft using the d^2 relation is $(250/500)^2$ or 25 percent of the NMACs less than 500 ft. By this relation, 180 NMACs less than 250 ft should have occurred while in fact, 161 were reported. This data seems to validate the d^2 relationship fairly well.

The N^2 and the d^2 relationships have been validated by data. It has also been shown that the hub model correlates highly with empirical data and can be used with confidence in future work.

One problem remaining in collision probability theory is the problem of determining the probability of simultaneous encounters or collisions.

3.5 Simultaneous Threats

This problem is defined as finding the probability that a near-miss between two aircraft will occur in a time interval (0,t) and that at least one of the involved aircraft will then encounter another aircraft in $(t, t + \Delta t)$. The reason for considering this problem is that it has been implicitly assumed in all the published

literature as well as in the previous analyses that this probability is small, but no quantative or analytical results have been previously presented. The analytic formulation of this problem is presented as Appendix B. The basic results of this analysis are given below. An application to the New York Terminal using 1968 statistics is used for quantifying the formulation.

The number of multiple incidents are related to the number of single incidents by

$$N_{mult} \approx 2(N-1)\ \mu\tau N_{sing}$$

where

$$\mu \approx 2N_{sing}/N(N-1)T$$

From the available statistics for the New York area, T = 4380 hours, N = 3, N_{sing} = 170 and μ = 0.013/hr. By substitution one obtains

$$N_{mult} = 0.073/year$$

so that the expected number of critical multiple incidents in the New York area is about 1 in 13-1/2 years under the assumptions cited. Another point of view is to look at the probability of a multiple or simultaneous critical incident occurring. This probability is given by

$$P \approx 2(N-1)\mu\tau$$

Now, using the statistics for the New York area and a system warning time τ = 30 sec., the probability that a multiple incident will occur is approximately 1 in 2000 over a one-year period.

Next, if one is interested in the probability of failure of an airborne collision avoidance system designed to resolve one critical encounter at a time, then this is given approximately by the probability of encountering one intruder and then encountering a second intruder while the system is resolving the first conflict. For this case, the probability of system failure is given by

$$P \approx (N-1)(N-2)\mu^2 T_f \tau$$

Again using the New York area statistics to quantify this result, the probability of system failure under the above assumptions is calculated to be 1 part in 10^6 per terminal operation (terminal flight time T_f is estimated at 20 min).

3.6 Evaluation Criteria Formulae

Conflict Ratio

Based on the previous analyses, the collision frequency is linearly related to the traffic factor as was indicated analytically by (3.11) and (3.15). This agrees with the empirical results reported in (36). Further, from (3.4), (3.16) and (3.24) it is seen that the collision frequency is proportional to the area of the projection of the protected volume on a plane

perpendicular to the relative velocity vector. For a spherical protected volume it is proportional to the radius squared. For a cylindrical protection volume, it is proportional to the height and radius of the cylinder. The values of critical miss distance in these models give the collision frequency or critical encounter frequency. Alternatively, the values of the system alarm thresholds give the system encounter frequency, which can be written as

$$\mu_s = K_\mu F(\varepsilon_L \varepsilon_V)_s \tag{3.25}$$

and the critical encounter frequency as

$$\mu_C = K_\mu F(\varepsilon_L \varepsilon_V)_C \tag{3.26}$$

where K_μ is the model constant and $\varepsilon_L, \varepsilon_V$ are the dimensions of the system alarm region or the critical miss distances. The formula for the Conflict Ratio is given by

$$CR = \frac{\mu_s}{\mu_c} = \frac{(\varepsilon_L \varepsilon_V)_s}{(\varepsilon_L \varepsilon_V)_C} \tag{3.27}$$

and is seen to be <u>independent</u> of both traffic factor F and model constant.

<u>Probability of Missed Critical Alarm</u>

To compute this parameter, begin by assuming that it is desired to protect a range ρ_ε about aircraft No. 1. This can be done by setting an alarm threshold ρ_T at a specified value.

Then the probability of false alarm will have a discrete value when the predicted range is equal to the threshold. Figure 3.3 illustrates the statistical situation for the threshold ρ_T greater than the protection range ρ_ε and for a standard deviation of the uncertainty in the predicted range given by σ_ρ.

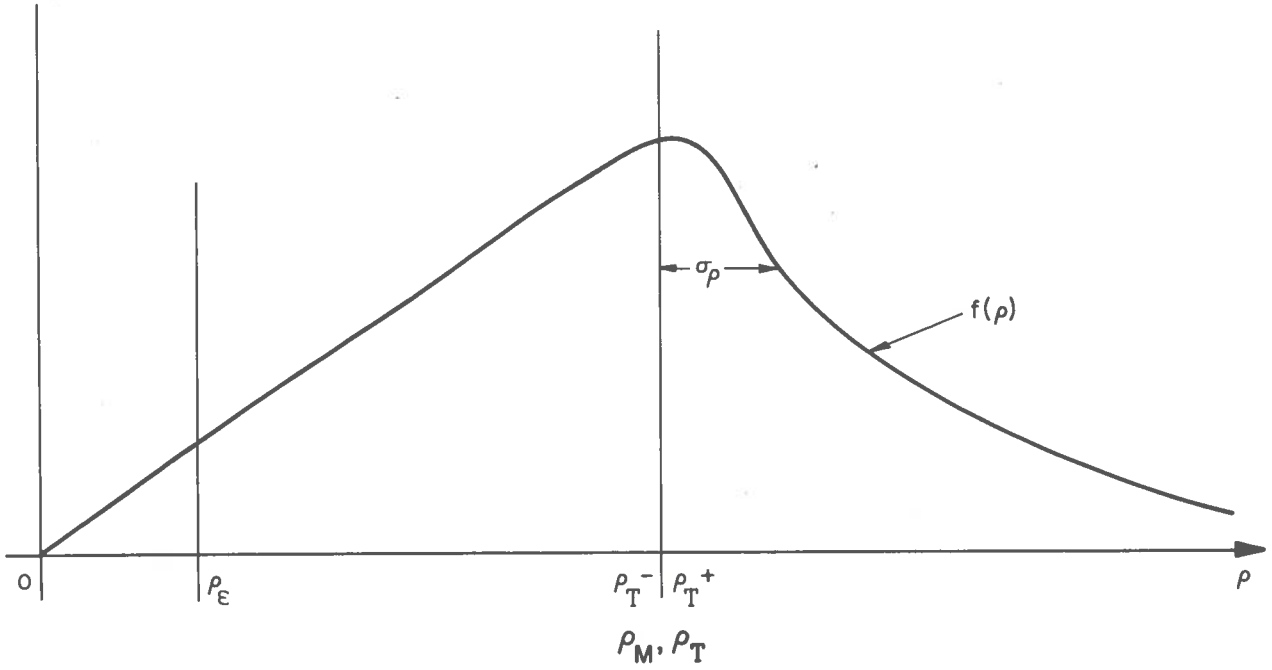

Figure 3.3.- Statistics of alarm probability theory

Consider that an alarm is given when the predicted value of range ρ_M is equal to ρ_T^- and is not given for ρ_M equal to ρ_T^+. A false alarm will occur if $\rho_M = \rho_T^-$; $|\rho| > \rho_\varepsilon$ while a missed alarm will occur for $\rho_M = \rho_T^+$; $|\rho| < \rho_\varepsilon$. The conditional probability of missed alarms can be written

$$P_{M/C} = P_r(\rho < \rho_\varepsilon / \rho_M = \rho_T^+)$$

where the condition is that the predicted value of range is equal to the threshold and has an uncertainty described by σ_ρ.

Next, consider that if $f(\rho)$ is the probability density function of the random variable ρ, one has

$$P_{M/C} = \int_0^{\rho_\varepsilon} f(\rho)d\rho \; ; \; \hat{\rho} = \rho_M = \rho_T^+$$

For purposes of illustration, consider the following example. Suppose that

$$\rho = |\bar{\rho}| = (\rho_1^2 + \rho_2^2 + \ldots + \rho_n^2)^{1/2}$$

and $\bar{\rho}$ is normally distributed in n dimensions with mean value $\bar{\rho}_M$ and a positive definite covariance matrix

$$P = \sigma_\rho^2 \, I$$

Under these assumptions, from reference (35), the probability density function of $|\rho|$ is a Rayleigh distribution and is given by

$$f(\rho) = \frac{\rho_M}{\sigma_\rho^2} \left(\frac{\rho}{\rho_M}\right)^{n/2} e^{\frac{-(\rho^2+\rho_M^2)}{2\sigma_\rho^2}} \; I_{\frac{1}{2}(n-2)} \left(\frac{\rho\rho_M}{\sigma_\rho^2}\right)$$

where $\rho>0$; $\rho_M = |\bar{\rho}_M|$ and I_α is the modified Bessel function of the first kind and of order α. Further, from reference (38) is obtained the relation (n=1)

$$I_{-\frac{1}{2}}(x) = \sqrt{\frac{2}{\pi x}}\cosh x$$

so that

$$f(\rho) = \frac{1}{\sqrt{2\pi}\,\sigma_\rho}\left[e^{\frac{-(\rho-\rho_M)^2}{2\sigma_\rho^2}} + e^{\frac{-(\rho+\rho_M)^2}{2\sigma_\rho^2}}\right]$$

Substitution and integration yields

$$P_{M/C} = \Phi\left(\frac{\rho_\varepsilon-\rho_T}{\sigma_\rho}\right) + \Phi\left(\frac{\rho_\varepsilon+\rho_T}{\sigma_\rho}\right) \;;\; \rho_T \to \rho_M \tag{3.28}$$

where $\Phi(x)$ is the probability error function given by

$$\Phi(x) = \frac{1}{\sqrt{2\pi}}\int_0^x e^{-\xi^2/2}\,d\xi$$

The probability of failure to detect a critical threat during a single data cycle is approximated by (3.28). After n data cycles, the probability of failure to detect a critical threat is conservatively approximated by

$$\boxed{P_M = P_{M/C}^n = \left\{\Phi\left(\frac{\rho_\varepsilon-\rho_T}{\sigma_\rho}\right) + \Phi\left(\frac{\rho_\varepsilon+\rho_T}{\sigma_\rho}\right)\right\}^n} \tag{3.29}$$

where n is the number of data cycles.

From (3.29), it is seen that ρ_T must be chosen larger than the critical miss distance ρ_ε in order to achieve small probabilities. Further, the threshold must be chosen greater than the prediction uncertainty for the same reason as well as to insure sufficient escape time. Because of prediction uncertainty and escape time, thresholds must be chosen large to insure low probabilities of missing critical alarms while conversely, small threshold values are desired in order to achieve low Conflict Ratio. Consequently, a trade-off between these two parameters is indicated in any system design. If the thresholds are chosen slightly larger than the critical miss distance (by an infinitesimal amount) and if one has a perfect position prediction, then $P_{M/C} = 0$ and $CR = 1$ as one would expect. As a result of (3.27) and (3.29), it is necessary to establish methods for computation of system thresholds. This is discussed in the following chapter.

CHAPTER 4

SYSTEM ALARM THRESHOLD ANALYSIS

4.1 Introduction

In Chapter 3, it has been shown that the system evaluation criteria, *conflict ratio* and *probability of missed critical alarm*, are both independent of the statistical traffic model and the traffic factor. These criteria depend only on the system alarm thresholds, the critical miss distance and the position prediction uncertainty.

System alarm thresholds are chosen in order to provide a pilot with sufficient warning time to perform an evasive maneuver, i.e., to avoid a collision. Because of the uncertainties in the prediction of the relative position of potentially conflicting aircraft, these thresholds must be chosen larger than the critical miss distances for purposes of safety.

Predicted relative position uncertainty arises from two major error sources:

Measurement Errors

Model Errors

Measurement errors occur as a result of imperfections in the sensing devices used to estimate the relative state between conflicting aircraft. Model errors occur as a result of approximating the motion of the aircraft. For example, a constant velocity assumption might be made and the future relative position of the aircraft estimated on this basis. If the aircraft are in fact

turning, a prediction error resulting from the prediction model will result. The computation of system alarm thresholds requires a thorough understanding of both of these major error sources.

In this chapter, linear and curvilinear models for predicting relative position between conflicting aircraft are presented. Measurement error propagation for both of these models will also be discussed in order that measurement sensor errors can be related to *conflict ratio*. In addition, system warning time will be analyzed on the basis of both vertical and lateral evasion maneuvers.

Based on these analyses, system alarm thresholds can then be computed and various anti-collision system categories compared.

4.2 The Rectilinear Prediction Model

The geometry of this problem is presented as Figure 4.1. The assumption that both aircraft fly with constant velocity is made in the analysis of this problem. As a result of this assumption and the geometry of Figure 4.1, it is readily established that the equations of relative motion for this prediction model are given by

$$\bar{\rho}(t) = \bar{\rho}_o + \bar{w}t \tag{4.1}$$

where

$$\bar{w} = \bar{v}_2 - \bar{v}_1 \tag{4.2}$$

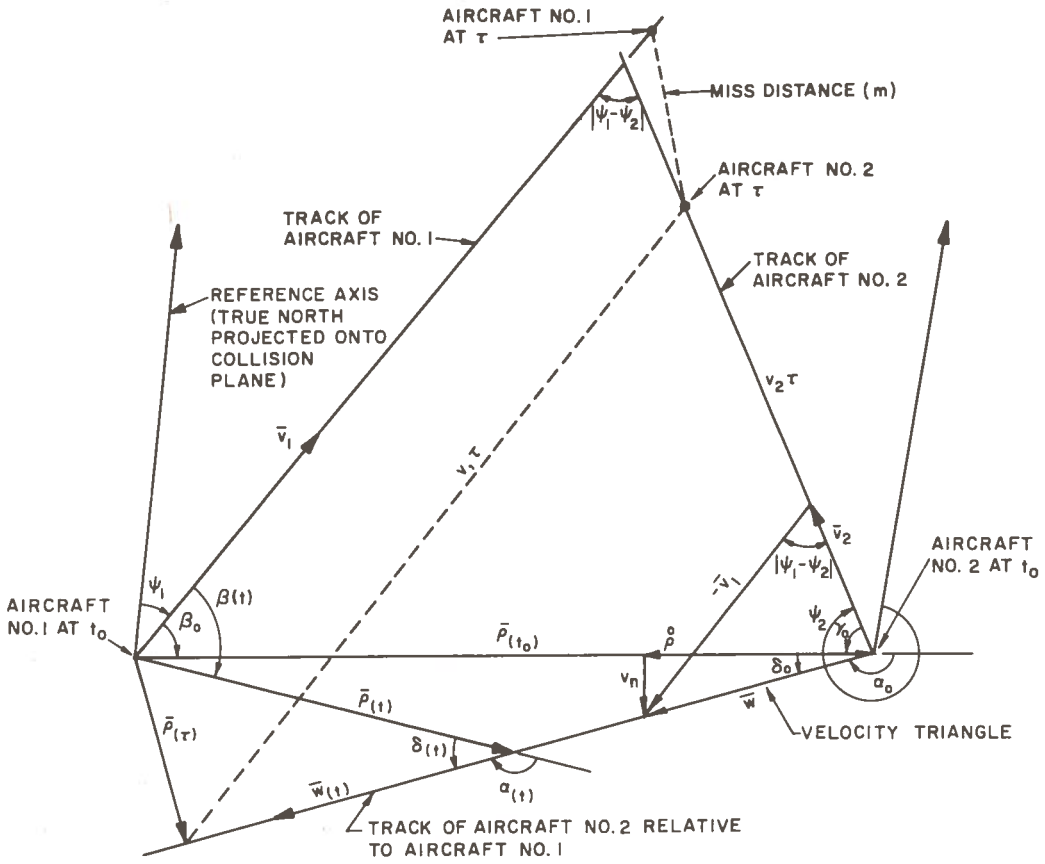

Figure 4.1.- Collision plane near miss geometry - rectilinear flight paths

The magnitude of the range vector is easily obtained from these equations and is given by

$$|\bar{\rho}(t)| = \{\rho_o^2 + 2w\rho_o t \cos\alpha + w^2 t^2\}^{1/2} \qquad (4.3)$$

The time of closest approach is obtained by computing the time at which

$$\frac{d\rho}{dt} = 0$$

Under the above assumptions, this time is computed from

$$\tau = -\rho_o \cos\alpha / w \; ; \; 0 \leq \alpha \leq \Pi \tag{4.4}$$

and the range at this time or the miss-distance is given by

$$|\bar{\rho}(t)| = \rho_o \sin\alpha \tag{4.5}$$

Many current systems, in particular the McDonnell-Douglas EROS system and the RCA Secant System use an approximation to the time of closest approach given by

$$\tau = \rho_o / \dot{\rho}$$

i.e., range/range-rate.

This approximation is valid however only in the case when a collision (as opposed to a near-miss) occurs; that is, when $\alpha = \Pi$. The error in the predicted time to closest approach caused by use of this approximation is presented as Figure 4.2.

From (4.3), it is noted that the form of the relative range as a function of time is given by

$$\rho^2(t) = a_o + 2a_1 t + a_2 t^2 \tag{4.6}$$

so that the time of closest approach is

$$\tau = -a_1/a_2 \tag{4.7}$$

and the miss-distance is

$$\rho(\tau) = \left(a_o - a_1^2/a_2\right)^{1/2} \tag{4.8}$$

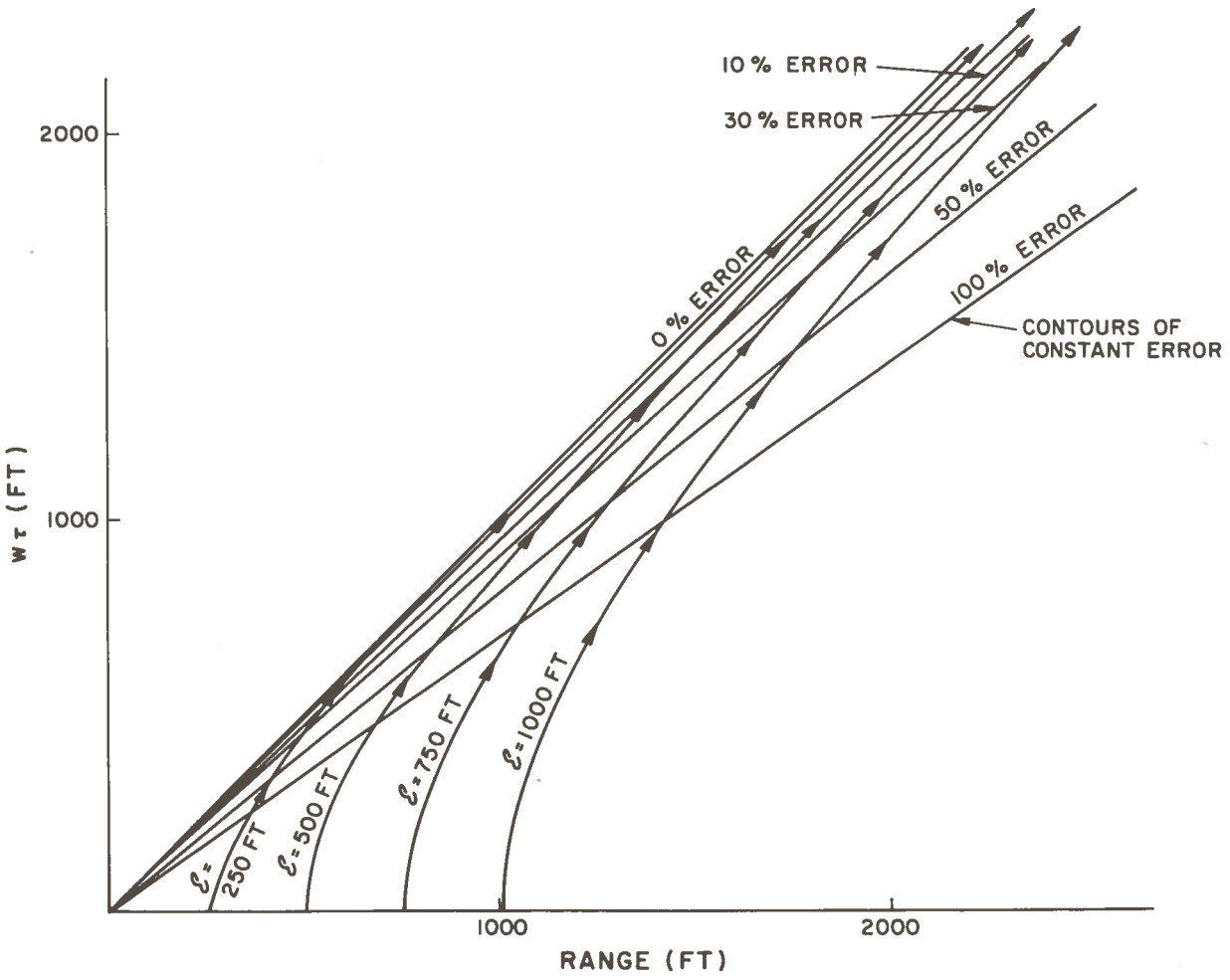

Figure 4.2.- Error in the TAU criterion

Equations (4.6), (4.7), and (4.8), show that the coefficients a_0, a_1, and a_2 can be estimated on the basis of range measurements only and that both the time of closest approach and the miss-distance can be computed from these coefficients. Under the assumption of constant velocity, a simple model for predicting relative position between potentially conflicting aircraft is available and requires only range information for the computation.

It is also of interest to note that in the collision case ($\alpha = \Pi$), the range vector and the relative velocity vector are

colinear. Examination of Figure 4.1 for the collision situation illustrates other commonly used collision criteria, namely:

The Rate of Change of the Line of Sight is Zero; ($\dot{\beta} = 0$)

The Range Acceleration is Zero; ($\ddot{\rho} = 0$)

The Normal Component of the Relative Velocity Vector is Zero; ($v_N = 0$)

4.3 The Curvilinear Prediction Model

The geometry of this problem is presented in Figure 4.3. In the analysis of this problem, assumptions are made that both aircraft fly with constant speed, constant rate of turn, and constant altitude rate. As a result of these assumptions and the geometry of Figure 4.3, it is readily established that the equations of relative motion for this prediction model are given by

$$\bar{\rho}(t) = \bar{\rho}(t_o) + \int_o^t \bar{w}(\sigma)\, d\sigma \tag{4.9}$$

where the relative velocity vector expressed in the navigational frame is

$$\bar{w}(t) = \begin{Bmatrix} v_2 \cos\phi_2 \cos(\psi_o+\omega_2 t) - v_1\cos\phi_1\cos\omega_1 t \\ -v_2 \cos\phi_2 \sin(\psi_o+\omega_2 t) - v_1\cos\phi_1\sin\omega_1 t \\ -\dot{h}_2 + \dot{h}_1 \end{Bmatrix} \tag{4.10}$$

and where the initial position vector coordinatized in the same frame is

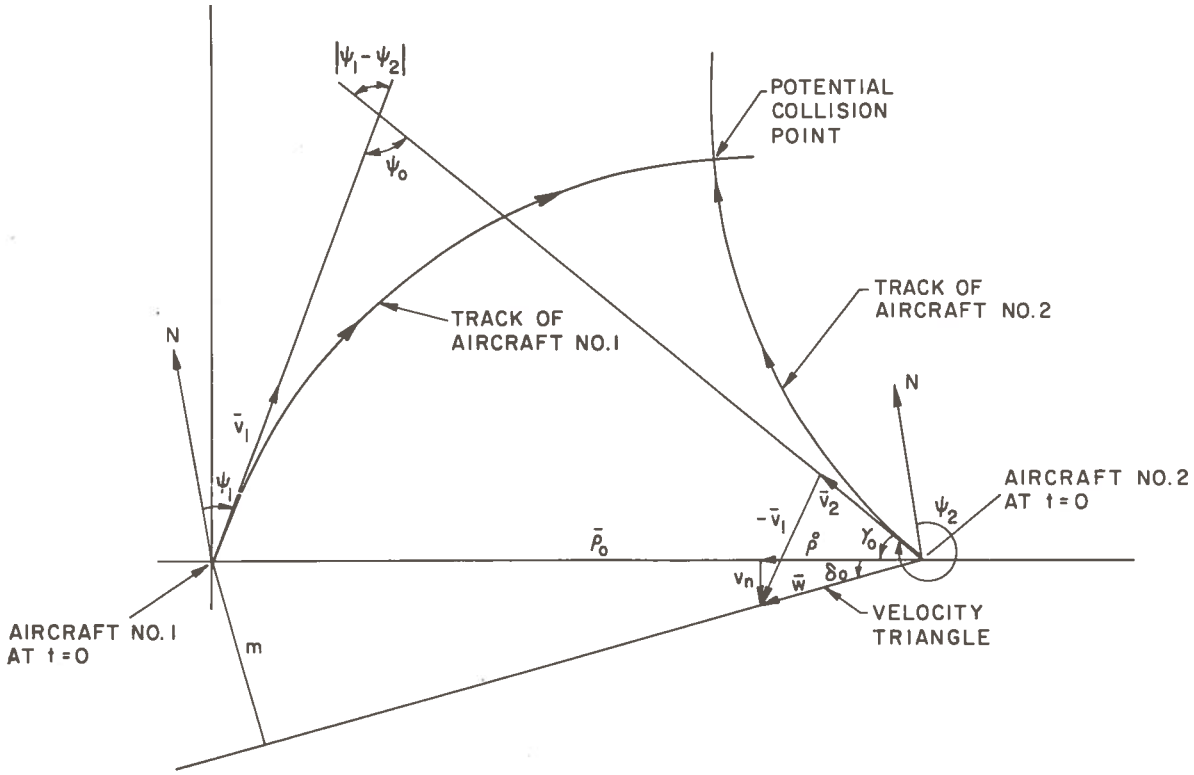

Figure 4.3a.- Curvilinear collision geometry (two dimensional)

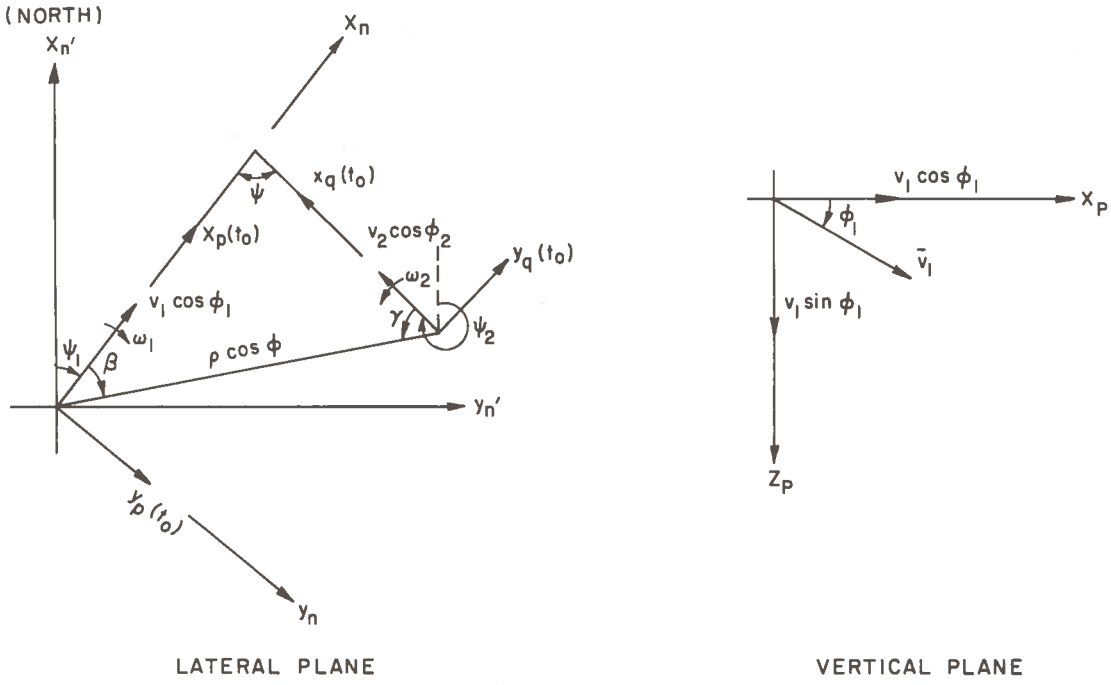

Figure 4.3b.- Curvilinear collision geometry (three dimensional)

$$\bar{\rho}(t_o) = \begin{Bmatrix} \rho_o \cos\phi \cos\beta_o \\ \rho_o \cos\phi \sin\beta_o \\ -h_{20} + h_{10} \end{Bmatrix} \tag{4.11}$$

A simple collision criterion for this model analogous to that obtained in the rectilinear model has not been obtained. A method for threat detection based on predicting future position as a function of present aircraft state is therefore chosen. However, one criterion for the case of planar flight and where the turn rates are given by

$$\omega_1 = -\omega_2 = \omega$$

is soluble. In this case, both aircraft are turning at the same rate and in the same direction. Under the above assumptions, (4.9) and (4.10) can be written as

$$\bar{\rho}(t) = \begin{Bmatrix} \rho_o - \frac{w}{\omega} \sin(\omega t - \delta_o) - \frac{w}{\omega} \sin\delta_o \\ - \frac{w}{\omega} \cos(\omega t - \delta_o) + \frac{w}{\omega} \cos\delta_o \end{Bmatrix} \tag{4.12}$$

and

$$\bar{w}(t) = -w \begin{Bmatrix} \cos(\delta_o - \omega t) \\ \sin(\delta_o - \omega t) \end{Bmatrix} \tag{4.13}$$

For collision, $\bar{\rho}(\tau)$ must be zero so that by applying this requirement to (4.12) the time to collision is found to be

$$\tau = 2\delta/\omega \tag{4.14}$$

and the collision condition is given by

$$\sin\delta = \omega\rho/2w \tag{4.15}$$

Also, from Figure 4.3, one can write that

$$\dot{\rho} = w\cos\delta \tag{4.16}$$

so that by differentiation of (4.15) and by substitution of (4.16) one obtains

$$\dot{\delta} = -\frac{\omega}{2} \tag{4.17}$$

Figure 4.3, shows that under the assumptions of same-sense-turns

$$\dot{\beta} = \dot{\delta} = -\frac{\omega}{2} \tag{4.18}$$

which yields the collision criterion that the rate of change of the line of sight is half the turn rate. Figure 4.4 is an illustration of this type of curvilinear collision path.

Prediction Equations

Integration of (4.9) yields the following equations for predicting relative position:

Curvilinear Flight Paths $\omega_1 \neq 0;\ \omega_2 \neq 0$ (4.19)

$$\bar{\rho}(\tau) = \begin{Bmatrix} \rho_o\cos\phi\cos\beta_o \\ \rho_o\cos\phi\sin\beta_o \\ -h_{20}+h_{10} \end{Bmatrix} + \begin{Bmatrix} \frac{v_2}{\omega_2}\cos\phi_2[\sin(\psi_o+\omega_2\tau)-\sin\psi_o]-\frac{v_1}{\omega_1}\cos\phi_1\sin\omega_1\tau \\ \frac{v_2}{\omega_2}\cos\phi_2[\cos(\psi_o+\omega_2\tau)-\cos\psi_o]+\frac{v_1}{\omega_1}\cos\phi_1[\cos\omega_1\tau-1] \\ (-\dot{h}_2+\dot{h}_1)\tau \end{Bmatrix}$$

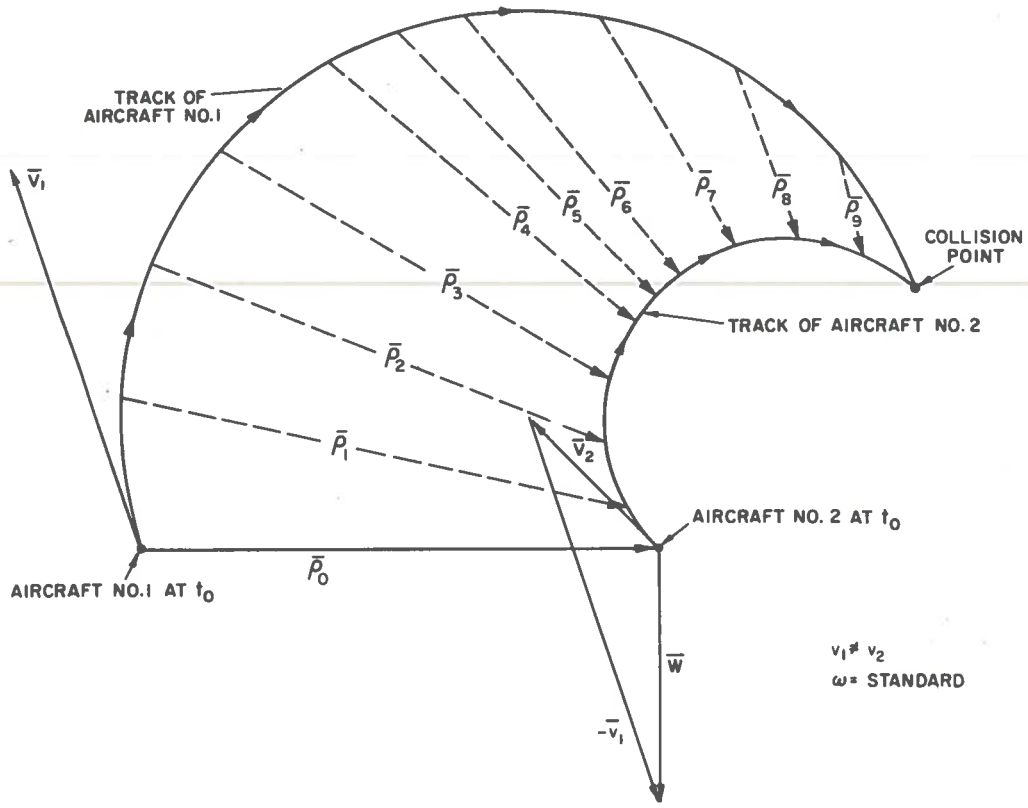

Figure 4.4.- Curvilinear collision flight paths - unequal speeds (same-sense-turns)

Rectilinear Flight Paths $\qquad \omega_1 = \omega_2 = 0$

$$\bar{\rho}(\tau) = \begin{Bmatrix} \rho_o \cos\phi \cos\beta_o \\ \rho_o \cos\phi \sin\beta_o \\ -h_{20}+h_{10} \end{Bmatrix} + \begin{Bmatrix} v_2\cos\phi_2\cos\psi_o - v_1\cos\phi_1 \\ -v_2\cos\phi_2\sin\psi_o \\ -\dot{h}_2+\dot{h}_1 \end{Bmatrix} \tau \qquad (4.20)$$

Mixed Flight Paths

$\omega_2=0;\omega_1\neq0$ (4.21)

$$\bar{\rho}(\tau) = \begin{Bmatrix} \rho_o\cos\phi\cos\beta_o \\ \rho_o\cos\phi\sin\beta_o \\ -h_{20}+h_{10} \end{Bmatrix} + \begin{Bmatrix} v_2\cos\phi_2\cos\psi_o \\ -v_2\cos\phi_2\sin\psi_o \\ -\dot{h}_2 + \dot{h}_1 \end{Bmatrix}\tau + \begin{Bmatrix} -\frac{v_1}{\omega_1}\cos\phi_1\sin\omega_1\tau \\ \frac{v_1}{\omega_1}\cos\phi_1[\cos\omega_1\tau-1] \\ 0 \end{Bmatrix}$$

$\omega_2\neq0;\omega_1=0$ (4.22)

$$\bar{\rho}(\tau) = \begin{Bmatrix} \rho_o\cos\phi\cos\beta_o \\ \rho_o\cos\phi\sin\beta_o \\ -h_{20}+h_{10} \end{Bmatrix} + \begin{Bmatrix} \frac{v_2}{\omega_2}\cos\phi_2[\sin(\psi_o+\omega_2\tau)-\sin\psi_o] \\ \frac{v_2}{\omega_2}\cos\phi_2[\cos(\psi_o+\omega_2\tau)-\cos\psi_o] \\ 0 \end{Bmatrix} + \begin{Bmatrix} -v_1\cos\phi_1 \\ 0 \\ -\dot{h}_2+\dot{h}_1 \end{Bmatrix}\tau$$

Examination of (4.19) thru (4.22) reveals the data requirements and measurements necessary for position prediction. The minimum data necessary to evaluate (4.19) thru (4.22) are: range, altitude, relative bearing, heading and air-speed or the equivalent.

A complete velocity fix is desirable. This type of information can be obtained indirectly from area navigation systems and cockpit information. For example, altitude, altitude-rate, airspeed, and heading are most easily obtained from aircraft instrumentation while range and relative bearing are most difficult to obtain from onboard instrumentation. Ground based radar could

provide these data or alternatively, an on-board area navigation system could provide the required position data. If this information were then transmitted to possible intruders and from possible intruders, range and relative bearing could then be computed and the future relative position predicted.

4.4 Position Prediction Errors

As mentioned previously, errors in the prediction of relative position can arise from both prediction model errors and measurement sensor errors. Both of these error sources are treated in detail in the following analyses.

Measurement Sensor Errors

To begin this analysis, recall that the range vector at a future time t is related to the present position and velocity vectors by

$$\bar{\rho}(t) = \bar{\rho}_o + \int_o^t \bar{w}(\sigma)d\sigma$$

where $\bar{w}(t)$ is the relative velocity vector. Variations in range are given by

$$\delta\bar{\rho}(t) = \delta\bar{\rho}_o + \int_o^t \delta\bar{w}(\sigma)d\sigma \qquad (4.23)$$

Consider that the relative position and velocity vectors are given by

$$\bar{\rho}_o = \begin{Bmatrix} [\rho_o^2 - (h_{10}-h_{20})^2]^{1/2} \cos\beta_o \\ [\rho_o^2 - (h_{10}-h_{20})^2]^{1/2} \sin\beta_o \\ h_{10}-h_{20} \end{Bmatrix} \tag{4.24}$$

$$\bar{w}(t) = \begin{Bmatrix} (v_2^2-\dot{h}_2^2)^{1/2} \cos[(\psi_{10}-\psi_{20})+\omega_2 t]-(v_1^2-\dot{h}_1^2)^{1/2} \cos\omega_1 t \\ -(v_2^2-\dot{h}_2^2)^{1/2} \sin[(\psi_{10}-\psi_{20})+\omega_2 t]-(v_1^2-\dot{h}_1^2)^{1/2} \sin\omega_1 t \\ \dot{h}_1 - \dot{h}_2 \end{Bmatrix} \tag{4.25}$$

The information required to calculate these vectors is seen to be the position information

$$\rho_o,\ h_{10},\ h_{20},\ \beta_o$$

and the velocity information

$$v_2,\ \dot{h}_2,\ v_1,\ \dot{h}_1,\ \psi_{10},\ \psi_{20},\ \omega_1,\ \omega_2$$

Twelve state variables are required. Some of these need not be measured directly however, and can be obtained by numerical differentiation of other data. For example, $\dot{h}_1$ and $\dot{h}_2$ can be obtained from altitude data while ω_1 and ω_2 can be obtained by differentiation of the heading information. Also, it is possible to use latitude, longitude and altitude data to obtain range and bearing or the relative range vector directly.

Equations which relate the variables measured to those used above are required for any method used however, in order that variations or uncertainties in the measurements can be related to the uncertainties in the state variables chosen. Therefore, the variations in $\bar{\rho}_o$ and in $\bar{w}$ based on the uncertainties in the state variables given above can be directly determined. From equation (4.24) one obtains

$$\delta\bar{\rho}_o = R(t) \begin{Bmatrix} \delta\rho_o \\ \delta\beta_o \\ \delta h_{10} \\ \delta h_{20} \end{Bmatrix} \tag{4.26}$$

where

$$R(t) = \begin{bmatrix} \frac{\rho_o}{\rho_L}\cos\beta_o & -\rho_L \sin\beta_o & -\frac{\Delta h}{\rho_L}\cos\beta_o & \frac{\Delta h}{\rho_L}\cos\beta_o \\ \frac{\rho_o}{\rho_L}\sin\beta_o & \rho_L \cos\beta_o & -\frac{\Delta h}{\rho_L}\sin\beta_o & \frac{\Delta h}{\rho_L}\sin\beta_o \\ 0 & 0 & 1 & -1 \end{bmatrix}$$

and where

$$\rho_L = \left[\rho_o^2 - (h_{10}-h_{20})^2\right]^{1/2} \quad ; \quad \Delta h = h_{10}-h_{20}$$

Similarly,

$$\delta\bar{w}(t) = W(t)\ \{\delta v_2, \delta\mathring{h}_2, \delta\psi_2, \delta\omega_2, \delta v_1, \delta\mathring{h}_1, \delta\psi_{10}, \delta\omega_1\}^T \tag{4.27}$$

where W is given by the matrix

$$\begin{bmatrix} \frac{v_2}{v_{2L}}\cos\theta_2 & \frac{-\dot{h}_2}{v_{2L}}\cos\theta_2 & -v_{2L}\sin\theta_2 & v_{2L}t\sin\theta_2 & \frac{-v_1}{v_{1L}}\cos\theta_1 & \frac{\dot{h}_1}{v_{1L}}\cos\theta_1 & v_{2L}\sin\theta_2 & v_{1L}t\sin\theta_2 \\ \frac{-v_2}{v_{2L}}\sin\theta_2 & \frac{\dot{h}_2}{v_{2L}}\sin\theta_2 & v_{2L}\cos\theta_2 & -v_{2L}t\cos\theta_2 & \frac{-v_1}{v_{1L}}\sin\theta_1 & \frac{\dot{h}_1}{v_{1L}}\sin\theta_1 & -v_{2L}\cos\theta_2 & -v_{1L}t\cos\theta_2 \\ 0 & -1 & 0 & 0 & 0 & 1 & 0 & 0 \end{bmatrix} \qquad (4.28)$$

and where

$$v_{2L} = (v_2^2 - \dot{h}_2^2)^{1/2} \quad ; \quad \theta_2 = \psi_{10} - \psi_{20} + \omega_2 t$$

$$v_{1L} = (v_1^2 - \dot{h}_1^2)^{1/2} \quad ; \quad \theta_1 = \omega_1 t$$

Substitution of (4.26) and (4.27) into (4.23) yields

$$\delta\bar{\rho}(t) = S(t)\delta\bar{x} \qquad (4.29)$$

where

$$S(t) = [R(t) \vdots \int_0^t W(\sigma)d\sigma]$$

and

$$\delta\bar{x}^T = \{\delta\rho_o, \delta\beta_o, \delta h_{10}, \delta h_{20}, \delta v_2, \delta h_2, \delta\psi_{20}, \delta\omega_2, \delta v_1, \delta\dot{h}_1, \delta\psi_{10}, \delta\omega_1\}$$

From (4.29), the covariance matrix of the errors in the predicted range vector as a function of the measurement errors is given by

$$P(t) = E(\delta\bar{\rho}\delta\bar{\rho}^T) = S(t)E(\delta\bar{x}\delta\bar{x}^T)\ S^T(t)$$

where E is the expectation operator. The trace of the position covariance matrix can be used as a measure of system accuracy and is given by

$$\text{Tr } P(t) = \sum_{i=1}^{12} \sum_{j=1}^{12} S_{ij}^2 \, \widetilde{\delta x_j^2}$$

but the trace of the covariance matrix is also equal to

$$\text{Tr } P(t) = \widetilde{\delta\rho^2} = \widetilde{\delta\rho_x^2} + \widetilde{\delta\rho_y^2} + \widetilde{\delta\rho_z^2} \qquad (4.30)$$

and minimum errors in predicted range occur for minimum measurement error as would be expected. Straight-forward minimization of this quantity, however could lead to an imbalance in the system design, since if one error is large and dominates, little is gained by making all other errors small. Of equal importance is the fact that

$$\int_o^T W(t)dt$$

has a different form based on the flight paths being flown. For example, if both aircraft are turning, the integral is bounded for all uncertainties except that in angular velocity. If on the other hand both aircraft are in rectilinear flight, then each velocity error source causes an error in predicted position which grows linearly with time while the error in angular velocity causes a quadratic error growth. In the rectilinear case, equation (4.28) remains the same except that

$$\theta_1 = 0 \; ; \; \theta_2 = \psi_{10} - \psi_{20}$$

Let

$$V(t) = \int_o^t W(\sigma)d\sigma$$

so that for the rectilinear case one obtains V(t) =

$$t\begin{bmatrix} \frac{v_2}{v_{2L}}\cos\psi_o & \frac{-\dot{h}_2}{v_{2L}}\cos\psi_o & v_{2L}\sin\psi_o & \frac{v_{2L}t}{2}\sin\psi_o & \frac{-v_1}{v_{1L}} & \frac{\dot{h}_1}{v_{1L}} & v_{2L}\sin\psi_o & 0 \\ \frac{-v_2}{v_{2L}}\sin\psi_o & \frac{\dot{h}_2}{v_{2L}}\sin\psi_o & v_{2L}\cos\psi_o & \frac{-v_{2L}t}{2}\cos\psi_o & 0 & 0 & -v_{2L}\cos\psi_o & \frac{-v_{1L}t}{2} \\ 0 & -1 & 0 & 0 & 0 & 1 & 0 & 0 \end{bmatrix}$$

From (4.30),

$$\widetilde{\delta\rho^2} = \left(\frac{\rho_o}{\rho_L}\right)^2 \widetilde{\delta\rho_o^2} + \rho_L^2\widetilde{\delta\beta_o^2} + \left(\frac{\Delta h^2}{\rho_L^2}+1\right)\widetilde{\delta h_1^2} + \left(\frac{\Delta h}{\rho_L^2}+1\right)\widetilde{\delta h_2^2}$$

$$+ \left(\frac{v_2}{v_{2L}}t\right)^2 \widetilde{\delta v_2^2} + \left[\left(\frac{\dot{h}_2}{v_{2L}}\right)^2+1\right]t\,\widetilde{\delta\dot{h}_2^2} + (v_{2L}t)^2\,\widetilde{\delta\psi_{20}^2}$$

$$+ \left(\frac{v_{2L}}{2}t^2\right)^2 \widetilde{\delta\omega_2^2} + \left(\frac{v_1}{v_{1L}}t\right)^2 \widetilde{\delta v_1^2} + \left[\left(\frac{\dot{h}_1}{v_{1L}}\right)^2+1\right]t\widetilde{\delta\dot{h}_1^2}$$

$$+ (v_{2L}t)^2\,\widetilde{\delta\psi_{20}^2} + \left(\frac{v_{1L}t^2}{2}\right)^2 \widetilde{\delta\omega_1^2}$$

For purposes of simplicity, assume that

$$\rho_o = \rho_L + \varepsilon_1$$

$$\left[\left(\frac{\Delta h^2}{\rho_L^2}\right) + 1\right]^{1/2} = 1 + \varepsilon_2$$

$$v_2 = v_{2L} + \varepsilon_3$$

and

$$\left[\left(\frac{\dot{h}}{v_L}\right)^2 + 1\right]^{1/2} = 1 + \varepsilon_4$$

By retaining only second order terms, one obtains

$$\begin{aligned}\widetilde{\delta\rho^2} = {} & \widetilde{\delta\rho_o^2} + \rho_o^2\,\widetilde{\delta\beta_o^2} + \widetilde{\delta h_1^2} + \widetilde{\delta h_2^2} + t^2\,\widetilde{\delta v_2^2} + t^2\,\widetilde{\delta\dot{h}_2^2} \\ & + (v_2 t)^2\,\widetilde{\delta\psi_{20}^2} + \left(\frac{v_2 t^2}{2}\right)^2 \widetilde{\delta\omega_2^2} + t^2\,\widetilde{\delta v_1^2} + t^2\,\widetilde{\delta\dot{h}_1^2} \\ & + (v_2 t)^2\,\widetilde{\delta\psi_{10}^2} + \left(\frac{v_1 t^2}{2}\right)^2 \widetilde{\delta\omega_1^2} \end{aligned} \qquad (4.31)$$

Further simplification is possible if it is assumed that the measurement uncertainties for the parameters of each aircraft are the same, in which case (4.31) can be written as

$$\begin{aligned}\widetilde{\delta\rho^2} = {} & \widetilde{\delta\rho_o^2} + 2t^2\,\widetilde{\delta v^2} + 2t^2\,\widetilde{\delta\dot{h}^2} + 2(vt)^2\,\widetilde{\delta\psi^2} \\ & + 2\left(\frac{vt^2}{2}\right)^2 \widetilde{\delta\omega^2} + 2\widetilde{\delta h^2} \end{aligned} \qquad (4.32)$$

In (4.32), it is also assumed that

$$v_1 = v_2 = v_{max} = v$$

which in general yields a conservative result. As an example, assuming the following measurement uncertainties yields the errors in predicted position given in table 4.1 and the total uncertainty in position after 25 seconds is on the order of 2000 ft lateral and 225 ft vertical (1σ).

$\widetilde{\delta\rho_o} \approx$ 1000 ft.

$\widetilde{\delta v} \approx$ 20 to 50 f.p.s.

$\widetilde{\delta \dot{h}} \approx$ 5 f.p.s.

$\widetilde{\delta h} \approx$ 100 ft.

$\widetilde{\delta\psi} \approx$ 2 degrees

$\widetilde{\delta\omega} \approx$ 0.2 deg/sec.

$v \approx$ 250 knots

TABLE 4.1.- ERRORS IN PREDICTED RANGE

Measurement Uncertainty		Range Uncertainty (τ_W = 25 sec.)	
initial range	1000 ft.	1000 ft.	
speed	20-50 f.p.s.	705-1760 ft.	
alt. rate	5 f.p.s.	176 ft.	225 ft.
altitude	100 ft.	141 ft.	
heading	2 degrees	512 ft.	
turn rate	0.2 deg/sec.	648 ft.	

TOTAL UNCERTAINTY .....1480 - 2200 ft.

A graphical presentation of predicted range uncertainties as a function of information error and warning time is given in figure 4.5. These plots are based on equation (4.32) and help to quantify the results of this sensitivity analysis.

Model Errors

Model errors are caused by approximating aircraft motion with an equation set or predictor which does not represent reality. If for example, rectilinear theory is used when the aircraft are turning, an error in predicted relative position results. For this case, suppose that two aircraft are initially in parallel flight (see Figure 4.6). Linear theory will predict a future position with separation equal to the initial separation under these conditions. If however the aircraft are turning as indicated and will in fact collide at some time τ, then the error in the prediction caused by the use of the linear model is ρ_o. For the geometry illustrated by Figure 4.6, collision will occur at a time τ if ω, ρ_o, and v are such that the relation

$$\rho_o = \frac{2v}{\omega} (1 - \cos\omega\tau) \tag{4.33}$$

is satisfied.

Other model errors can occur if, for example, the curvilinear model is used and the aircraft turn rates are not constant. This error could be predicted by the methods of the previous section. Alternatively, these errors can be avoided by use of a level 1 control as described in Chapter 2 of this thesis.

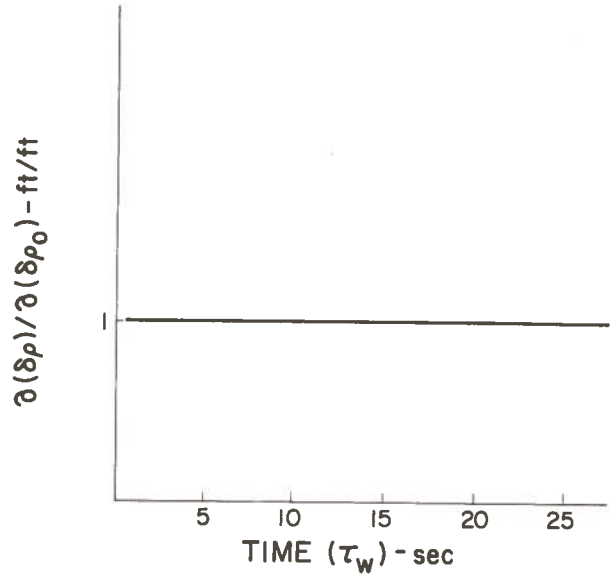

Figure 4.5a.- Predicted range uncertainty due to initial position uncertainty

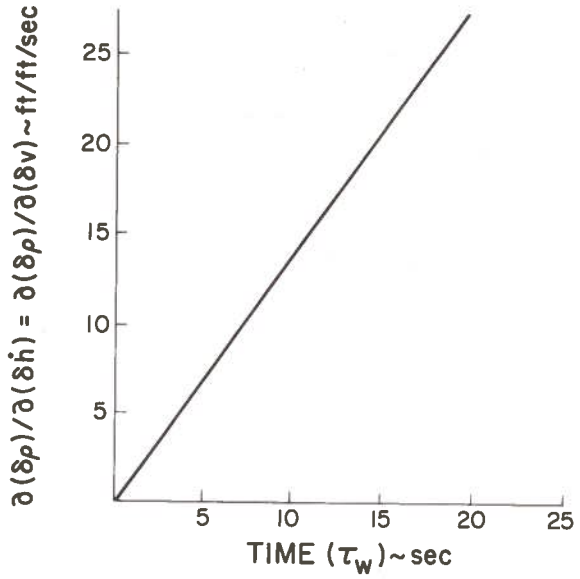

Figure 4.5b.- Predicted range uncertainty due to speed uncertainty (lateral & vertical)

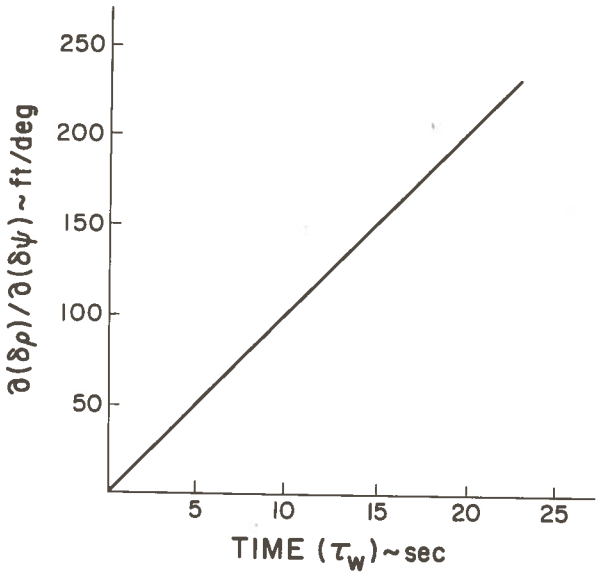

Figure 4.5c.- Predicted range uncertainty due to heading uncertainty

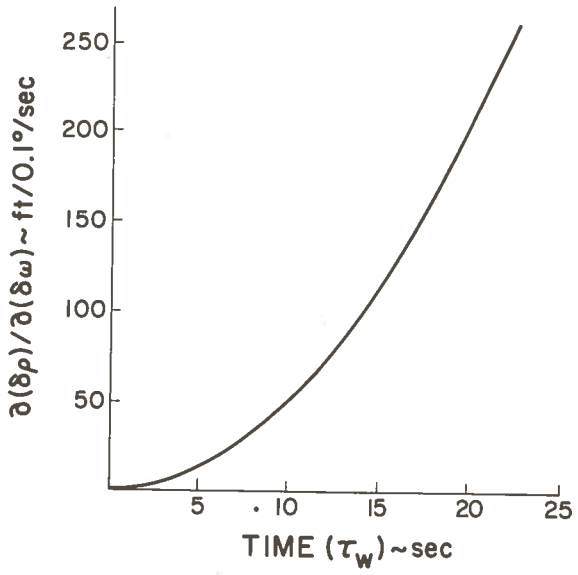

Figure 4.5d.- Predicted range uncertainty due to turn rate uncertainty

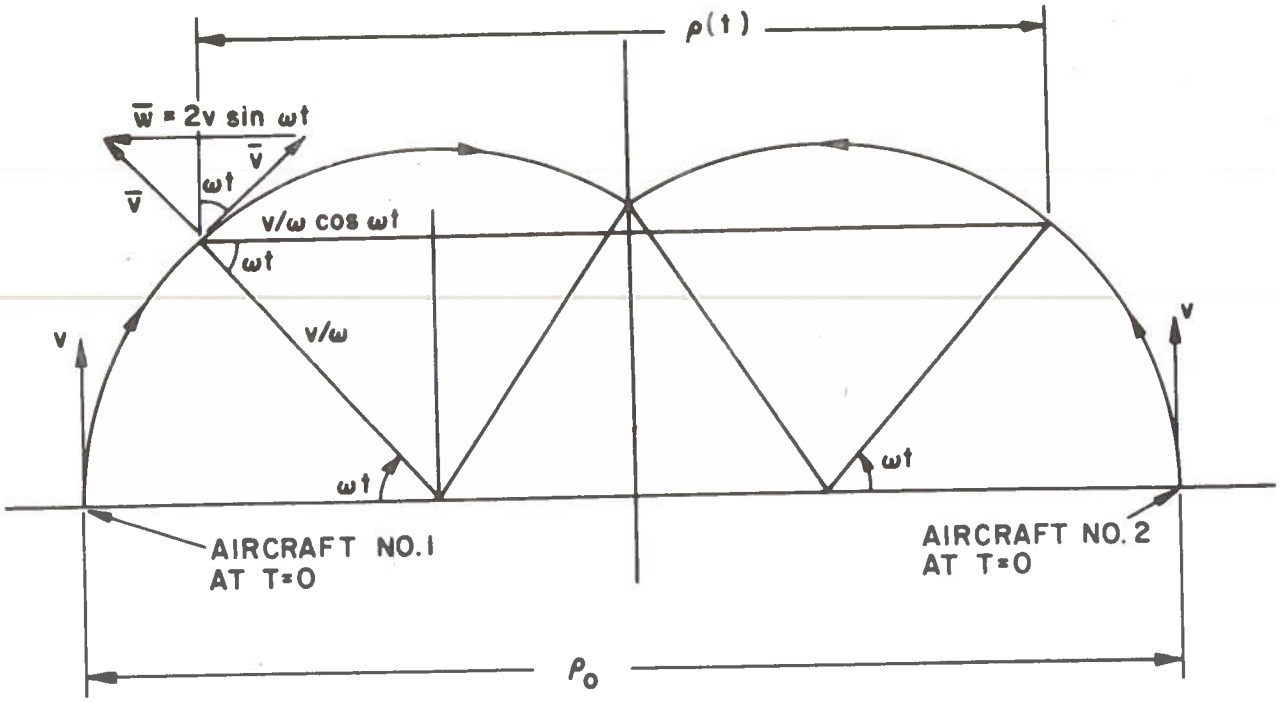

Figure 4.6.- Rectilinear/curvilinear model error

Finally, model errors can occur in the event that no model is used. In this case no prediction of position is made, so that a range alarm threshold which will provide protection against the head-on situation must be provided. This alarm threshold magnitude is a function of warning time τ_W and relative speed, i.e.

$$\varepsilon_L = w\tau_W \tag{4.34}$$

A plot of this relation is presented in Figure 4.7. A similar argument applies in the case where altitude information is unavailable. In this case, a vertical rather than a lateral range threshold must be used to compensate for this model error.

Based on these results, it is apparent that a study of system warning time must be made in order to establish the system threshold values.

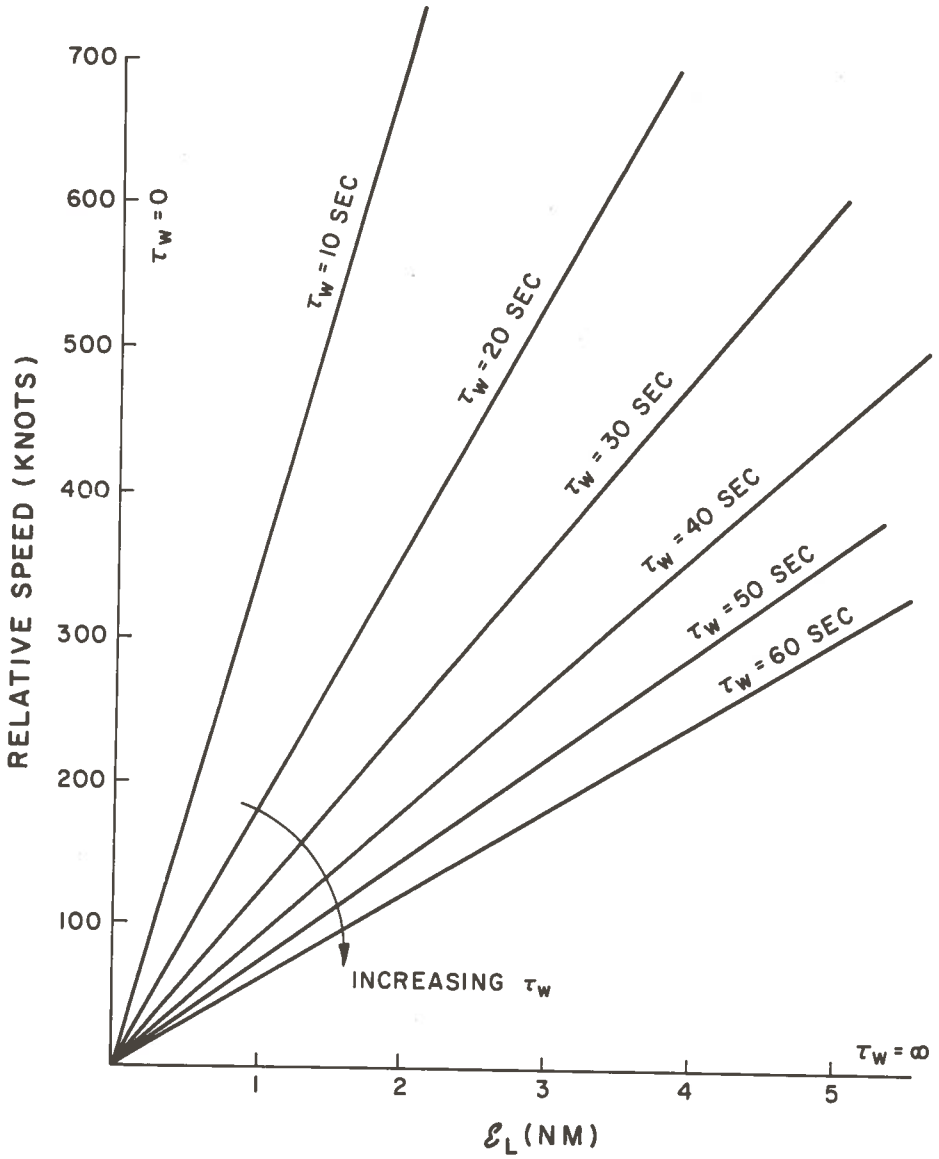

Figure 4.7.- Range threshold for head-on collisions

4.5 Escape Time and Avoidance Maneuvers

In the previous sections of this chapter, reference is frequently made to "time-to-collision" and "escape time." Both of these quantities are extremely important to a collision-avoidance system design since once it has been established that a

collision or a critical near-miss will occur, there must be sufficient time to successfully execute a maneuver to avoid the threat. The escape time must be smaller than the time-to-collision. Further, it is necessary for data to be collected and processed as well as for the pilot and aircraft to react. In general then, the warning time τ_W, can be stated as

$$\tau_W = T_e + T_P + T_R \geq \tau_c \tag{4.35}$$

where T_p is the time required for data collection and processing and T_R is the time for pilot and aircraft reaction. T_e is the time required to generate the necessary miss distance at the predicted time of closest approach. It is counted from the time that the aircraft reacts to the pilot's input until the new course of the aircraft is such that the threat is eliminated. To put it simply, enough warning time must be given in order to evaluate and avoid the threat. Before trying to evaluate T_e, T_R, and T_p, aircraft capability must first be determined. Once this is determined, it must then be considered what is most advantageous for the aircraft to do in light of the fact that it has a collision to avoid and a destination to reach. Based on this information, it can then be established that $T_e \cdot T_p$ is a function of data rate and processing time while T_R is a function of pilot and aircraft response. After establishing these parameters, a value of warning time τ_W can then be specified for use in prediction of range as well as for establishing the thresholds mentioned in previous sections.

Consider first what an aircraft is capable of doing in the way of maneuvers to avoid a collision. An aircraft may change speed; climb, dive, or level-off; turn, or roll-out; and combine various of these maneuvers. A detailed treatment of each of these maneuvers is presented as follows:

Lateral Speed Change

The difference in future position of an aircraft caused by a speed change is given by

$$|\Delta\bar{r}| = at^2/2$$

A plot of this relation is presented in Figure 4.8.

A value of a = 1/10g is chosen as representative of current aircraft capability. If both aircraft execute a speed change in a head-on situation, collision will still occur. Only the time of collision will be changed. In the overtaking situation, if the overtaking aircraft slows down and the other aircraft speeds up, the value of Δr given above will be doubled but collision can still occur depending on the initial velocity difference. For this reason as well as the small displacement achieved, a speed change is considered to be unsatisfactory for collision avoidance.

Vertical Maneuvers

For an aircraft in level flight at altitude h_0, the change in altitude due to a climb or dive is given by

$$\Delta h = h-h_o = \pm (\overset{oo}{h}\, t^2/2) \quad ; \quad 0 < t \leq T$$

$$\Delta h = \frac{\overset{oo}{h}T^2}{2} + \overset{o}{h}_{max}\,(t-T) \quad ; \quad t > T$$

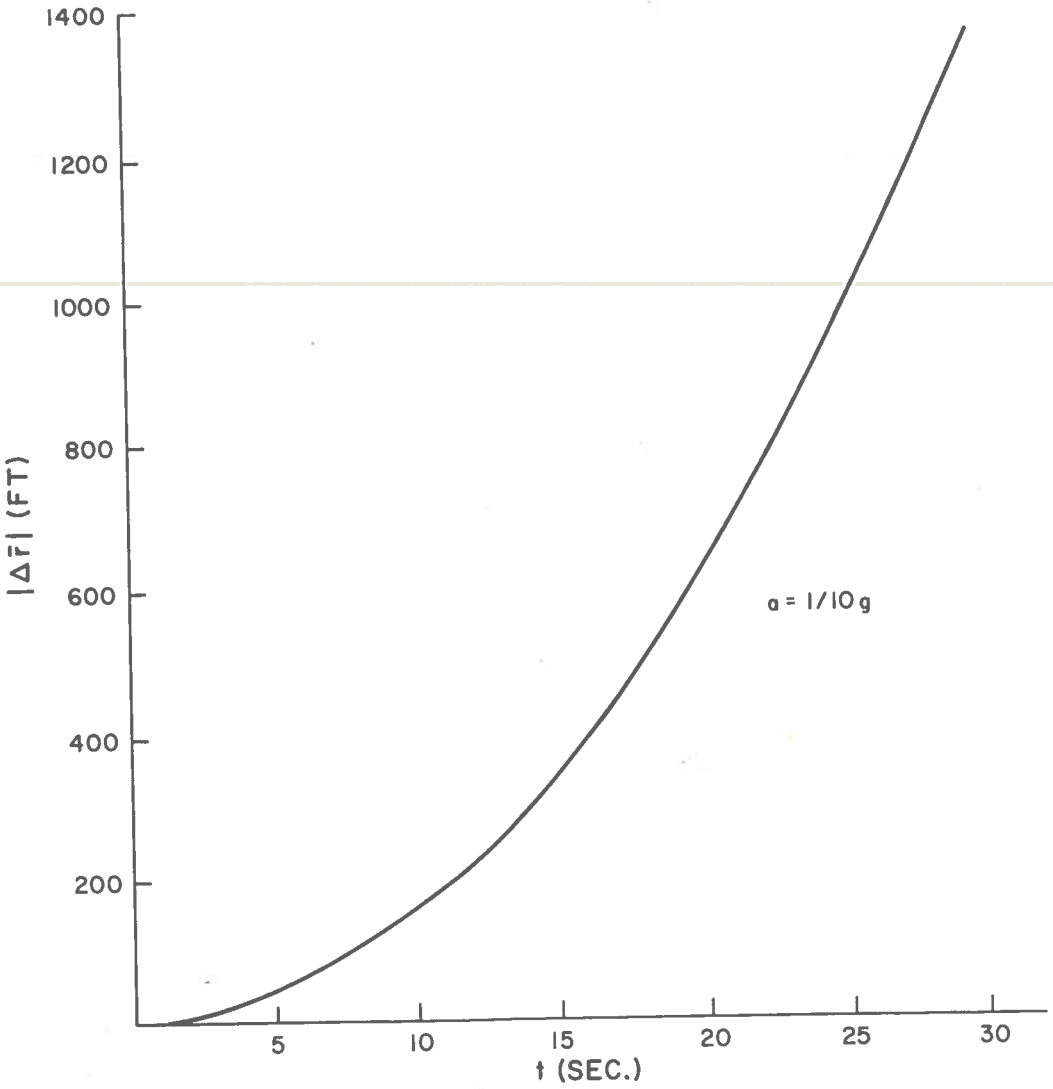

Figure 4.8.- Position displacement for speed maneuver

T is the time required to achieve maximum rate of climb or dive. A plot of these relations is presented as Figure 4.9, and from this figure, it is immediately noted that large changes in altitude can be achieved in a short period of time. This is a highly desirable feature and therefore this maneuver should be considered as a candidate maneuver for collision avoidance systems. Next, consider a lateral turn maneuver.

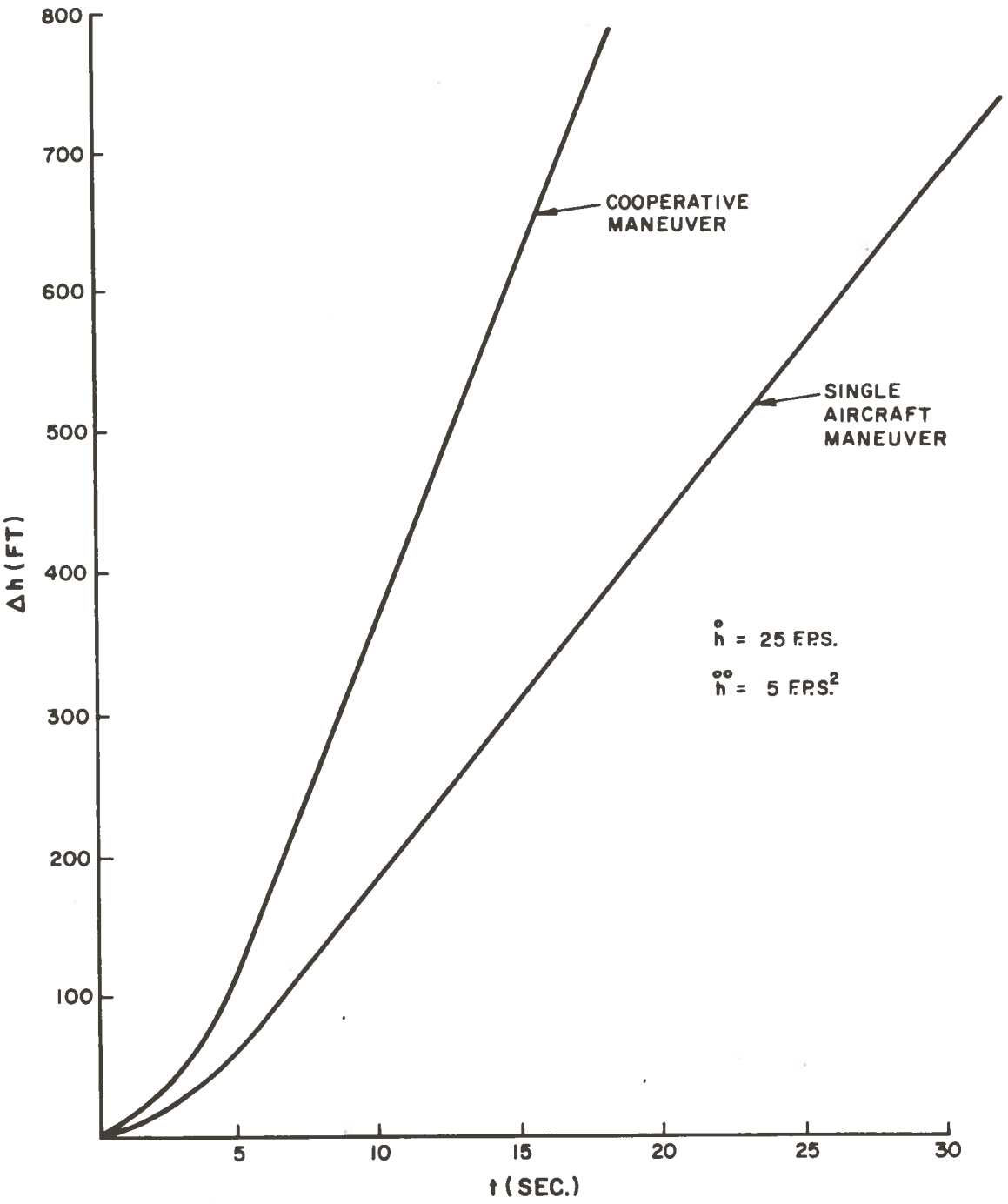

Figure 4.9.- Position displacement for altitude maneuver

Lateral Maneuvers

The lateral displacement achieved by a turning aircraft in a time t is given by $\Delta R_L = \frac{V}{\omega} (1 - \cos \omega t)$

A plot of ΔR_L is presented as Figure 4.10 and a number of speeds are considered for a standard turn rate. Similar to the climb-dive maneuver, the lateral turn maneuver also looks encouraging and should be considered as a candidate for collision avoidance.

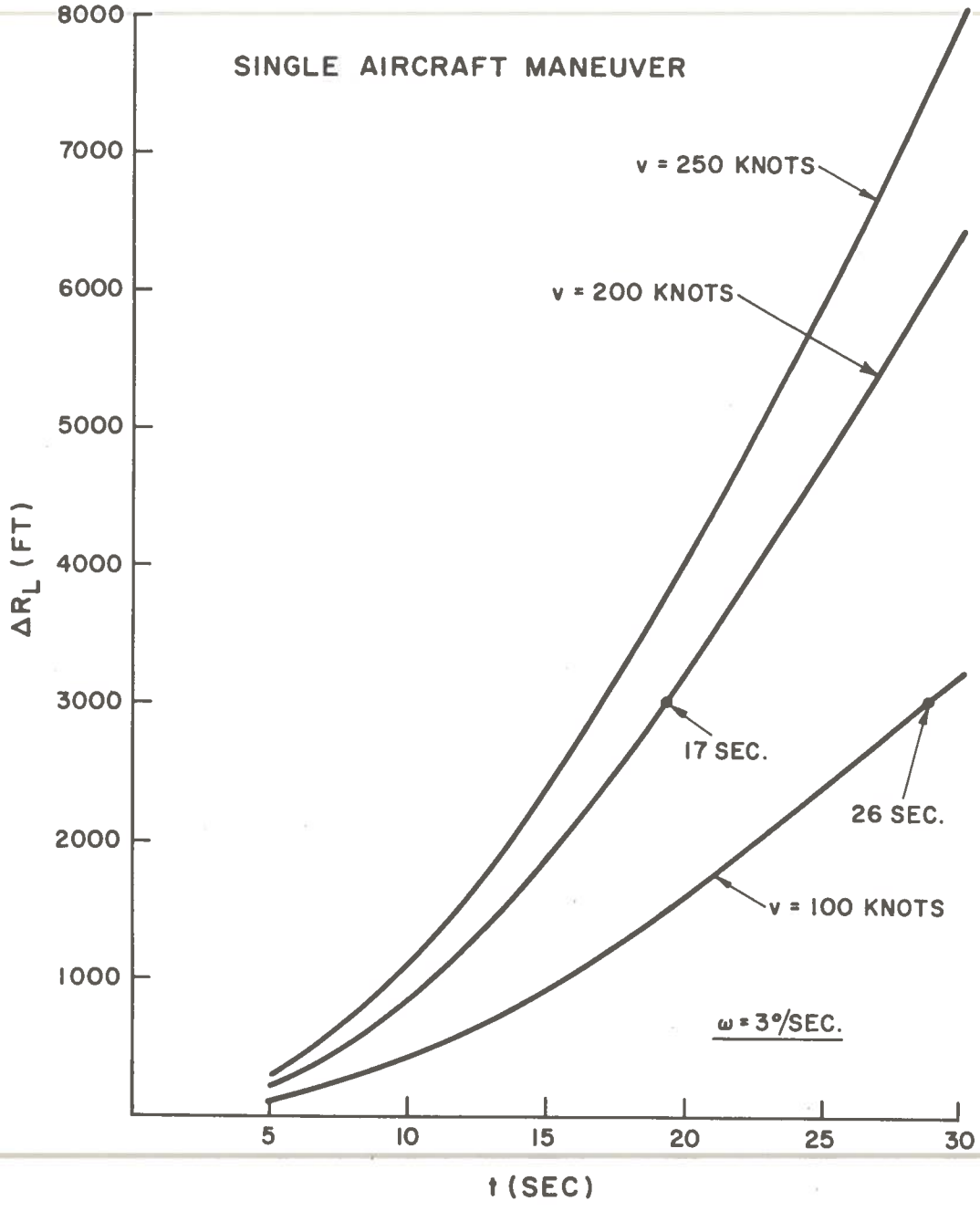

Figure 4.10.- Position displacement for lateral maneuver

Figures 4.9 and 4.10 show that relatively large displacements can be achieved in short periods of time using either vertical or lateral evasion maneuvers. Separations greater than 600 ft. vertical and 1000 ft. lateral can be achieved in about 15 sec. Allowing 5 sec. for reaction time and 5 sec. for processing time results in a system warning time on the order of 25 sec. A choice of system warning time on the order of 30 sec. appears to be completely adequate and is consistent with current design practice.

Based on the preceding analyses, system alarm thresholds can be estimated for a variety of anti-collision system design concepts. Calculation of these thresholds and numerical evaluation of these systems are presented in the following chapter.

CHAPTER 5

ANTI-COLLISION SYSTEM DESIGN AND EVALUATION

5.1 Introduction

System evaluation criteria have been defined in Chapter 2 and formulated in Chapter 3. Methods for computing system thresholds based on measurement and model error were presented in Chapter 4. In this chapter, a variety of system types in each of the anti-collision system categories defined in Chapter 2 will be evaluated by numerically computing both *conflict ratio* and *probability of missed critical alarm.*

Also of interest in system design is the alarm rate of the system or the system encounter frequency. This parameter is also discussed along with estimates of traffic factor and model constant.

In addition to the criteria for system evaluation and the system encounter frequency, a number of anti-collision system design options are possible. Among these are:

Self contained vs cooperative system design

Ground based vs airborne hardware

Single vs multiple intruder capability

Continuous vs intermittent control

Linear vs curvilinear threat evaluation

Vertical vs lateral evasion maneuvers

Each of these options is discussed in detail in this chapter and the design of a low conflict ratio anti-collision system is

presented. This design is based on the preceding work and includes the formulation of a collision avoidance algorithm and a display.

5.2 Anti-Collision System Evaluation

Evaluation of anti-collision systems has been reduced to the computation of the protection volumes for specific system concepts. Protection volumes for various system types are discussed below.

Range Only Systems

In this system, a range guard is used for pilot warning indication. The alarm threshold for this type of system in the lateral direction is given by

$$\varepsilon_L = w_{max}\ \tau_W$$

and in the vertical direction by

$$\varepsilon_V = 2\ \dot{h}_{max}\ \tau_W$$

Range/Altitude Systems

This system is similar to the range only system except that altitude discrimination is used. The lateral alarm threshold is the same as above but the vertical alarm threshold is the minimum separation standard. This value is taken to be

$$\varepsilon_V = \begin{cases} 500 \text{ ft.} & \text{(terminal area)} \\ 1000 \text{ ft.} & \text{(en-route)} \end{cases}$$

NOTE

It is assumed that the uncertainty in the altitude information is less than the minimum separation standard. If this is not the case, then the vertical alarm threshold must be at least as large as the altitude uncertainty.

Range/Altitude/Range-Rate

In this type of system, it is assumed that the standard TAU criterion (range/range-rate) is used to predict the time to closest approach and the miss-distance as illustrated in Chapter 4. Rectilinear theory is used for position prediction and the lateral threshold must be chosen to compensate for the potential error caused by turning aircraft. The dimensions of this threshold may be estimated by using equation (4.33), i.e.

$$\varepsilon_L = \frac{2v}{\omega} (1 - \cos \omega\tau_W)$$

The vertical threshold is the same as in the Range/Altitude System.

Certain systems of this type (McDonnell Douglas EROS) use a range guard in addition to the miss-distance prediction and give an alarm if this threshold is violated. In this case, the dimension of the lateral threshold is equal to this range guard. Typically, the value of this threshold is 1 nm so that in this case ε_V = 1 nm.

Full State System

This system requires a complete estimate of the relative states of the potentially conflicting vehicles. In addition it is assumed that curvilinear theory is used for threat detection and that the 3 control levels structured in Chapter 2 are mechanized. Under these assumptions, the vertical and lateral thresholds are functions of measurement error only and are given by

$$\varepsilon_L \approx \left\{ \widetilde{\delta\rho_o^2} + 2\tau_W^2 \widetilde{\delta v^2} + 2(v\tau_W)^2 \widetilde{\delta\psi^2} + 2\left(\frac{v\tau_W^2}{2}\right) \widetilde{\delta\omega^2} \right\}^{1/2}$$

and

$$\varepsilon_v \approx \left\{ \widetilde{2\delta h^2} + 2\tau_W^2 \widetilde{\delta \dot{h}^2} \right\}^{1/2}$$

(see equation (4.32)).

Based on the above equations for the threshold computation, *conflict ratio* and *probability of missed critical alarm* can be computed for both the terminal area and the en-route environments.

The following assumptions for system warning time, relative speed, critical miss distance, altitude rate, and turn rate are made for purposes of numerical evaluation.

Terminal Area Data

τ_W = 30 sec ; w_{max} = 480 knots ; v_{max} = 240 knots

m_c = 200 ft ; ω = 3°/sec. ; $\dot{h}_{max}$ = 25 f.p.s.

En-Route Data

τ_W = 30 sec. ; w_{max} = 1200 knots; v_{max} = 600 knots

$$m_c = \begin{cases} \text{1000 ft. lateral} \\ \\ \text{500 ft. vertical} \end{cases} ; \omega = 3^{o}/\text{sec} ; \dot{h}_{max} = 25 \text{ f.p.s.}$$

Substitution of these data into the system threshold equations as well as the conflict ratio (3.27) and probability of missed critical alarm (3.29) equations produces the data shown in tables 5.1 and 5.2. Measurement errors consistent with those used in Chapter 4 are used in this evaluation.

TABLE 5.1.- TERMINAL AREA SYSTEM EVALUATION

SYSTEM TYPE	ε_L(NM)	ε_V(ft)	CR	Lateral P_M*	Vertical P_M*
Range only	4	1500	900	$0.03\text{x}10^{-10}$	$1.14\text{x}10^{-6}$
Range/Alt	4	500	300	$0.03\text{x}10^{-10}$	$4.5\text{x}10^{-5}$
Range/Alt/Range-Rate	2-1/2	500	187	$0.03\text{x}10^{-10}$	$4.5\text{x}10^{-5}$
Range/Alt/Range-Rate and Range Guard	1	500	75	$6.4\text{x}10^{-10}$	$4.5\text{x}10^{-5}$
Full State	1/3	500	25	$1.75\text{x}10^{-8}$	$4.5\text{x}10^{-5}$

*P_M for 5 data cycles

TABLE 5.2.- EN-ROUTE SYSTEM EVALUATION

SYSTEM TYPE	ε_L(NM)	ε_V(ft)	CR	Lateral P_M	Vertical P_M
Range only	10	1500	90	$<1x10^{-10}$	$<1x10^{-10}$
Range/Alt	10	1000	60	$<1x10^{-10}$	$.32x10^{-8}$
Range/Alt/Range-Rate	6-2/3	1000	40	$<1x10^{-10}$	$.32x10^{-8}$
Range/Alt/Range-Rate and Range Guard	1	1000	6	$<1x10^{-10}$	$.32x10^{-8}$
Full State	1/2	1000	3	$4.5x10^{-5}$	$.32x10^{-8}$

The result of this evaluation is that all systems have a probability of missed critical alarm less than 5×10^{-5} while conflict ratios range from 900 to 25 in the terminal area and from 90 to 3 in the en-route environment. This includes only alarms which require positive evasion. For the full state system, the negative alarm conflict ratio is 560 in the terminal area and 60 in the en-route environment. These alarms however do not require positive action on the part of the pilot but are simply alerts not to maneuver in a specific direction.

Based on the above evaluation of system types, approximate conflict ratio ranges for the basic anti-collision system categories can be assigned.

	Terminal	En-Route
PWI	1000 < CR < 200	100 < CR < 50
CDS	200 < CR < 100	50 < CR < 10
CAS	100 < CR < 1	10 < CR < 1

Also of interest in anti-collision system design is the system alarm or encounter frequency. This is discussed in the following section. A graph for the simple computation of conflict ratio is presented in Figure 5.1.

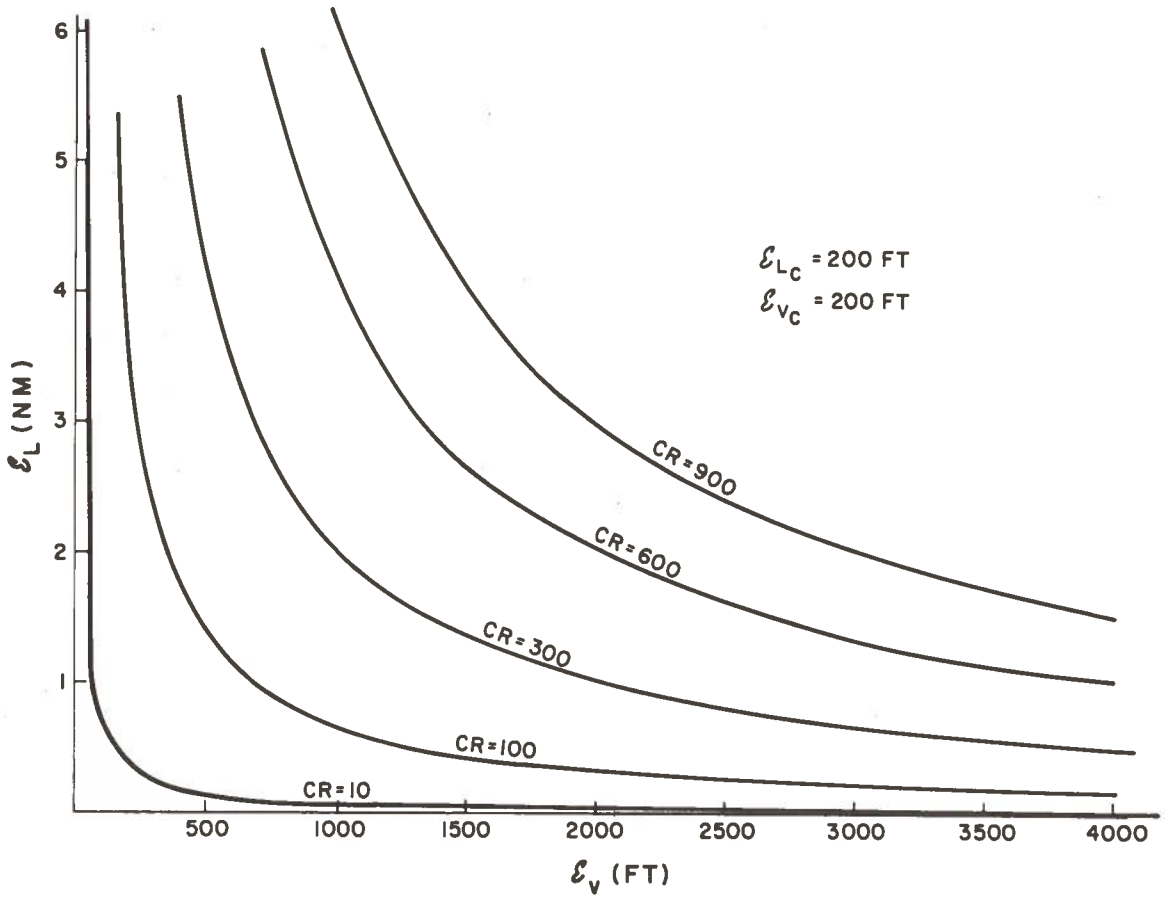

Figure 5.1.- Conflict ratio as a function of protection volume

Combination of Figure 5.1 and tables 5.1 and 5.2 as well as equations (3.27) and (3.29) provides the necessary information for performing tradeoff studies of *conflict ratio* and *probability of missed critical alarm* as a function of system thresholds. This type of study is essential to the system design process.

5.3 System Encounter Frequency

In equation (3.25), the system encounter frequency is given as

$$\mu_s = K_\mu F(\varepsilon_L \varepsilon_V)_s$$

Based on this equation, both the model constant K_μ and the traffic factor F are required for evaluation of μ_s.

Traffic factor data is available in the literature (15) and is summarized for 10 major terminals in table 5.3. These data are based on 1968 information. Extrapolation of these data is possible using traffic forecasts from the Alexander report(36) which are presented as table 5.4.

NOTE

In any extrapolation, traffic factor is proportional to the square of the number of annual operations.

Model constant K_μ is summarized in table 5.5(a) for a variety of traffic models. Included in this summary is the basic model constant for the gas model, the Arcon(43) models and the

TABLE 5.3.- TRAFFIC FACTOR DATA (1968)

Air Terminal	Traffic Factor* $x10^{-12}$
NY	0.73
LAX	0.72
CHI	0.38
SFO	0.35
MIA	0.28
DAL	0.15
DCA	0.13
ATL	0.12
DEN	0.10
BOS	0.08

*average values

TABLE 5.4.- TRAFFIC PREDICTIONS

User	Annual Operations $x10^6$		
	1968	1980	1995
Air Carrier	11	21	31
General Aviation	84	167	448
Military	33	34	40
Total	128	222	519

hub model developed in this thesis. Model constants adjusted to account for the reduction in incidents resulting from "see-and-be-seen" incident avoidance is also presented. Other models

based on simulation results and empirical data are also presented. These model constants account for all types of incidents. Estimates of the number of incidents by type can be obtained by using the factors presented in table 5.5b.

TABLE 5.5a.- MODEL CONSTANTS

Model Type	K_μ* (Basic)	K_μ (adjusted for see and be seen)
Gas Model	4.22×10^{-12}	1.32×10^{-12}
Arcon Model		
(square grid)	3.32×10^{-12}	1.04×10^{-12}
(triangular grid)	3.82×10^{-12}	1.20×10^{-12}
Hub Model		
Total Conflicts	$.539 \times 10^{-12}$	$.168 \times 10^{-12}$
In-Lane Conflicts	$.307 \times 10^{-12}$	$.096 \times 10^{-12}$
Cross Lane Conflicts	$.232 \times 10^{-12}$	$.073 \times 10^{-12}$
†ATL Simulation	0.165×10^{-12}	$.165 \times 10^{-12}$
†Alexander Report	0.143×10^{-12}	$.143 \times 10^{-12}$

*Units: encounters/min/$(nm)^2$/$(\text{annual operations})^2$
†Empirical Data

TABLE 5.5b.- ENCOUNTER TYPES*

Type	Percentage	Type	Percentage
AC/AC	1.1%	ML/ML	9.9%
AC/GA	22%	IFR/VFR	64%
AC/ML	6.2%	VFR/VFR	33%
GA/GA	34.6%	IFR/IFR	3%
GA/ML	26.4%		

*Based on 1968 statistics

Using the information from table 5.5, it is interesting to compute the system encounter frequency and to compare this to the work of Britt and Schreader(19). This comparison is presented as table 5.6. The traffic factor for Atlanta has been increased by a factor of nine to account for the fact that the data used in (19) was taken during peak periods. This corresponds to an increase in traffic density on the order of three.

Having illustrated the methods for computing encounter frequency and having completed the numerical evaluation of various systems, it remains to discuss a variety of system design options and then to discuss the design of a low conflict ratio anti-collision system.

TABLE 5.6.- COMPARISON OF ALARM RATE

Detection Criterion	Simulation Results	Hub Model	Gas Model	Alexander Report
Range	0.17-0.22	0.18	4.5	0.15
TAU/Alt.	0.052	0.06	1.5	0.052
TAU/Miss Dist.	0.036-0.044	0.038	0.95	0.032
Full State	None	0.005	0.125	0.004

5.4 System Design Options

A variety of system design options are discussed in this section.

Self-Contained vs Cooperative System Design

A number of reasons for choosing a cooperative system design exist. The first of these is that a larger miss distance can be achieved by cooperative maneuvers. The second is that unless systems cooperate or communicate, avoidance maneuvers could be chosen which cancel. The third reason is that discrimination between a safe passage and a collision is difficult using self-contained systems as is indicated by Figures 5.2 and 5.3. In these figures it is seen that measurement accuracy of the rate of change of the relative bearing on the order of 0.013 deg/sec. or of range on the order of inches in miles is required for adequate discrimination.

Ground-Based vs Airborne Hardware

For this design option consider that it is desired to minimize airborne interference with ground control directives. To accomplish this objective, low conflict ratio is required for the airborne system. This implies small alarm thresholds and accurate measurements. Use of data from ground tracking could be helpful in this respect. Alternatively, an airborne display as well as information readily available from cockpit instrumentation is required for relative position prediction. This indicates that a mix of ground-based and airborne instrumentation is needed at least for terminal area operation.

Single vs Multiple Intruder Capability

Based on the Atlanta simulation(19), it was found that 40 percent of the alarms for a range threshold of 4 nm involved

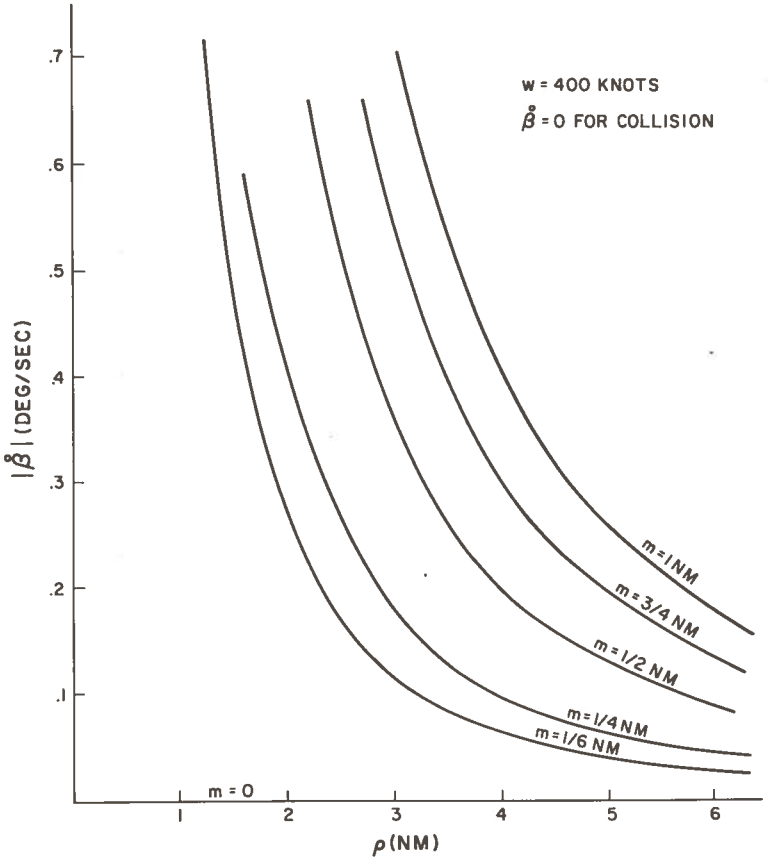

Figure 5.2.- LOS collision criterion sensitivity

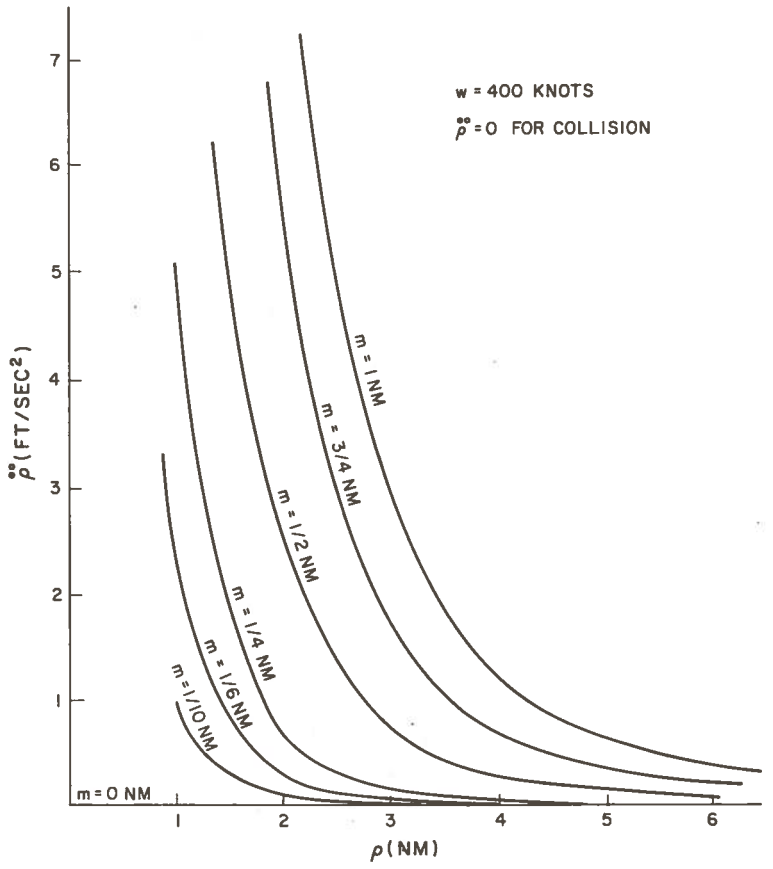

Figure 5.3.- Range acceleration criterion sensitivity

more than one aircraft. For this reason, the capability of simultaneous processing of intruders is recommended. Further, based on the results of Chapter 3, a simultaneous multiple critical threat had a probability of occurence of 1×10^{-6} per approach in the N.Y. terminal during 1968. For this reason, the ability to avoid simultaneous multiple threats is also recommended.

Continuous vs Intermittent Control

In reference (34), a theory of *intermittent positive control* (IPC) is described and defined as follows. "The concept of intermittent positive control is to issue commands to normally uncontrolled aircraft only when it is necessary to avoid a hazardous mid-air circumstance . . ."

With regard to resolving the question of whether intermittent control or continuous ground control should be used, it is conceivable that traffic could become so dense that the frequency of intermittent control commands and the resulting time under intermittent control would begin to approach continuous control. The problem then of estimating the percent of time that an aircraft would be under control as a function of density must be considered in order to determine the feasibility of the intermittent control concept.

To analyze this feasibility question, it is appropriate to concentrate on the terminal area because of the high densities involved. Further, even though aircraft are under ground control in this flight regime, 60 percent of the hazardous mid air incidents reported during 1968 (15) occurred in the terminal area.

If these statistics are used and feasibility is established, it is reasonable to assume that en-route feasibility of the concept will also apply since fewer incidents and less workload will be placed on the system en-route.

Based on the hub model and the assumption that 30 seconds is required to resolve an encounter, Figure 5.4 was constructed to indicate the percent of time in an encounter status in the terminal area.

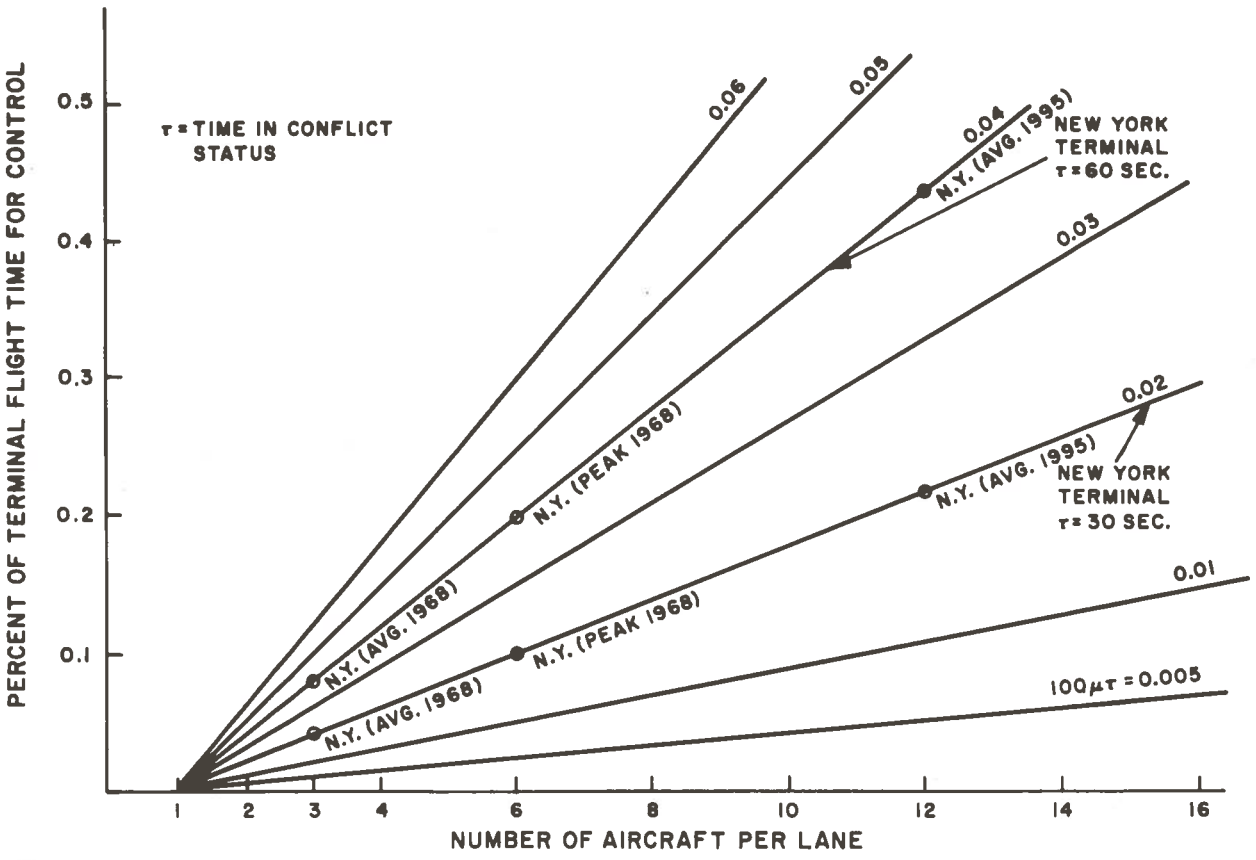

Figure 5.4.- Percent of terminal flight time for hazard avoidance

Figure 5.4 shows that the percent of terminal flight time required for collision avoidance control is small (less than 1 percent) even for large increases in density. This result is reasonable when it is considered that in 1968, a total of 719 hazardous encounters occurred in the United States as compared to 128×10^6 terminal operations. Further, it indicates that interference with ground control would be rare providing that a system capable of determining only critical incidents were designed. If however, a system has a high conflict ratio, interference with ground control would be more severe. Also of interest is the result that if one aircraft experienced one encounter during an approach, 2.5 percent of his flight time would be required to resolve the threat under the assumption of a 20 min. flight and a 30 sec. resolution time. Finally, it must be emphasized that the control times involved are estimated on the basis of requiring positive control action. Negative command encounter status can be estimated on the basis of the negative conflict ratio and is found to be on the order of 4 percent for 1995 in New York.

Linear vs Curvilinear Threat Evaluation

This design option has been previously discussed in Chapter 4 and it suffices to state that if a low conflict ratio system is desired, curvilinear theory should be used.

Vertical vs Lateral Evasion Maneuvers

Both vertical and lateral evasion capability are recommended for the design of a collision avoidance system. Although

vertical evasion is preferable because aircraft heading is unaltered, a vertical maneuver may not always be possible. This situation can result from a physical obstacle such as a mountain or from another aircraft which presents a potential threat. Having discussed the above design options, the design of a low conflict ratio anti-collision system is presented.

5.5 Low Conflict Ratio Anti-Collision System Design

A collision avoidance system is one which *detects* the presence of other aircraft, *evaluates* a collision threat, *indicates* the proper evasive maneuver, and *confirms* that proper evasive action has been taken. These systems may be self-contained, in which case the system is complete within itself, or cooperative, i.e. complementary equipments which exchange information are required in the different aircraft and/or on the ground.

In Section 5.4, it was shown that self-contained systems are not feasible based upon measurement requirements and state-of-the-art capability. Cooperative systems therefore become necessary and imply the need for a communications subsystem in addition to a measurement subsystem, a data collection subsystem, a data processing subsystem, and a command and display subsystem. A system block diagram of the essential components of a collision avoidance system is presented in Figure 5.5. No comment as to location of these subsystems is made however, since a full airborne concept would require all aircraft to have each subsystem

while a full ground concept would require only a communications and display subsystem on-board each aircraft. The relative navigation, data collection, data processing, and the command subsystems could be located on the ground.

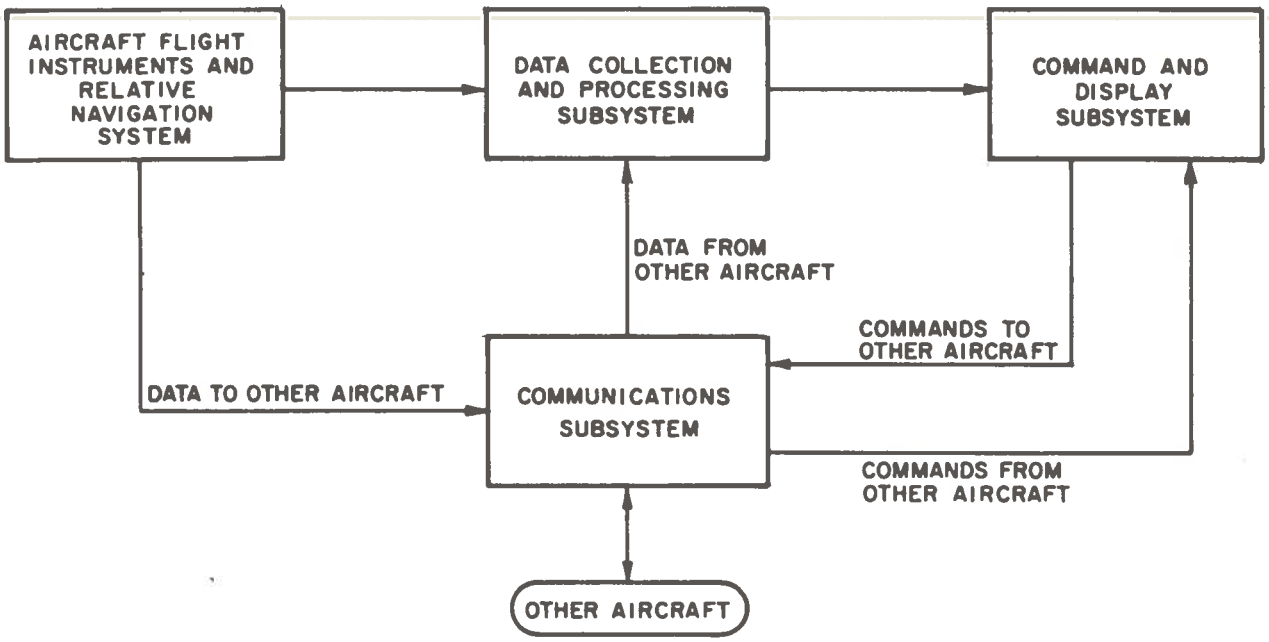

Figure 5.5.- Collision avoidance system block diagram

The object of this section is to establish the design requirements for detection, evaluation, and avoidance of a threat as well as to establish certain hardware requirements such as computer sizing, sensor accuracies, and data frequency. System software is also discussed from the point of view of algorithm formulation, position prediction, threat evaluation, aircraft monitoring, and positive and negative command computation. Features of this system are:

Full measurement of relative state

Curvilinear threat evaluation

3-level intermittent control

Multiple intruder capability

Vertical and lateral evasion

Variable alarm thresholds

Directional display

The discussion of the design of this system begins with an examination of the system functions.

Data Collection and Intruder Detection

The data set which must be collected from each aircraft was also discussed in the preceding chapter but the preprocessing of this data was not discussed. Preprocessing of data consists of the determination of the relative range $\bar{\rho}_{ij}(0)$. Differentiation of heading and altitude to obtain turn-rate and altitude-rate is also required. This can be accomplished by numerical differentiation. The test for determining if $\bar{\rho}_{ij}$ is in the control region is performed by comparing the lateral range with the radius of the control region and the vertical range with the half altitude of the control region. If the intruder aircraft is not in the control region, the data set is rejected. If it is in the control region, a prediction of the range vector at time $t = \tau_W$ is made.

The shape of the control region is assumed to be cylindrical. In the case of ground control, the control region is assumed to be between 30 and 60 nm in radius and from 0 to 10,000 ft.

in altitude. This is totally arbitrary and the dimensions can be easily changed particularly in the vertical direction. These values were chosen because they coincide with the present definition of terminal area. The control region about an aircraft is constructed by considering maximum relative speed and warning time. In the terminal area for example, the maximum relative speed is 480 knots lateral under 10,000 ft. so that a radius of 4 nm lateral about each aircraft must be controlled. Vertically, the maximum rate of climb or dive is assumed to be 25 f.p.s. so that a vertical distance of ±1250 ft. about each aircraft must also be controlled. A 25 sec. warning time is assumed for these computations.

A monitor region must be defined larger than the control region in order that an aircraft can be detected when it enters the control region. Allowing say 10 sec. for monitoring yields an aircraft monitor region which has a 5 nm radius and a height of ±1750 ft. in the terminal area. Figure 5.6 is presented to illustrate the choice of these thresholds as a function of relative speed.

Also to be considered is the possibility of changing the safety region defined by ε_L and ε_V. In the terminal area these values could be set small in order to minimize system interference with ground control. In the cruise environment however, these values could be set in accordance with existing separation standards.

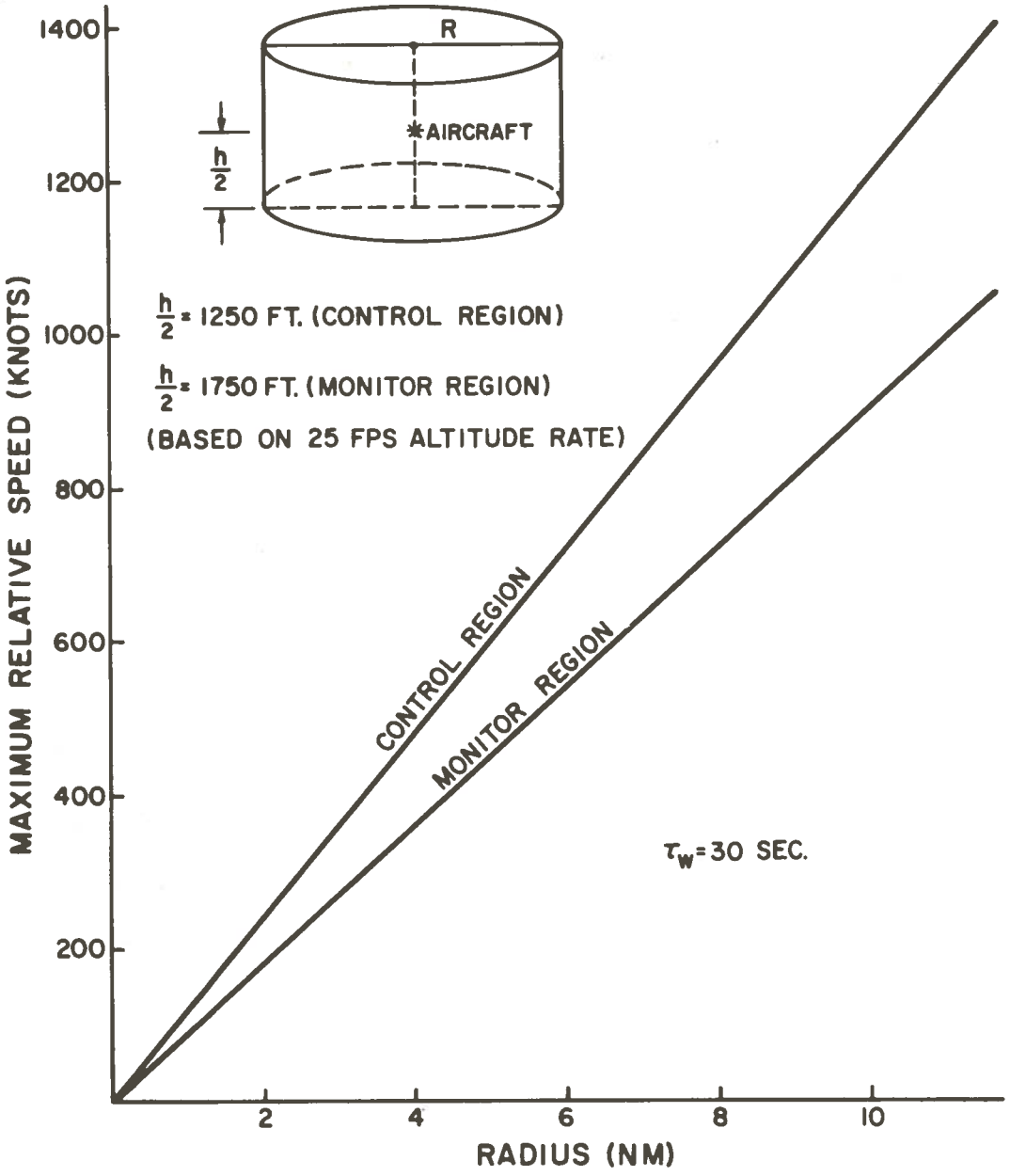

Figure 5.6.- Monitor and control region dimensions

Threat Detection and Avoidance

In Chapter 4, a system warning time of 30 sec. was established for terminal area collision avoidance under the assumption of current flight constraints. This provides sufficient time for detection, evaluation, and avoidance of an actual threat.

An actual threat is defined to exist when both aircraft are on flight paths which will cause a violation of the separation criteria if no maneuvers are made to alter the current state. A potential threat is defined to exist when both aircraft are on flight paths which do not constitute an actual threat but, because of geometry and maneuverability, are capable of causing an actual threat if one or both aircraft make an improper maneuver.

In designing collision avoidance systems, protection from both actual and potential threats must be provided, since ignoring potential threats can result in the creation of an actual threat with insufficient time for avoidance.

The protection against an actual threat consists of both prevention by means of negative commands and resolution of existing conflicts by positive commands. Negative commands are used to prevent potential threats from becoming actual threats. This is accomplished by issuing commands to prohibit the dangerous maneuvers.

In Chapter 4, it was shown that if a proper range threshold (4 nm in the terminal area) is chosen based upon the maximum aircraft speed (250 knots in the terminal area) and on the system warning time (30 sec. in the terminal area) that actual threat detection can be accomplished by a range prediction technique based on equations (4.19) through (4.22). This assumes that sufficient data is available for this prediction. It is emphasized that a monitoring function for collision avoidance is also critical, since avoidance of an actual threat can create a new

potential threat which must be controlled in order to prevent the creation of a new actual threat.

It now remains to discuss methods for determination of potential threats. A potential threat is a situation which under certain maneuver combinations could result in an actual threat. Examination of equations (4.19) through (4.22) reveals that a large number of future positions are possible for both aircraft if all combinations and values of turn rate and climb-dive rate are allowed. Prediction of potential threats could be quite tedious and time consuming. If however, one adopts the philosophy that various degrees of control are required to eliminate collisions, this problem can be simplified considerably. For example, if maneuvers are limited to standard maneuvers within a control region then the calculations for potential threat evaluation are very straight-forward.

In Appendix C, actual and potential threat detection and the associated positive and negative command computations are discussed in detail. In order to permit a simple computation of potential threats, the control structure defined in Chapter 2 will be used. This structure is as follows:

Level 1- Limit aircraft to their existing state or to standard maneuvers to change state

Level 2- Limit maneuvers by prohibiting those which are dangerous

Level 3- Command definite maneuvers for avoidance of an actual threat

A functional block diagram of this philosophy of collision avoidance is presented in Figure 5.7 and the logic for conflict detection and resolution in Figure 5.8.

Next, consider the problem of designing a display for the above system.

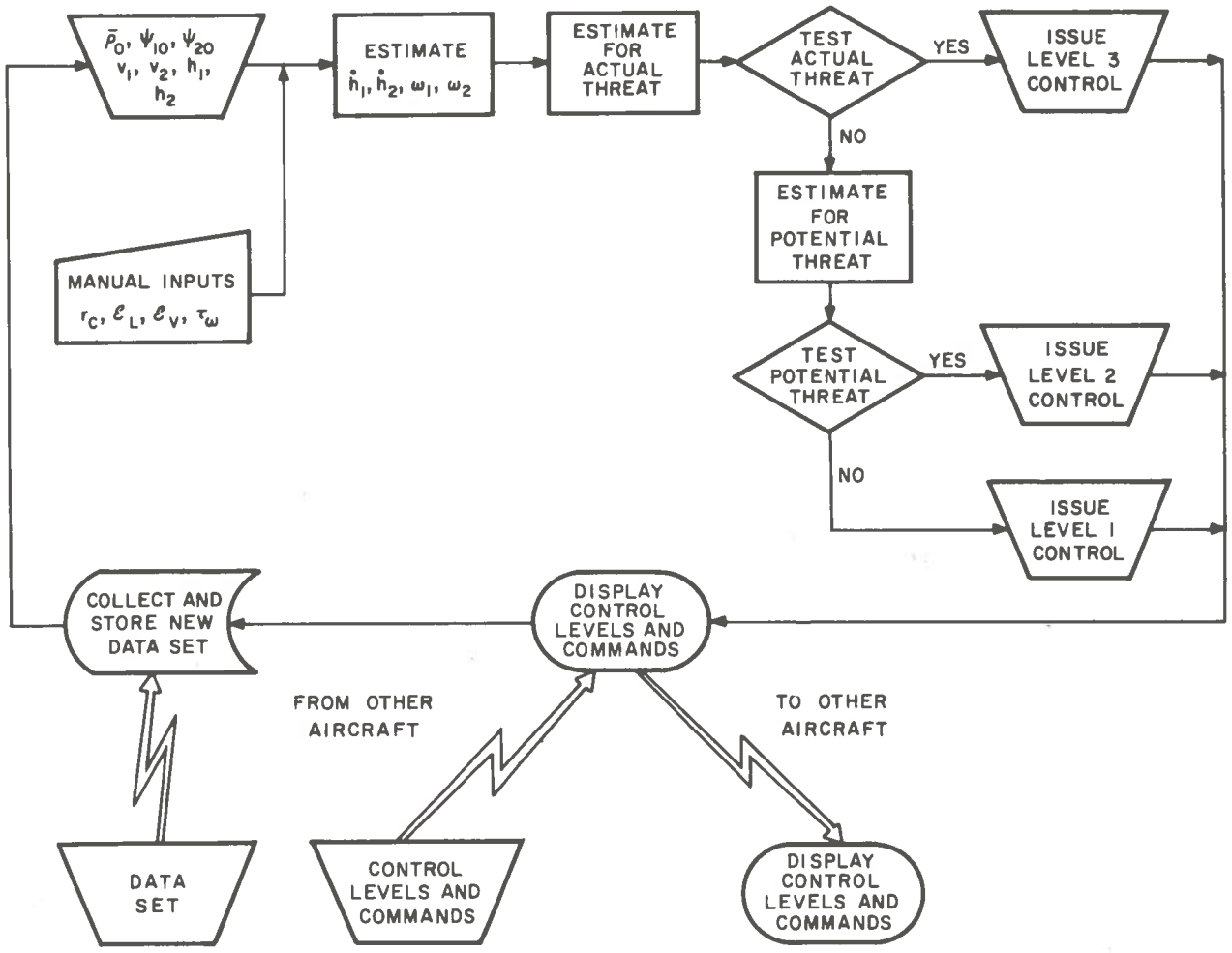

Figure 5.7.- Collision avoidance system functional flow

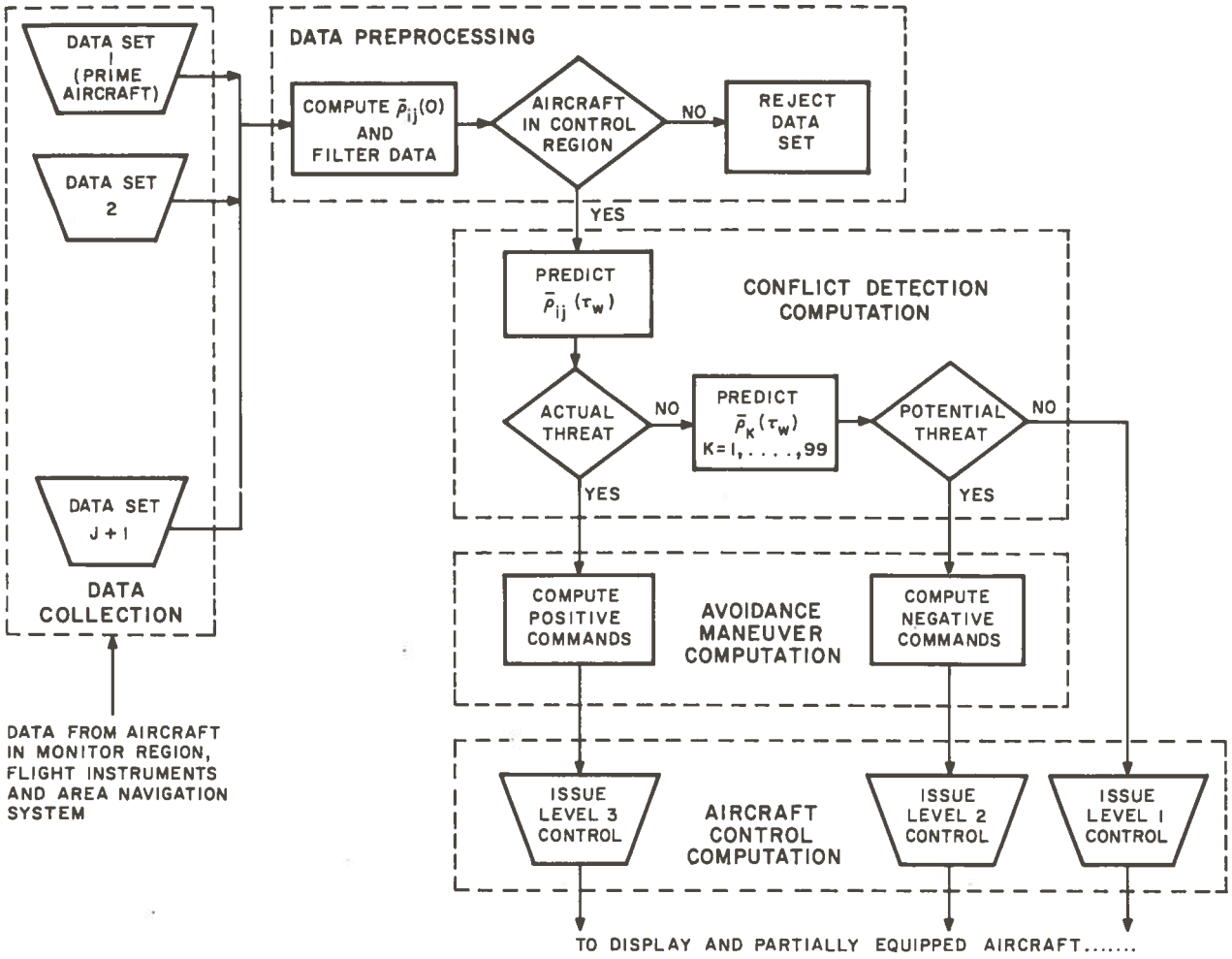

Figure 5.8.- Collision avoidance algorithm design

Display Design

Before attempting to design a display, consider the types of information which must be displayed. Basically, the various control levels must be displayed along with associated commands. For Level 1 control, no specific commands need be displayed. For Level 2 control, negative commands must be displayed. These negative commands consist of no right turn, no left turn, no climb, no dive or a combination such as no left turn and dive, etc. For Level 3 control, positive commands such as turn right

or left, or climb, or dive along with possible combinations must be displayed. One method of displaying these commands and controls is illustrated in Figure 5.9. This display is based upon the basic display of the McDonnell-Douglas EROS System and automobile traffic control concepts.

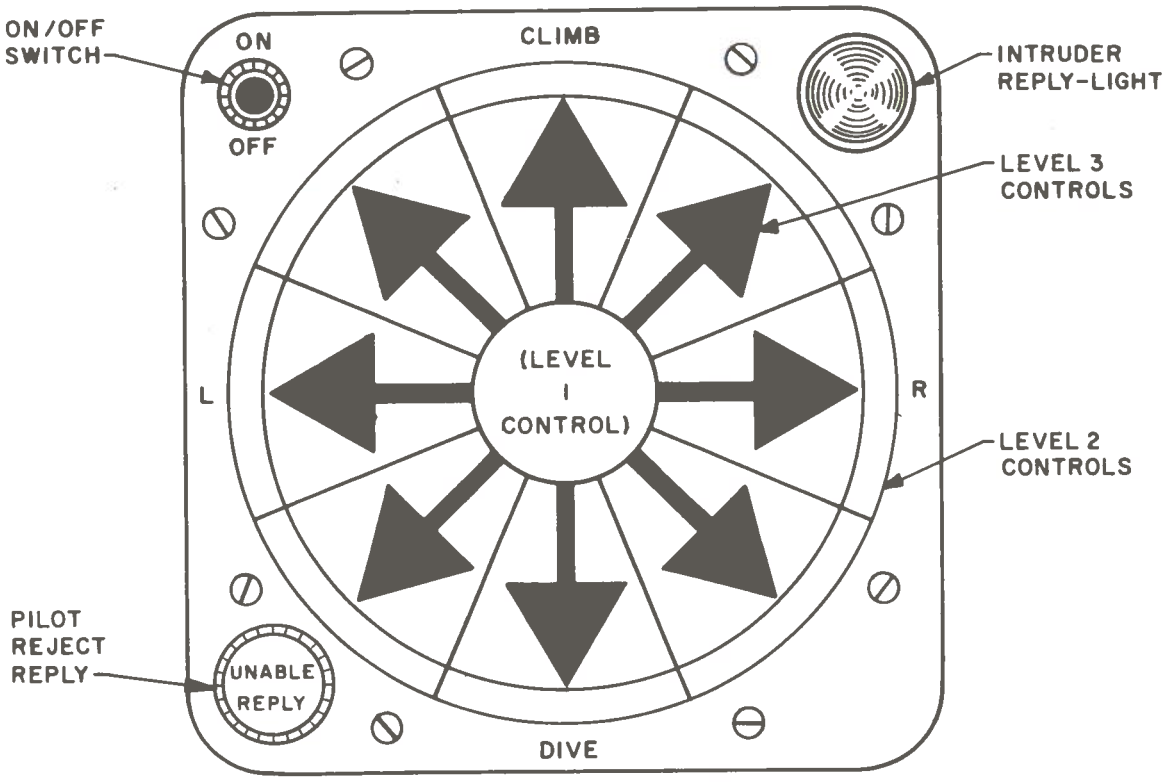

Figure 5.9.- Collision avoidance display

The display is separated into three basic regions. The inner region is used to indicate a Level 1 control condition. It is illuminated amber to indicate a warning, green to indicate no conflict at all and that the system is operational, and red to indicate system saturation or malfunction. The center ring of arrows is used to indicate a Level 3 control and a specific arrow

is illuminated green indicating a positive command to go in that direction. The outer ring is used to indicate a Level 2 control and a specific sector is illuminated red to prohibit a maneuver in that direction.

A digital method of driving this display can easily be designed. For example, a four bit word could be constructed where each bit would be assigned a value of 1, 0, or -1. The word configuration could be as indicated in Figure 5.10. An example of a Level 3 control command to climb and turn right would be the configuration 1111, while a Level 3 climb only command would appear as 1101.

BIT MEANING / VALUE	CONTROL LEVEL	CENTER BALL LIGHT	LATERAL MANEUVER	VERTICAL MANEUVER
+1	Level 3	Amber	Right	Climb
0	Level 2	Green	No Turn	Level
-1		Red	Left	Dive

Figure 5.10.- Digital display drive word structure

A command reject option is provided by means of the button located at the bottom of the display, and the intruder accept/reject reply indicator is located at the top of the display. Red indicates rejection and green indicates acceptance of a Level 3 avoidance command. Illumination of the accept/reject message is easily accomplished by the addition of a bit to the word configuration illustrated in Figure 5.10.

Display of the monitor function is also desirable. This could be accomplished by flashing the appropriate command indicator to evidence satisfactory conflict resolution. The frequency of the flashing could also be varied such that at low frequency, the conflict would almost be resolved while at high frequency, resolution of the conflict is just being initiated. The flashing frequency could be a direction function of the predicted range at the system warning time τ_W.

System Requirements

In discussing the requirements for a collision avoidance system, it is helpful to refer to the system block diagram of Figure 5.5. Figure 5.5 shows that a collision avoidance system is composed of four basic subsystems namely:

Measurement Subsystem

Communications Subsystem

Computation Subsystem

Display Subsystem

The function of the measurement subsystem is to provide all the data pertinent to the protected aircraft required by the data set. This subsystem is composed of all the sensors necessary to measure these data. A typical complement of sensors consists of an altimeter, compass, airspeed indicator, and an area-navigator.

The communications subsystem is also required for data collection. It has the function of collecting the basic data sets of all aircraft within the monitor region of the system. Further it is necessary for command transmission in fully equipped

aircraft. If the aircraft is partially equipped, only the basic data set augmented with aircraft identity, and system type, an accept/reject message must be transmitted. This system could be a standard telemetry system which requires no special equipment.

The computation subsystem is used for all computation and logic functions such as data preprocessing, threat detection and evaluation, and avoidance command computation. This subsystem consists of an airborne computer and all required instrumentation for interface with the measurement, communications, and display subsystems. The logic for the construction of the display drive signal as illustrated in Figure 5.10 is also included in this subsystem.

The remaining major subsystem is the display subsystem which has as its function the requirement to present system status, collision avoidance commands, control levels, intruder response and conflict resolution status to the pilot. One method of display is illustrated in Figure 5.9.

The problem of requirements for each major subsystem are discussed here in detail. For the measurement subsystem, the primary requirement is accuracy for which an analysis is made in section 4.4 of this thesis. It was shown that sensor accuracy and the conditional probabilities of false alarm and missed alarm are directly related. With given specifications, the sensor accuracies are readily established by the methods of section 4.4. Sensor location is also important. Since an altimeter, compass

and air-speed indicator are usually included as part of aircraft instrumentation and since altitude, heading and airspeed are very difficult to measure from the ground, the obvious choice is to obtain these data from the airborne sensors. Further, aircraft identification, system type, and accept/reject messages must also originate from the aircraft. The major question of sensor location is therefore associated with the location of the position sensing devices. Area navigation represents one solution, but is not absolutely necessary since a measure of relative range and bearing is all that is required for collision avoidance. A recent development by Honeywell(40) for the U.S. Army offers the possibility of fairly inexpensive ($5,000) range and relative bearing data.

In terminal areas, radar beacon systems such as used for automated ground control (AGC) are being developed and are likely to be highly accurate. In terms of sensor location, the following locations appear to be feasible:

Airborne sensors

- Altimeter
- Compass
- Air-speed indicator
- Area navigator (or range and relative bearing sensors)

Ground based sensors

- Area navigator (radar beacon or other surveillance equipment)

One method of system implementation is use of the onboard sensor complement of equipment in the cruise environment where accuracy is not as critical as in the terminal area since large separation standards can be used. In the terminal area however, provision could be made to use the ground-based navigation system in conjunction with the onboard sensors to provide for collision avoidance. Also, onboard data could be received by the ground system for use in terminal area guidance and control. If collision avoidance logic were included in the ground based system, a desirable form of system redundancy could be achieved.

Concerning the requirements for the communications system, consider that a typical data set consists of latitude, longitude, range or relative bearing, altitude, heading, air-speed, aircraft identification, system type, accept/reject message, and avoidance commands. A minimum of seven words must be transmitted by both partially and fully equipped aircraft. Word length is associated with the problem of accuracy and is easily determined once the sensor accuracy is established. One further communications requirement is the frequency of data transmission. The interval of time between data transmissions can be thought of as a lag in the system. Assuming perfect and instantaneous computation as well as perfect data, the maximum error in the prediction of future position will be as large as the data interval times the maximum relative velocity. A plot of this error is presented in Figure 5.11. With this chart data frequency can be chosen so that the error will be compatible with the measurement errors.

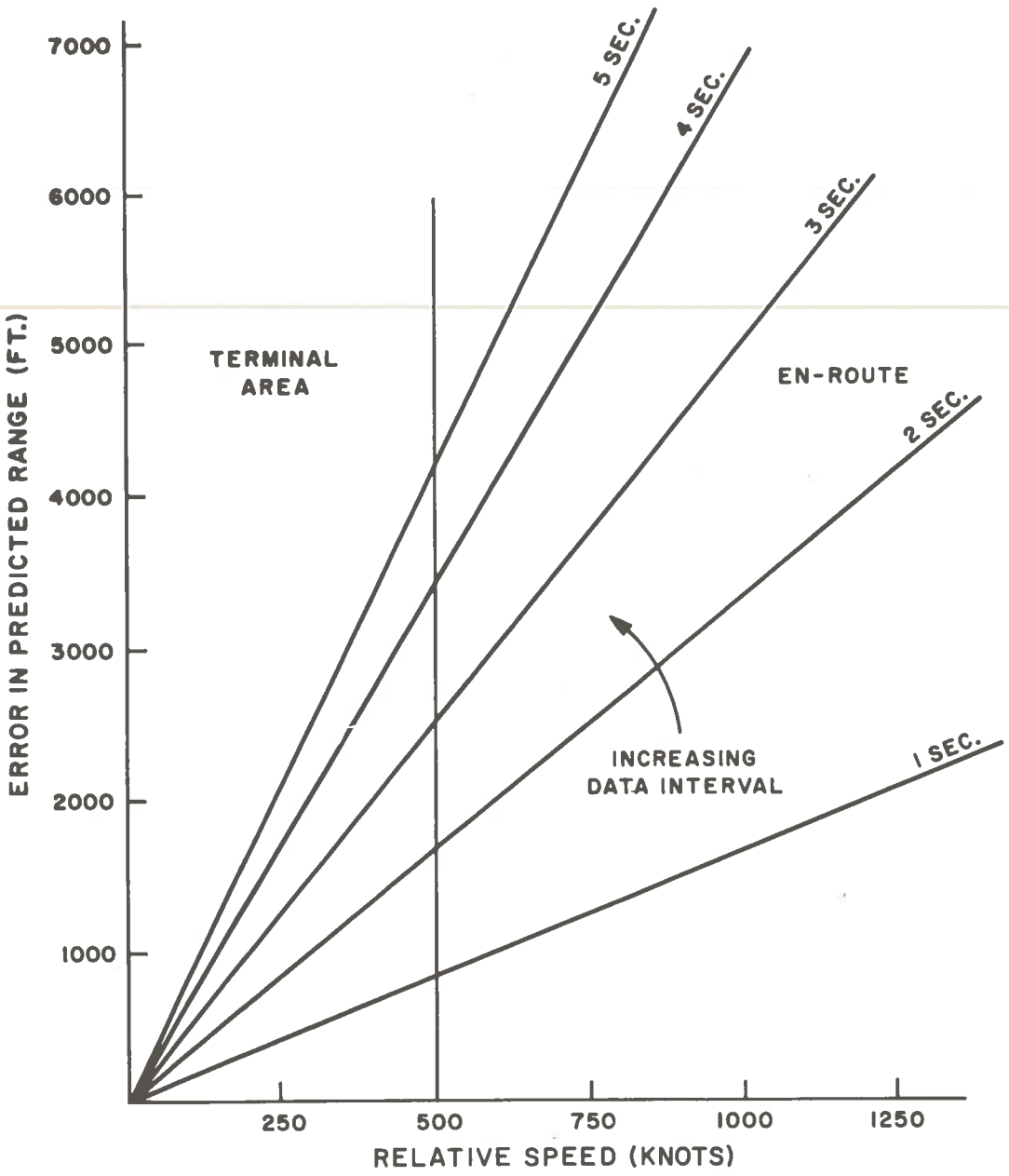

Figure 5.11.- Predicted position error due to data interval

The computation cycle time is closely associated with the data interval. One of the major subsystem requirements is that the computation subsystem have the equipment necessary to interface with the measurement, display, and communications subsystems.

It must also have a word length consistent with the communications subsystem. Computation cycle is determined by the maximum number of computations required to process one aircraft, the number of aircraft that a system must process simultaneously, and the computational speed of the computer used. The maximum number of computations required to process one aircraft occurs when a potential threat exists. In this case, in addition to standard preprocessing and command computations, approximately 100 values of the relative range vector must be computed and tested. This prediction alone accounts for approximately 2000 multiplies and 1000 adds since it is estimated that one range prediction takes the equivalent of 20 multiply and 10 add operations.

The number of aircraft that an airborne system must process should be no more than three simultaneous actual threats and on the order of 15 aircraft in the control region at any given time. This value depends directly on the density of the aircraft in the flight environment and the system design option being considered. For example, in the terminal area of New York during 1968 there were roughly 60 aircraft airborne at any given time within a 30 nm radius and below 10,000 ft. A ground based system operating in this area must be capable of processing at least 100 aircraft simultaneously to account for times of peak density, and does not provide for the expected increase of density in the near future. One method of alleviating this problem is to process only actual threats every data cycle and to process potential threats, say every five data cycles. This would reduce the computation load.

The basic requirements for the display subsystem are that it be capable of indicating the necessary commands and controls, as well as system status to the pilot. Furthermore, it should be designed so that it is acceptable to the pilot, i.e., human factors should be considered.

Design Summary

A basic philosophy of collision-avoidance has been developed which provides three levels of aircraft control, consistent with the degree of collision threat. The first level of control requires that an aircraft use standard maneuvers to change flight path. The second level prohibits specific maneuvers which could cause an actual threat. The third level requires that a specific maneuver be executed in order to avoid a threat.

Measurement sensitivities have been calculated and a probabilistic method of relating these sensitivities, as well as the dimensions of the aircraft safety region, to the conditional probability of false or missed alarm has been formulated.

Avoidance maneuvers and commands for resolving both actual and potential threats have been developed. Further, various system design options ranging from fully airborne to ground-based have been discussed. A method of collision avoidance algorithm design capable of treating three-dimensional curvilinear flight paths and simultaneous threats has also been presented. This algorithm design is also applicable to any of the system design options discussed.

Methods of control and display have also been formulated. A specific display has been designed based upon the McDonnell-Douglas EROS system and present automotive traffic control concepts.

Requirements for each major subsystem of a collision avoidance system have been discussed. These include the measurement, communications, computation and display subsystems, and the overall system. A method of relating data rate, word length, and computation cycle to the error in predicted range as a function of relative speed has also been presented.

In summary, it is estimated that the *conflict ratio* for a system of this type is on the order of 25 in the terminal area and 3 in the en-route environment.

CHAPTER 6

CONCLUSION

6.1 Summary of Results

The primary conclusion of this research is that closed-form deterministic and statistical methods can be used to evaluate anti-collision systems. These methods, verified by empirical data, provide the insight required to define a system design approach which will satisfy specific design goals. Two figures-of-merit called *conflict ratio* and *probability of missed critical alarm* are developed. The *conflict ratio* is a measure of system efficiency, while the *probability of missed critical alarm* is a measure of system safety. These two parameters relate both system thresholds and prediction accuracies to the critical miss distances, but are independent of environment. With these parameters, simple trade-off studies can determine the proper choice of system thresholds, sensors and collision avoidance criteria which will satisfy specified system design goals.

Low conflict ratios are achieved by choosing small system thresholds while low probability of missed critical alarm and sufficient escape time are obtained by choosing large system thresholds requiring a compromise solution to resolve these conflicting requirements. Systems which provide both low probability of missed critical alarm and sufficient escape time have the following ranges of conflict ratio.

	Terminal	En-Route
Pilot warning indicators (PWI);	1000<CR<200	100<CR<50
Collision detection (CDS) or partial state CAS	200<CR<100	50<CR<10
Full state collision avoidance (CAS)	100<CR<1	10<CR<1

The conflict ratio for a perfect system is 1.

In addition to the foregoing, a number of other factors affecting the design of anti-collision systems have been analyzed. It has been established that anti-collision systems should be co-operative and capable of processing simultaneous intruders. It has been shown that the intermittent-positive-control (IPC) concept as opposed to continuous collision avoidance control is feasible and will be applicable as a terminal area control method through the 1995 time period based on FAA traffic estimates. Further, it was established that a system capable of cooperating with the ground as well as with other aircraft was desirable.

Anti-collision systems are by their nature predictive devices. They attempt to reduce the probability of collision by preventing intruders from violating a protected volume about the aircraft. The dimensions of the protected volume are determined by the accuracy of the system in predicting future relative position between the intruder and the protected aircraft and by the

required system warning time. In an attempt to establish a collision avoidance system design philosophy, it was found that the use of curvilinear theory reduces drastically the dimensions of the protection volume, and the use of negative commands provides adequate time for the execution of escape maneuvers by preventing potential threats from becoming actual threats. Further, by use of three basic levels of control, the amount of positive action required by the pilot for collision avoidance is significantly reduced by comparison to systems using only one control level. Finally, it is suggested that variable system thresholds be used in order to minimize interference with the ground controller in the terminal area and also be capable of providing protection in the high speed en-route environment.

A method of economically providing collision protection for both general aviation and air carriers is also suggested by this research. This method consists basically of providing a CAS type device for the air carrier while simultaneously providing a PWI device for general aviation. This can be accomplished by both the AC and the GA aircraft transmitting and receiving the basic data sets of all aircraft within a specified monitor region. The PWI would then simply display the relative position of intruder aircraft. The CAS would perform the detection, evaluation, avoidance and monitoring functions. The GA aircraft would also be equipped with a display which would enable him to receive commands from fully equipped aircraft or from an in-range ground station. This scheme provides protection of the CAS type for all

aircraft in the terminal area and for AC vs GA conflicts en-route. PWI protection only is provided for GA vs GA encounters in the en-route environment when no ground station is in range.

System design methods which include the measurement, communication, computation, command and display subsystems have also been presented. For example, a method of relating data rate, word length and computation cycle to the range prediction error as a function of relative speed has been established. Further, suggestions for a typical CAS display are presented.

In order to provide the technical understanding necessary to achieve the above results, a study of traffic models and threshold computation was performed. Certain fundamental conclusions resulted from these studies. In the study of threshold computation for example, a minimum data set for predicting relative position between two vehicles under Level 1 control was established. This data set consists of the altitude, heading, air-speed, latitude and longitude of each aircraft or the equivalent data set of altitude, heading and air-speed of each aircraft supplemented with a relative range and bearing measurement.

In the study of traffic models, a collision probability theory was developed. This was used to formulate a closed-form terminal area traffic model which was then verified by empirical data. A method for quantifying the probability of a multiple collision was presented as well as a method for determining the ability of a pilot to spot and resolve conflicts without the aid of a CAS. This was also based on empirical data. Finally, it

was verified that the occurrence of mid-air incidents varied linearly with the traffic factor but, in addition, it was shown that this variation is independent of the density distributions of the aircraft. The distributions simply determine the slope of the relation.

6.2 Suggestions for Further Study

A number of areas that require further study have been revealed by this research. These areas range from the purely mathematical and statistical to the evaluation of hardware.

In the areas of mathematics and statistics, problems concerning the integration of multivariate Gaussian and Rayleigh distributions should be investigated to obtain more accurate approximations to the *probability of missed critical alarm*. Both analytic and numerical solutions to this problem should be sought. A successful study in this area would enhance the ability of the engineer to specify system thresholds and evaluate collision avoidance systems. Also of importance in this area is the reduction of existing data and even the collection of new data where necessary in order to determine the actual position and velocity distributions of aircraft, both in the terminal area and in the en-route environment. For this type of data reduction, a determination should be made, from either existing or new data of the exact percentage of NMACs that are attributable to accelerating or turning aircraft. Analysis of the curvilinear collision criterion developed in this thesis would be useful to find

additional general closed-form solutions. Additional solutions beyond those discovered in this work would be useful for both evasive maneuver analysis and detection algorithms.

Other work in the area of the computer sciences would also contribute to the implementation of a successful collision avoidance system. For example, a detailed collision avoidance algorithm should be designed based upon the design philosophy presented in Chapter 5. This could then actually be inserted into an existing simulation program such as the Langley Program(19) and compared with other CAS methods.

In the final area of development, hardware implementation, it is recommended that a display containing all of the elements of the display designed in Chapter 5 be fabricated and linked to the simulation mentioned above. This procedure would enable evaluation of the effectiveness of the display under simulated conditions and would indicate modifications which would make it more suitable to pilots. This experiment would also make it possible to determine values of *conflict ratio* and *probability of missed critical alarm* which are acceptable to a pilot. It would be highly desirable to have a final flight test program for evaluating the techniques developed in this work under actual flight conditions.

This work is a beginning to the solution of the complex problem of designing a specific collision avoidance system compatible with present and future ATC systems, applicable to both AC and GA aircraft, that will reliably prevent mid-air collisions.

REFERENCES

1. Bulford, D.E.; "Collision Avoidance, A Bibliography, 1955 to Sept. 1968," Federal Aviation Agency, Atlantic City, N.J., AD 677 942, Nov. 1968.

2. Russell, B.W.; "Error Analysis, Typical Collision Avoidance System," WADC TR 59-199, AD 213 839, May, 1959.

3. Crafton, P.A.; "The Avoidance of Collision Between Aircraft on Curvilinear Flight Trajectories," Naval Research Lab. Rpt. 5344, Aug. 1959; Jnl. Aerospace Science, Vol. 29, Jan. 1962.

4. McKown, C.S., Marrone, J.J.; "Prevention of Mid-Air Collisions," Sperry Engineering Review, Vol. 16, Winter 1963.

5. Morrel, J.S.; "Fundamental Physics of the Aircraft Collision Problem," Bendix TM 465 1016 39, June 1956.

6. Joy, R.D., Killham, D.E., Belden, L.K.; "Computer-Simulation Study of Air Derived Separation Assurance Systems in Multiple Aircraft Environment," Collins Radio Co., Interim Rpt., FAA Rpt. # RD 64-138, AD 612 363, Oct. 1964.

7. Holt, J.M., Marner, G.R.; "Separation Hazard Criteria," Collins Radio Co., Company Rpt. Dec. 1968.

8. Catalano, J., McKown, C.; "A Study of Requirements for Visual Airborne Collision Avoidance," Sperry Gyroscope Co. AD 614 622, Dec. 1963.

9. Blatt, J.D.; "System Considerations for Airborne Collision Prevention," In: The Collision Prevention Advisory Group Symposium, Report of the Proceeding, Potential of Airborne Collision Prevention Devices, Washington D.C., AD 415 918, 1963.

10. LaRochelle, P.J.; "Technical Feasibility of Collision Avoidance Systems" (same as 9).

11. Tibbs, A.M.; "Summary of Collision and Near Miss Collision Statistics" (same as 9).

12. Marks, B.L.; "Air Traffic Control Separation Standards and Collision Risk," RAE Tech. Note Math. 91, AD 407 312, Feb. 1963.

13. Piggot, B.A.M.; "A Non-Linear Maximization Problem Arising in the Study of Aircraft Collision Risk," RAE Tech. Note 65044, AD 465 707, Feb. 1965.

14. National Transportation Safety Board; "Mid-Air Collision Statistics," N68-18223, Dec. 1967.

15. Department of Transportation; "Near Mid-Air Collision Report of 1968," prepared by NMAC Study Group, July 1969.

16. Flanagan, P.D., Willis, K.E.; "Frequency of Air Space Conflicts in the Mixed Terminal Environment," Lambda paper 32, Lambda Corporation, Arlington, Va., Mar. 1969.

17. Bellantoni, J.F.; "Vehicle Collision Probability," S.M. Dissertation in the Dept. of Mathematics, New York University, N.Y., N.Y., June 1962.

18. Present, R.D.; Kinetic Theory of Gases. New York: McGraw Hill Book Company, Inc. 1958.

19. Britt, C.L., Schraeder, J.H.; "A Statistical Evaluation of Aircraft Collision-Hazard Warning System Techniques in the Terminal Area," NASA Langley Working Paper LWP 777, 1969.

20. vanSaun, H.R.; "Pilot Warning Systems," Journal of the Institute of Navigation, Vol. 14, No. 3, Fall 1967.

21. Meilander, W.C.; "The Associative Processor in Aircraft Conflict Detection," NAECON '68 Proceedings of the 20th National Aerospace Electronics Conf., Dayton, Ohio, May 1968.

22. Jenkins, J.L.; "An Airborne Collision Warning Device," Rand Corp., P-1178, Rev., Nov. 1957.

23. Nagy, A.S.L.; "Operational Analysis of Time Frequency Collision Avoidance Systems," Boeing Co., Commercial Airplane Division, Rpt. # D6-1 9535, AD 668 163, 1968.

24. Matusche, H.; "KOLLARM, a New-Collision Warning Equipment," Luftfahrttechnik Raumfahrttenchnik, Vol. 9, Feb. 1963, RAE Trans. 1053, Dec. 1963.

25. National Company, Inc.; "Evaluation of a Collision Avoidance Technique," Final Report, Contract # ARDS-530, Project # 305-15-1D, Sept. 1963, AD 427 142L.

26. Zboril, F.R.; "Assessment of Air Collision Avoidance Techniques in the 1970's," In: Annual East Coast Conference on Aerospace and Navigational Electronics, 11th, Baltimore, Md., Oct. 1964.

27. Russell, B.W.; "Characteristics of Airborne Anti-Collision Devices and Their Role in Air Traffic Control," WADC TR 59-209, AD 214 388, May 1959.

28. ISC/Telephonics; "Aircraft Collision Avoidance System Final Engineering Report - Phase I," Contract # N0 019-68-c-0196, AD 854 529, May 1969.

29. Frye, E.O., Killham, D.E.; "Aircraft Collision Avoidance Systems," IEEE Spectrum, Vol. 3, No. 1, Jan. 1966.

30. Dinerman, B.V., Burkard, K.; "Evaluation of a Ground Bounce Ranging/Altitude Exchanging Collision Avoidance System Technique," FAA, NAFEC Rpt. # RD 64-5, AD 431 914, Oct. 1963.

31. Lederer, J.; "Air Collision Avoidance," Paper at Institute of Navigation Annual Meeting 23rd, Washington, D.C. June 1967.

32. Jazwinski, A.H.; "Limited Memory Optimal Filtering," Rpt. 67-11, Contract NAS-5-11058, Analytical Mechanics Associates, Aug., 1967.

33. Britting, K.R.; "Analysis of Space Stabilized Inertial Navigation Systems," Experimental Astronomy Lab. Rpt. # RE-35, Massachusetts Institute of Technology, Cambridge, Mass., Jan. 1968.

34. Willis, K.E., Currier, J.B., Flanagan, P.; "Intermittent Positive Control," Proceedings of the IEEE, Vol. 58, No. 3, Mar. 1970.

35. Miller, K.S.; Multidimensional Gaussian Distributions. New York: John Wiley & Sons, Inc., 1964.

36. Department of Transportation; "Report of the Department of Transportation Air Traffic Control Advisory Committee," Vols. 1 & 2, Dec. 1969.

37. Freye, E.O., Killham, D.E.; "Aircraft Collision Avoidance Systems," Collins Radio Co., IEEE Spectrum, Jan. 1966.

38. Hildebrand, F.B.; Advanced Calculus for Engineers. New Jersey: Prentice-Hall, Inc., 1948.

39. Litchford, G.; "Making General Aviation Safer and More Effective Through Universal Electronic Design," Aeronautics and Astronautics, Jan. 1971.

40. Klass, Philip J.; "Army Plans Test of Improved PWI," Aviation Week and Space Technology, Feb. 15, 1971.

41. Ruetenik, J.R., Thompson, J.H.; "Computer Simulation Model of Terminal Air Traffic and PWI Systems," Kaman Avidyne TR-57, NASA Contract No. NAS 12-698, Mar. 28, 1969.

42. Martin Marietta Co.; "Flight Test and Evaluation of Airborne Collision Avoidance System," for the Air Transport Association of America, Apr. 1970.

43. ARCON Corporation; "Air Traffic Control Theory and Design," for the Mitre Corporation, Report No. 1-61, Jul. 1961.

APPENDIX A

ESTIMATION OF AVERAGE COLLISION FREQUENCY

A.1 Mathematical Method

Consider that the average value, or the expected value of λ_{ij} when averaged over all combinations of N aircraft is given by

$$E(\lambda_{ij}) = \frac{\Sigma_i \Sigma_j \lambda_{ij} (1-\delta_{ij})}{N(N-1)} \tag{A.1}$$

Also consider that the collision frequency among N aircraft is known to be

$$\Lambda_{NN} = \frac{1}{2} \sum_i \sum_j \lambda_{ij} \ (1-\delta_{ij}) \tag{A.2}$$

By substitution one obtains the relation

$$\Lambda_{NN} = \frac{N(N-1)}{2} E(\lambda_{ij}) \tag{A.3}$$

so that an approximation to $E(\lambda_{ij})$ is indicated.

In general, it has been established that

$$\lambda_{ij} = \int_{\substack{\text{Vel} \\ \text{Sp}}} d(\bar{w}) W(0, \bar{w}_{ij}, t) \ V_c(\bar{w}_{ij}) \tag{A.4}$$

where W is a function of $\tilde{\bar{r}}_i$, $\tilde{\bar{r}}_j$, $\tilde{\bar{v}}_i$, $\tilde{\bar{v}}_j$, i.e., the nominal or average position and velocity of the i^{th} and the j^{th} aircraft, therefore integration over the relative velocity space will yield a function

$$\lambda_{ij} = \lambda_{ij}(\tilde{\bar{r}}_i, \tilde{\bar{r}}_j, \tilde{\bar{v}}_i, \tilde{\bar{v}}_j) \tag{A.5}$$

Suppose that a probability density distribution of nominal position and velocity for a large number of aircraft in a defined airspace is known, and is given by

$$U(\tilde{\bar{r}}_i, \tilde{\bar{v}}_i, t)$$

Then, the probability that the i^{th} aircraft is at position $(\bar{r}, \bar{r}+\Delta\bar{r})$ with velocity $(\bar{v}, \bar{v}+\Delta\bar{v})$ at time t is given by

$$U(\tilde{\bar{r}}_i, \tilde{\bar{v}}_i, t)\ \Delta(\tilde{\bar{r}}_i)\ \Delta(\tilde{\bar{v}}_i)$$

where

$$\Delta(\tilde{\bar{r}}_i) = \Delta x\ \Delta y\ \Delta z$$

$$\Delta(\tilde{\bar{v}}_i) = \Delta \mathring{x}\ \Delta \mathring{y}\ \Delta \mathring{z} \tag{A.6}$$

If there are N aircraft in the airspace, the density distribution can be found by looking at the probable number of aircraft in an element of volume $\Delta(\tilde{\bar{r}}_i)$. This is given by

$$\Delta N = N\ U_r(\tilde{\bar{r}}_i, t)\ \Delta(\tilde{\bar{r}}_i)$$

and the density by

$$D_r(\tilde{\bar{r}}_i, t) = \frac{\Delta N}{\Delta V} = N\ U_r(\tilde{\bar{r}}_i, t)$$

where

$$U_r(\tilde{\bar{r}}_i,t) = \int_{Vel} U(\tilde{\bar{r}}_i,\tilde{\bar{v}}_i,t)\, d(\tilde{\bar{v}}_i)$$

and where the probable number of aircraft in an element of volume $(\bar{r},\bar{r}+\Delta\bar{r})$ having velocity $(\bar{v},\bar{v}+\Delta\bar{v})$ is given by

$$\Delta N = NU(\tilde{\bar{r}}_i,\tilde{\bar{v}}_i,t)\Delta(\tilde{\bar{r}}_i)\Delta(\tilde{\bar{v}}_i) \qquad (A.7)$$

Note, in this case that

$$D(\tilde{\bar{r}}_i,\tilde{\bar{v}}_i,t) = \frac{\Delta N}{\Delta V} = NU(\tilde{\bar{r}}_i,\tilde{\bar{v}}_i,t) \qquad (A.8)$$

where in this equation

$$\Delta V = \Delta(\tilde{\bar{r}}_i)\Delta(\tilde{\bar{v}}_i) \qquad (A.9)$$

Consider that

$$N = \int D(\tilde{\bar{r}}_i,\tilde{\bar{v}}_i,t)dV$$

so that

$$N = N\int_{\substack{\text{Pos \& Vel}\\ \text{Space}}} U(\tilde{\bar{r}}_i,\tilde{\bar{v}}_i t)\Delta(\tilde{\bar{r}}_i)\Delta(\tilde{\bar{v}}_i)$$

But,

$$\int_{-\infty}^{\infty} U\Delta(\tilde{\bar{r}}_i)\Delta(\tilde{\bar{v}}_i) = 1$$

so that N = N and the relation is satisfied providing the airspace volume is large compared to the error volume of the average position distribution. The term $D(\tilde{\bar{r}}_i, \tilde{\bar{v}}_i, t)$ is the probability density distribution of average or nominal position and velocity of N aircraft in an airspace. For convenience, let

$$\tilde{\bar{x}}_i = \begin{Bmatrix} \tilde{\bar{r}}_i \\ \\ \tilde{\bar{v}}_i \end{Bmatrix} \tag{A.10}$$

so that one can write

$$D(\tilde{\bar{x}}_i, t) = NU(\tilde{\bar{x}}_i, t) \tag{A.11}$$

From basic probability theory, the average or expected value of a function of a random variable is given by

$$E(\lambda_{ij}) = \frac{\int d(\tilde{\bar{x}}_i) \int d(\tilde{\bar{x}}_j) D(\tilde{\bar{x}}_i, t) D(\tilde{\bar{x}}_j, t) \lambda_{ij}(\tilde{\bar{x}}_i, \tilde{\bar{x}}_j)}{\int d(\tilde{\bar{x}}_i) \int d(\tilde{\bar{x}}_j) D(\tilde{\bar{x}}_i, t) D(\tilde{\bar{x}}_j, t)}$$

but,

$$\int d(\tilde{\bar{x}}_i) D(\tilde{\bar{x}}_i, t) = N$$

so that the expression for $E(\lambda_{ij})$ is finally given in integral form as a function of the probability density distributions as

$$E(\lambda_{ij}) = \int d(\tilde{\bar{x}}_i) \int d(\tilde{\bar{x}}_j) U(\tilde{\bar{x}}_i) U(\tilde{\bar{x}}_j) \lambda_{ij}(\tilde{\bar{x}}_i, \tilde{\bar{x}}_j) \tag{A.12}$$

Also, in a completely analogous fashion, it can be shown that

$$\Lambda_{1,N} = N \int d(\tilde{\bar{x}}_i)\ U(\tilde{\bar{x}}_i)\ \lambda_{1,i}(\tilde{\bar{x}}_1, \tilde{\bar{x}}_i) \quad ; \quad i \neq 1 \tag{A.13}$$

The major problem at this point is to determine the distributions $U(\tilde{\bar{x}}_i)$ for realistic situations and to compare the results with actual data to determine their validity. Two brief examples will be presented to illustrate the results achieved to this point.

EXAMPLE I. Uniform Distribution in Nominal Position and Velocity and in their Deviations

In this example there is the following equation for collision frequency

$$\Lambda_{1,N} = N \int d(\tilde{\bar{x}}_i)\ U(\tilde{\bar{x}}_i)\ \lambda_{1,i}(\tilde{\bar{x}}_1, \tilde{\bar{x}}_i)$$

where, under the assumption of a uniform distribution, $\lambda_{1,i}$ is given by

$$\lambda_{1,i} = \frac{4}{3}\pi d^2 v / V_{a/s}$$

Consider that the assumption of a uniform distribution in position and velocity yields the probability density function

$$U(\tilde{\bar{r}}_i, \tilde{\bar{v}}_i) = 1/4\pi\ V_{a/s}$$

where $V_{a/s}$ is the space over which the assumption is made. Substitution and integration obtains

$$\Lambda_{1,N} = \frac{N}{V_{a/s}} \cdot \frac{4}{3}\pi d^2 v$$

which agrees with the gas theory.

Similarly, considering the overall collision frequency among the N aircraft, i.e.

$$\Lambda_{N,N} = \frac{N(N-1)}{2}\int d(\tilde{\tilde{x}}_i)\int d(\tilde{\tilde{x}}_j)U(\tilde{\tilde{x}}_i)U(\tilde{\tilde{x}}_j)\lambda_{ij}(\tilde{\tilde{x}}_i,\tilde{\tilde{x}}_j)$$

and further considering that

$$N\int d(\tilde{\tilde{x}}_j)U(\tilde{\tilde{x}}_j)\lambda_{ij} = \frac{N}{V_{a/s}} \cdot \frac{4}{3}\pi d^2 v$$

further integration yields

$$\Lambda_{N,N} = \frac{N(N-1)}{V_{a/s}} \cdot \frac{2}{3}\pi d^2 v$$

which also agrees with the gas theory.

EXAMPLE II. Uniform Distribution in Nominal Position and Velocity with Normally Distributed Deviations

In this example, there is the following equation for the collision frequency

$$\Lambda_{1,N} = N\int d(\tilde{\tilde{x}}_i)U(\tilde{\tilde{x}}_j)\lambda_{i,j}(\tilde{\tilde{x}}_i,\tilde{\tilde{x}}_j) \quad ; \quad j\neq 1$$

where $U(\tilde{\tilde{x}}_j)$ is given by

$$U(\tilde{\tilde{x}}_j) = 1/4\pi V_{a/s}$$

and $\lambda_{i,j}$ in this case is given by

$$\lambda_{i,j} = \frac{d^2 e^{-\frac{1}{2}\tilde{\tilde{\rho}}_{i,j}^{T} P^{-1} \tilde{\tilde{\rho}}_{i,j}}}{|P|^{1/2}} \left(\frac{\sigma_v}{\pi} + \frac{\tilde{w}}{2(2\pi)^{1/2}} \right)$$

where

$$\tilde{\tilde{\rho}}_{i,j} = \tilde{\tilde{r}}_j - \tilde{\tilde{r}}_i$$

Substitution and integration obtains

$$\Lambda_{1,N} = \frac{N}{V_{a/s}} \cdot 4\pi d^2 \left(\frac{\sigma_v}{\sqrt{2\pi}} + \frac{\tilde{w}}{4} \right)$$

and similarly, further integration (see example I) obtains

$$\Lambda_{N,N} = \frac{N(N-1)}{V_{a/s}} \cdot 2\pi d^2 \left(\frac{\sigma v}{\sqrt{2\pi}} + \frac{\tilde{w}}{4} \right)$$

Consider the case of two groups of aircraft namely group N and group M and consider the probability of collision between these two groups. The probability of no collision Q_{NM} is given by

$$Q_{NM} = \prod_{i=1}^{N} \prod_{j=1}^{M} q_{ij}$$

where

$$q_{ij} = e^{-\int_0^t \lambda_{ij}(\tau) d\tau}$$

so that by substitution,

$$Q_{NM} = e^{-\int_o^t \sum_i^N \sum_j^N \lambda_{ij}(\tau)d\tau}$$

Define

$$\Lambda_{NM} = \sum_{i=1}^{N} \sum_{j=1}^{M} \lambda_{ij}$$

so that

$$Q_{NM} = e^{-\int_o^t \Lambda_{NM}(\tau)d\tau}$$

and

$$P_{NM} = 1-e^{-\int_o^t \Lambda_{NM}(\tau)d\tau} \qquad \text{(A.14)}$$

Examination of Λ_{NM} yields the relation

$$E(\lambda_{ij}) = \sum_{i=1}^{N} \sum_{j=1}^{M} \lambda_{ij/NM} \qquad \text{(A.15)}$$

where

$$\Lambda_{NM} \approx NM\ E(\lambda_{ij}) \qquad \text{(A.16)}$$

For group N, we see that the density distribution can be expressed as

$$D_N(\tilde{\tilde{x}}_i,t) = N\, U_N(\tilde{\tilde{x}}_i,t) \tag{A.17}$$

and for group M by

$$D_M(\tilde{\tilde{x}}_j,t) = M\, U_M(\tilde{\tilde{x}}_j,t) \tag{A.18}$$

so that

$$E(\lambda_{ij}) = \frac{\int d(\tilde{\tilde{x}}_i)\int d(\tilde{\tilde{x}}_j) D_N(\tilde{\tilde{x}}_i,t) D_M(\tilde{\tilde{x}}_j,t)\lambda_{ij}(\tilde{\tilde{x}}_i,\tilde{\tilde{x}}_j)}{\int d(\tilde{\tilde{x}}_i)\int d(\tilde{\tilde{x}}_j) D_N(\tilde{\tilde{x}}_i,t) D_M(\tilde{\tilde{x}}_j,t)} \tag{A.19}$$

Independence of distributions between the two groups has been assumed. Next, consider that

$$\left.\begin{aligned} &\int d(\tilde{\tilde{x}}_i)\; D_N(\tilde{\tilde{x}}_i,t) = N \\ &\text{and that} \\ &\int d(\tilde{\tilde{x}}_j)\; D_M(\tilde{\tilde{x}}_j,t) = M \end{aligned}\right\} \tag{A.20}$$

which gives the final relationship

$$E(\lambda_{ij}) = \int d(\tilde{\tilde{x}}_i)\int d(\tilde{\tilde{x}}_j) U_N(\tilde{\tilde{x}}_i,t) U_M(\tilde{\tilde{x}}_j,t)\lambda_{ij}(\tilde{\tilde{x}}_i,\tilde{\tilde{x}}_j) \tag{A.21}$$

Suppose that correlation between the states of the M aircraft and the N aircraft exists. In this case,

$$E(\lambda_{ij}) = \int d(\tilde{\tilde{x}}_i)\int d(\tilde{\tilde{x}}_j) U_{NM}(\tilde{\tilde{x}}_i,\tilde{\tilde{x}}_j)\lambda_{ij}(\tilde{\tilde{x}}_i,\tilde{\tilde{x}}_j) \tag{A.22}$$

where U_{NM} is the joint distribution between the states of the two groups of aircraft. Also

$$D_{NM} = NM\ U_{NM}$$

and

$$\left.\begin{aligned} \int d(\tilde{\tilde{x}}_i) \int d(\tilde{\tilde{x}}_j) D_{NM}(\tilde{\tilde{x}}_i, \tilde{\tilde{x}}_j) &= NM \\ \int d(\tilde{\tilde{x}}_j) D_{NM}(\tilde{\tilde{x}}_i, \tilde{\tilde{x}}_j) &= MD_N(\tilde{\tilde{x}}_j) \end{aligned}\right\} \qquad (A.23)$$

A slight generalization may now be made for the case of more than two groups. Suppose that three groups exist, groups M, N, and K. In this case,

$$\Lambda_{M,N,K} = \Lambda_{MN} + \Lambda_{MK} + \Lambda_{NK} \qquad (A.24)$$

where Λ_{MNK} is the collision frequency among the different groups of the aircraft.

One final example is given. If one assumes all distributions are uniform, then the collision frequency among two groups of aircraft is given by

$$\Lambda_{MN} = \frac{4}{3} \frac{\pi d^2 v}{V_{a/s}} MN$$

and among three groups of aircraft by

$$\Lambda_{MNK} = \frac{4}{3} \frac{\pi d^2 v}{V_{a/s}} (MN + MK + NK)$$

APPENDIX B

MULTIPLE MID-AIR INCIDENT PROBABILITIES

Assume that N aircraft are in the airspace so that the probability of at least one encounter between two aircraft in (0,t) is given by

$$\left.\begin{aligned} P_{NN} &= 1 - e^{-\Lambda_{NN} t} \\ \text{where} \\ \Lambda_{NN} &= \frac{N(N-1)}{2} E(\lambda_{ij}) \end{aligned}\right\} \qquad (B.1)$$

The probability of a near miss between a specified aircraft among N other aircraft in $(t,t+\tau)$ is given by

$$\left.\begin{aligned} P_{1N} &= 1 - e^{-\Lambda_{1N} \tau} \\ \text{where} \\ \Lambda_{1N} &= (N-1)\ E(\lambda_{1k}) \end{aligned}\right\} \qquad (B.2)$$

Let P be the probability that a near-miss occurs and that at least one of the aircraft involved then experiences a second near-miss. This probability is given by

$$P = P_{NN}\ (P_{1N} + P_{2N} - P_{1N}\ P_{2N}) \qquad (B.3)$$

Substitution obtains

$$P = \left(1-e^{-\Lambda_{NN}t}\right)\left\{\left(1-e^{-\Lambda_{1N}\tau}\right)+\left(1-e^{-\Lambda_{2N}\tau}\right)-\left(1-e^{-\Lambda_{1N}\tau}\right)\left(1-e^{-\Lambda_{2N}\tau}\right)\right\}$$

which can be simplified to the expression

$$P = \left(1-e^{-\Lambda_{NN}t}\right)\left(1-e^{-(\Lambda_{1N}+\Lambda_{2N})\tau}\right) \tag{B.4}$$

For a fixed value of τ, the number of multiple incidents which can occur in a time T is given by

$$N_{mult} \approx \left(1-e^{-(\Lambda_{1N}+\Lambda_{2N})\tau}\right) \cdot \Lambda_{NN}T \tag{B.5}$$

and since in general $(\Lambda_{1N}+\Lambda_{2N})\tau$ will be small,

$$N_{mult} \approx (\Lambda_{1N}+\Lambda_{2N})\tau \; N_{sing} \tag{B.6}$$

where N_{sing} is the number of single encounters in time T. Next, consider that

$$\left.\begin{aligned} \Lambda_{NN} &= \frac{N(N-1)}{2} E(\lambda_{ij}) \\ &\text{and that} \\ \Lambda_{1N} &= (N-1)\; E(\lambda_{1k}) \\ \Lambda_{2N} &= (N-1)\; E(\lambda_{2k}) \end{aligned}\right\} \tag{B.7}$$

where

$$E(\lambda_{ij}) = \sum_{i=1}^{N} \sum_{j=1}^{N} \lambda_{ij}(1-\delta_{ij})/N(N-1)$$

and

$$E(\lambda_{Mj}) = \sum_{j=1}^{N} \lambda_{Mj}(1-\delta_{Mj})/N \qquad \text{(B.8)}$$

Then,

$$E(\lambda_{ij}) = \sum_{M=1}^{N} E(\lambda_{Mj})/(N-1)$$

Assume that

$$E(\lambda_{Mj}) = \mu \qquad \text{(B.9)}$$

for every M, so that

$$\sum_{M=1}^{N} \frac{E(\lambda_{Mj})}{N-1} = \mu$$

and under this assumption,

$$E(\lambda_{ij}) = E(\lambda_{Mj}) = \mu \qquad \text{(B.10)}$$

Then, consider that

$$\Lambda_{NN} \approx \frac{N(N-1)}{2}\mu$$

and

$$\Lambda_{1N} = \Lambda_{2N} \cong (N-1)\mu \qquad \text{(B.11)}$$

The number of multiple encounters is related to the number of single encounters by

$$N_{mult} = 2(N-1)\mu\tau N_{sing} \tag{B.12}$$

where

$$\mu = 2N_{sing}/N(N-1)T \tag{B.13}$$

The probability of a single near miss encounter over a one year period is almost a certainty, and the probability of a multiple encounter is given approximately by

$$P \cong \left[1-e^{-(\Lambda_{1N}+\Lambda_{2N})\tau}\right]$$

but since τ is small, this expression can be approximated by

$$P \approx (\Lambda_{1N}+\Lambda_{2N})\tau$$

or

$$P \approx 2(N-1)\mu\tau \tag{B.14}$$

To consider the probability of a specified aircraft experiencing a multiple encounter during an approach or departure operation, first consider that the probability of occurrence of the first encounter is given by

$$P_1 = 1-e^{-\Lambda_{1N}T_f} \tag{B.15}$$

Where T_f is the time of flight in the terminal area. It was shown that

$$\Lambda_{1N} = (N-1)\mu$$

so that one may use the approximation

$$P_1 \approx (N-1)\mu T_f$$

Also, the probability of a second encounter (assuming exclusive events) is given by

$$P_2 \approx (N-2)\mu\tau$$

So that the probability of multiple encounter is

$$P \approx (N-1)(N-2)\mu^2 T_f \tau \qquad \text{(B.16)}$$

APPENDIX C

POSITIVE AND NEGATIVE COMMAND COMPUTATION

Evasion of Actual Threats by Vertical Maneuvers

To begin, first assume that the vertical separation is predicted to be less than ε_V at a future time τ_W and that it is necessary to avoid this condition. The question which must be answered is, "What maneuver sequence must be performed to successfully resolve the imminent conflict?". To answer this question, consider the following cases:

CASE I. Both Aircraft Initially in Level Flight

Figure C.1 illustrates the possible geometries of this case. From this figure, it is seen that aircraft No. 1 can be in either position 1 or 2 and aircraft No. 2 in positions 3 or 4 when the conflict is detected. Table C.1 illustrates the possible maneuvers of the aircraft and the results of these maneuvers. As would be expected, a cooperative maneuver gives the largest change in relative position. It is also evident that if aircraft No. 2 is above aircraft No. 1, a simple interchange of the columns of table C.1 handles this case.

CASE II. Aircraft No. 1 Initially Level; Aircraft No. 2 Climbing or Diving

Figure C.2 illustrates the possible geometries of this case. The cases for aircraft No. 2 above aircraft No. 1 and climbing, or below aircraft No. 1 and diving are not considered to be of interest. Table C.2 illustrates the possible maneuvers of the

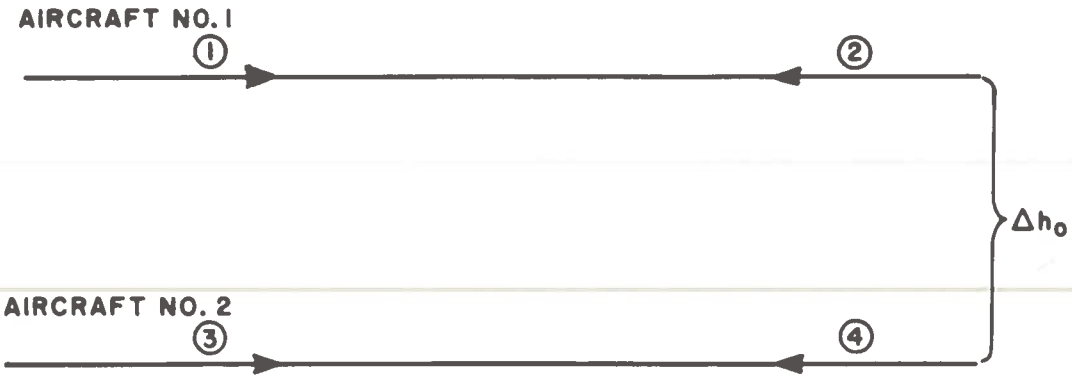

Figure C.1.- Vertical conflict geometry (Case I)

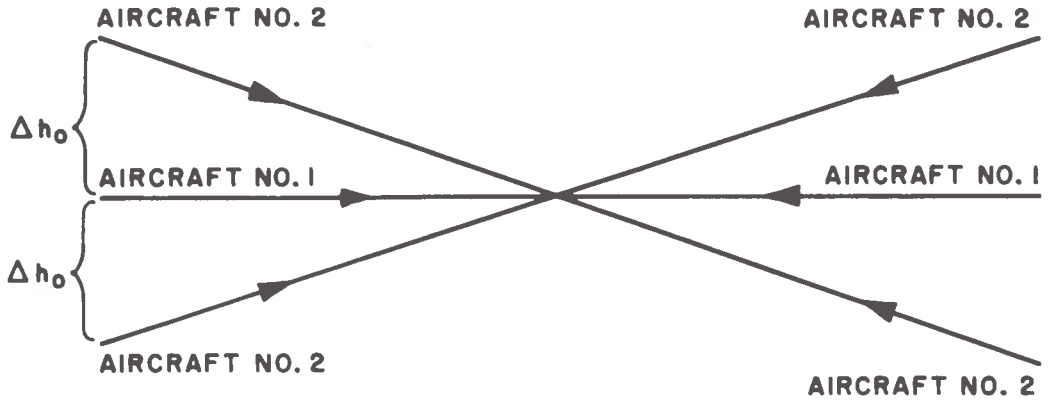

Figure C.2.- Vertical conflict geometry (Case II)

aircraft and the results of these maneuvers. Note also that for aircraft No. 2 climbing, it is assumed that aircraft No. 1 is higher than aircraft No. 2 and conversely. From table C.2, the maximum displacement is achieved by the climbing or diving aircraft leveling off and the level aircraft choosing the proper climb or dive maneuver. However, if only a level-off maneuver is executed, a net loss of 62.5 ft. in altitude results and it then reverts to a Case I situation. Since large displacements can be achieved in a short period of time, it appears that this

TABLE C.1.- VERTICAL CONFLICT RESOLUTION (CASE I)

State of aircraft after warning		Altitude Displacement
climb	dive	$\Delta h(t) = \Delta h_o + \ddot{h}_{t}^{2}$ $(0<t<5$ sec.)
		$\Delta h(t) = \Delta h(5) + 2\dot{h}_{max}(t-5)$ $t>5$ sec.
dive	climb	Bad maneuver for $\Delta h_o \neq 0$
		if $\Delta h_o = 0$ then $h(t)$ as above
level	climb	Bad maneuver for $\Delta h_o \neq 0$
dive	level	$\Delta h_o = 0$ $\Delta h(t) = \ddot{h}t^2/2$; $(0<t<5$ sec.)
		$\Delta h(t) = \dot{h}_{max}(t-5)+\Delta h(5)$; $t>5$ sec.
level	dive	$\Delta h(t) = \Delta h_o + \ddot{h}t^2/2$; $0<t<5$ sec.
climb	level	$\Delta h(t) = \dot{h}_{max}(t-5)+\Delta h(5)$; $t>5$ sec.
climb	climb	$\Delta h(t) = \Delta h_o$
dive	dive	
level	level	
Aircraft No. 1	Aircraft No. 2	

would be the most acceptable maneuver to execute. The final cases to be considered are when both aircraft are initially in a climb or dive situation.

CASE III. Both Aircraft in a Climb or Dive

In this case, if only one aircraft levels off, it reverts to a Case II situation and then possibly to a Case I situation.

TABLE C.2.- VERTICAL CONFLICT RESOLUTION (CASE II)

State of aircraft after warning		Altitude Displacement
level	level	$\Delta h(t) = \Delta h_o - \ddot{h}t^2/2$; $0<t<5$ sec. $\Delta h(t) = \Delta h(5)$; $t\geq 5$ sec.
climb dive	climb dive	$\Delta h(t) = \Delta h_o + \ddot{h}t^2/2$; $0<t<5$ sec. $\Delta h(t) = \Delta h(5) + \dot{h}_{max}t$; $t\geq 5$ sec.
dive* climb*	climb* dive*	$\Delta h(t) = \Delta h_o - \ddot{h}t^2/2$; $0<t<5$ sec. $\Delta h(t) = \Delta h(5) - h_{max}t$; $t>5$
		Aircraft 2 below aircraft 1
dive*	level*	$\Delta h(t) = \Delta h_o - \ddot{h}t^2$; $0<t<5$ sec. $\Delta h(t) = \Delta h(5) - \dot{h}_{max}t$; $t>5$ sec.
		Aircraft 2 above aircraft 1
		$\Delta h(t) = \Delta h_o + \ddot{h}\,t^2$; $0<t<5$ sec. $\Delta h(t) = \Delta h(5) + \dot{h}_{max}t$; $t>5$ sec.
climb*	level*	Same as dive-level with aircraft position change
Aircraft No. 1	Aircraft No. 2	

*indicates a dangerous maneuver combination

($\Delta h(t)$ can go through zero)

This could result in an excessive loss of time so that it is recommended that the most appropriate maneuver to execute is for both aircraft to level off in the event of a possible collision and then take further action based on Case I conditions.

Evasion of Actual Threats by Lateral Maneuvers

The first problem to be resolved is whether same-sense or opposite-sense turns should be used or at least to establish the rules governing the proper choice of turn. If opposite sense turns are chosen incorrectly, the linear collision can be accelerated rather than avoided. Further, Figure C.3 illustrates that in the case of a head-on conflict, opposite-sense turns can simply delay a collision. Also, in the overtaking situation, same sense turns will not in general lead to a satisfactory escape. As a result, some method for choosing the proper escape maneuvers must be established. This can be accomplished by considering that if two aircraft are in rectilinear flight and are on a collision course, then

$$\bar{\rho}(\tau_L) = 0 \tag{C.1}$$

so that the collision condition yields

$$\bar{\rho}_o = \left\{ \begin{array}{c} v_2 \cos\phi_2 \cos\psi_o + v_1 \cos\phi_1 \\ v_2 \cos\phi_2 \sin\psi_o \\ -\dot{h}_1 + \dot{h}_2 \end{array} \right\} \tau_L \tag{C.2}$$

The equation for the range between two aircraft after a turn maneuver has been made to avoid a rectilinear collision is given by

$$\rho^2(t) = \frac{v_2^2}{\omega_2^2}\cos^2\phi_2\left[(1-\cos\omega_2 t)^2+(\omega_2\tau_L-\sin\omega_2 t)^2\right]$$

$$+\frac{v_1^2}{\omega_1^2}\cos^2\phi_1\left[(1-\cos\omega_1 t)^2+(\omega_1\tau_L-\sin\omega_1 t)^2\right]$$

$$-\frac{2v_2\cos\phi_2 v_1\cos\phi_1}{\omega_1\omega_2}\left\{\begin{array}{l}\sin\psi_o[(1-\cos\omega_2 t)(\omega_1\tau_L-\sin\omega_1 t)\\ +(1-\cos\omega_1 t)(\omega_2\tau_L-\sin\omega_2 t)]\end{array}\right.$$

$$\left.\begin{array}{l}+\cos\psi_o[(\omega_2\tau_L-\sin\omega_2 t)(\omega_1\tau_L-\sin\omega_1 t)\\ -(1-\cos\omega_2 t)(1-\cos\omega_1 t)]\end{array}\right\} \qquad (C.3)$$

Consider the case for a same-sense turn. In this case,

$$\omega_1 = -\omega \;;\; \omega_2 = \omega \text{ or } \omega_1 = \omega \;;\; \omega_2 = -\omega$$

Substitution into equation 3 yields

$$\rho^2(t) = \frac{w_L}{\omega}\left[(1-\cos\omega t)^2 + (\omega\tau-\sin\omega t)^2\right] \qquad (C.4)$$

where

$$w_L^2 = v_2^2\cos^2\phi_2 + v_1^2\cos^2\phi_1 - 2v_1\cos\phi_1\, v_2\cos\phi_2\cos\psi_o$$

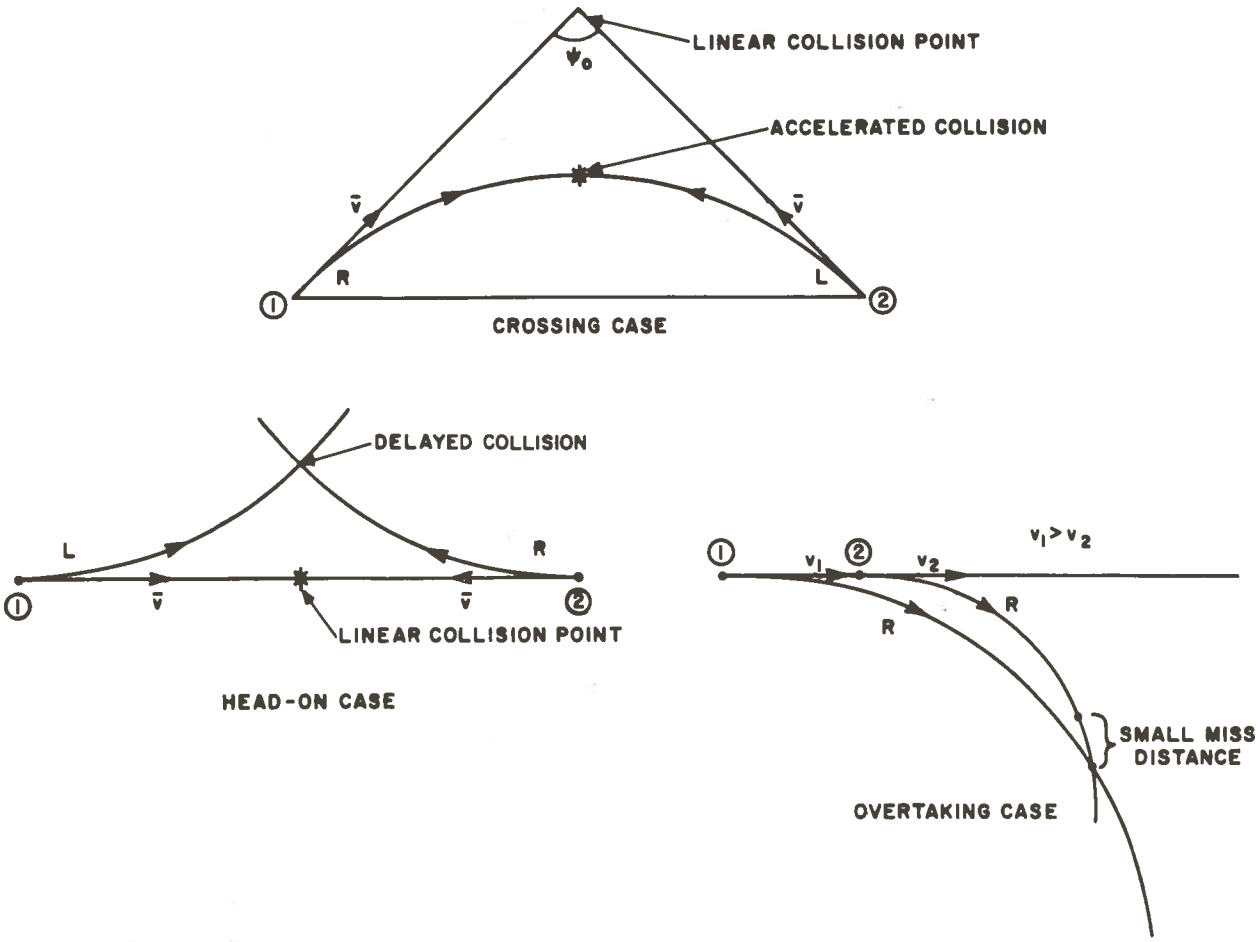

Figure C.3.- Dangerous turn maneuvers

It is immediately noted that when

$$\frac{\pi}{2} \leq \psi_o \leq \pi$$

equation (C.4) cannot go to zero, since

$$\begin{cases} -\frac{\pi}{2} < \phi_1 < \frac{\pi}{2} \\ -\frac{\pi}{2} < \phi_2 < \frac{\pi}{2} \end{cases}$$

Next, consider the opposite-sense turn case. In this situation,

$\omega_1 = \omega$; $\omega_2 = \omega$ or $\omega_1 = -\omega$; $\omega_2 = -\omega$. For $\omega_1 = \omega$; $\omega_2 = \omega$ the aircraft are turning toward each other and this has been shown to be dangerous. Consider the case of $\omega_1 = -\omega$; $\omega_2 = -\omega$ so that the aircraft turn away from each other. In this case, the range between the two aircraft is given by

$$\rho^2(t) = \frac{w_L^2}{\omega^2}\left[(1-\cos\omega t)^2 + (\omega\tau-\sin\omega t)^2\right]$$

$$+ \frac{4v_1}{\omega^2}\cos\phi_1 v_2\cos\phi_2(1-\cos\omega t)\left[\sin\psi_o(\omega\tau-\sin\omega t)\right.$$

$$\left. + \cos\psi_o(1-\cos\omega t)\right] \qquad (C.5)$$

so that if $\omega\tau_L > 1$ and if $0 \le \psi_o \le \pi/2$, $\rho(t)$ from (C.5) will always be greater than or equal to $\rho(t)$ from (C.4). Therefore, as a rule of thumb, the choice of avoidance maneuvers is given by

$$0 \le |\psi_o| \le \pi/2 \Rightarrow \text{opposite-sense turn}$$

$$\frac{\pi}{2} \le |\psi_o| \le \pi \Rightarrow \text{same-sense turn}$$

and if this rule is followed, the miss-distance between the two aircraft is given by

$$m(t) \ge \frac{w_L}{\omega}\left[(1-\cos\omega t)^2 + (\omega\tau_L-\sin\omega t)^2\right]^{1/2} \qquad (C.6)$$

and will occur at a time T_e given by

$$\tan\omega T_e = \omega\tau_L \qquad (C.7)$$

A plot of (C.7) is presented as Figure C.4. From (C.6) and (C.7), the minimum miss distance is given by

$$m(T_e) \geq \frac{w_L}{\omega} \frac{(1-\cos\omega T_e)}{\cos\omega T_e} \qquad (C.8)$$

A plot of (C.8) is presented in Figure C.5 along with a cross plot of

$$\rho_o \cos\phi = \frac{w_L}{\omega} \tan(\omega T_e) \qquad (C.9)$$

From this graph, it is seen that if the value T_e = 10 sec. is chosen that $m(T_e)$ will be greater than 750 ft. if the maneuver is initiated before the range is less than 1/2 nm.

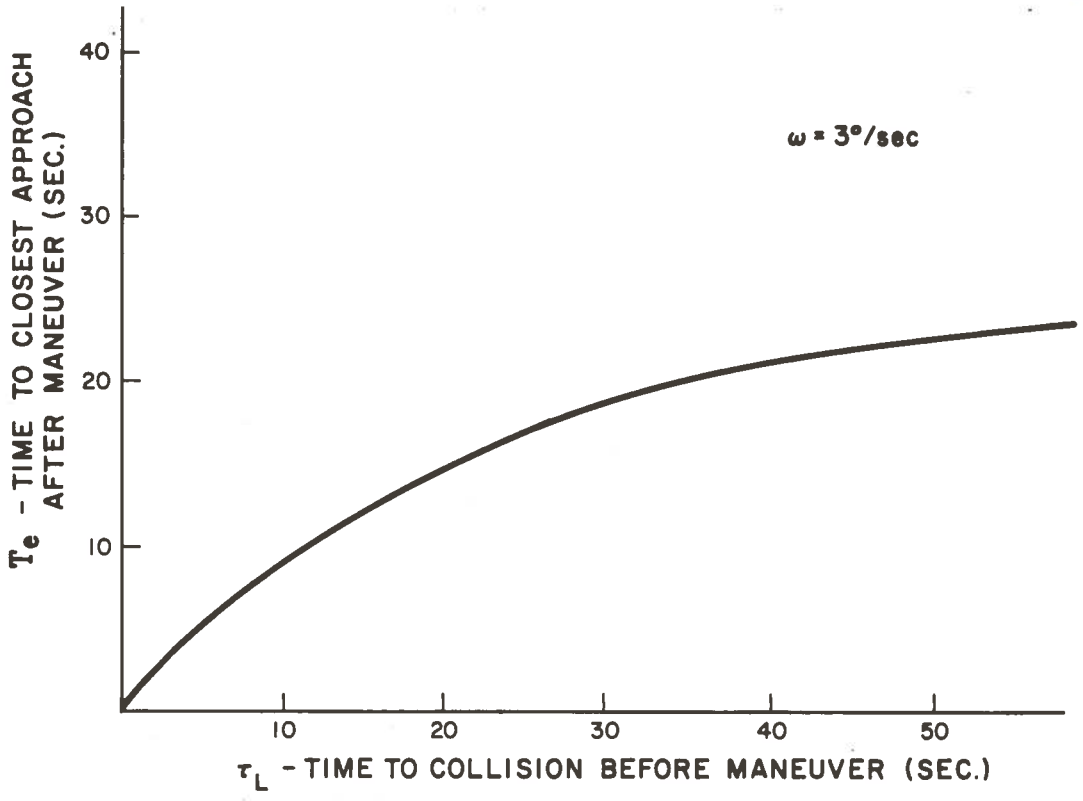

Figure C.4.- Escape time vs time to collision

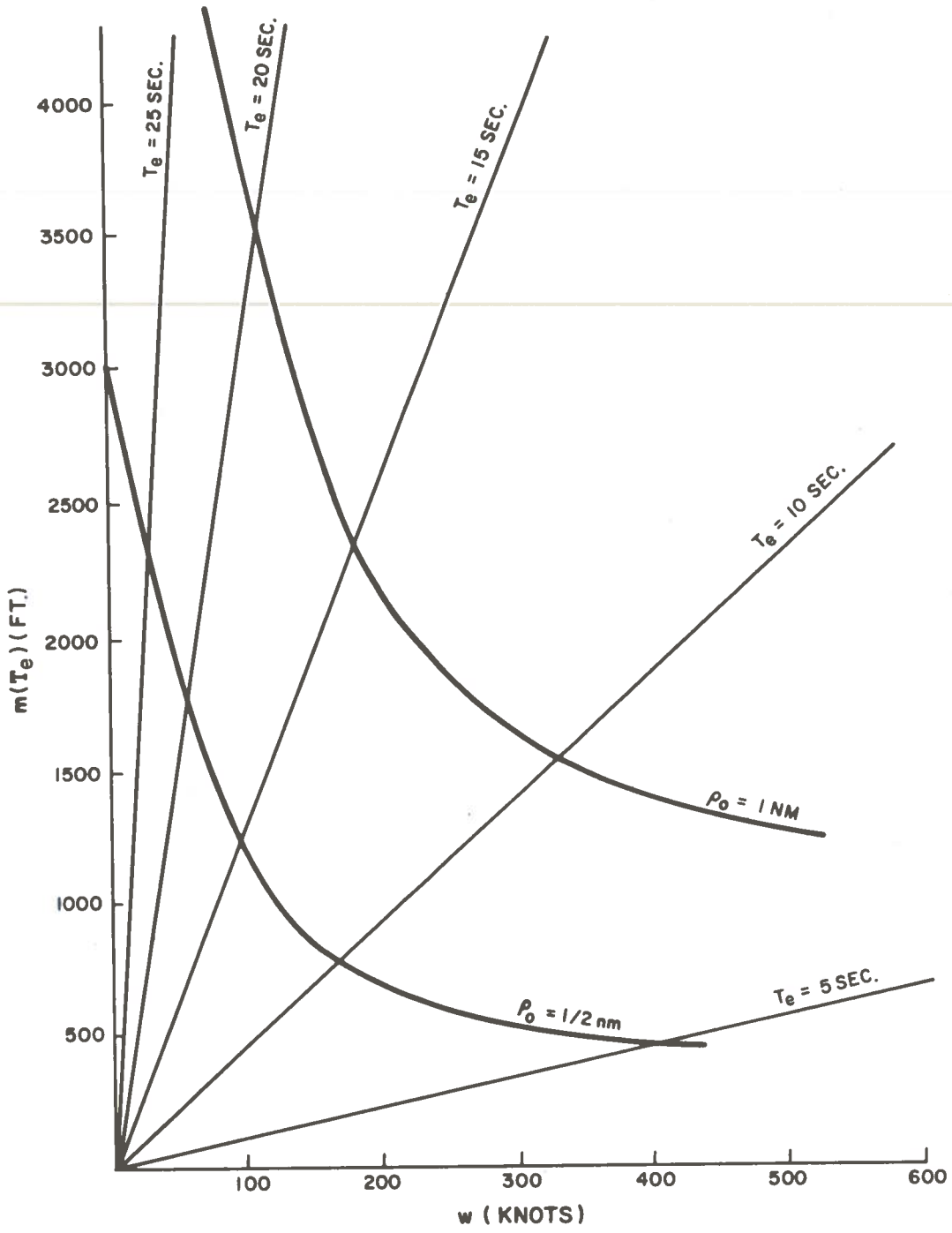

Figure C.5.- Miss distance and escape time

Next, suppose that a same-sense turn is indicated. In this case, if a miss rather than a collision is predicted, a question of whether both aircraft should make a right turn or a left turn

remains to be answered. This question is answered geometrically by Figure C.6. From Figure C.6a, the collision case, it is seen that no preferred direction of turn is indicated and standard passing rules should be employed. Figures C.6b and c however illustrate that a preferred direction of turn does exist in the near miss case. Based on these figures, the following same-sense turn rules should be observed:

$0 < \beta(\tau_W) < \pi \rightarrow$ Both aircraft go left

$-\pi < \beta(\tau_W) < 0 \rightarrow$ Both aircraft go right

These rules will insure that the existing value of miss distance will be made larger rather than being driven to or through zero. A brief analytical examination of this maneuver is presented. It was stated that the condition for collision with both aircraft in a same-sense turn is

$$\sin \delta_o = \omega \rho_o / 2w \qquad \text{(C.10)}$$

where δ_o is the angle between the range vector and the relative velocity vector (see Appendix). If two aircraft are initially on a rectilinear collision course ($\delta_o = 0$), a curvilinear collision cannot occur if a same-sense turn is executed. In the case of a small miss ($\delta_o = \pm\varepsilon$), the collision condition is

$$\sin \delta_o \approx \delta_o \approx \omega \rho_o / 2w \qquad \text{(C.11)}$$

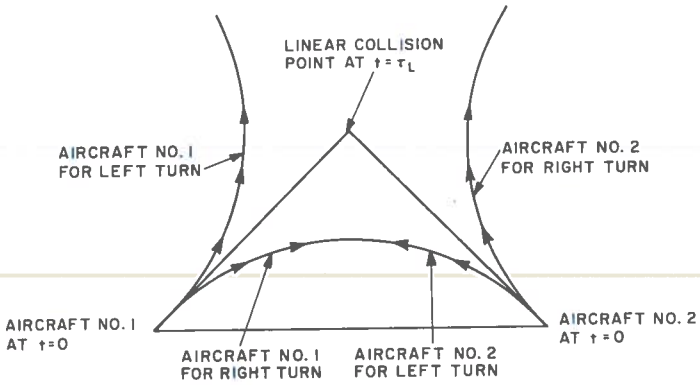

Figure C.6a- Turn from rectilinear collision course

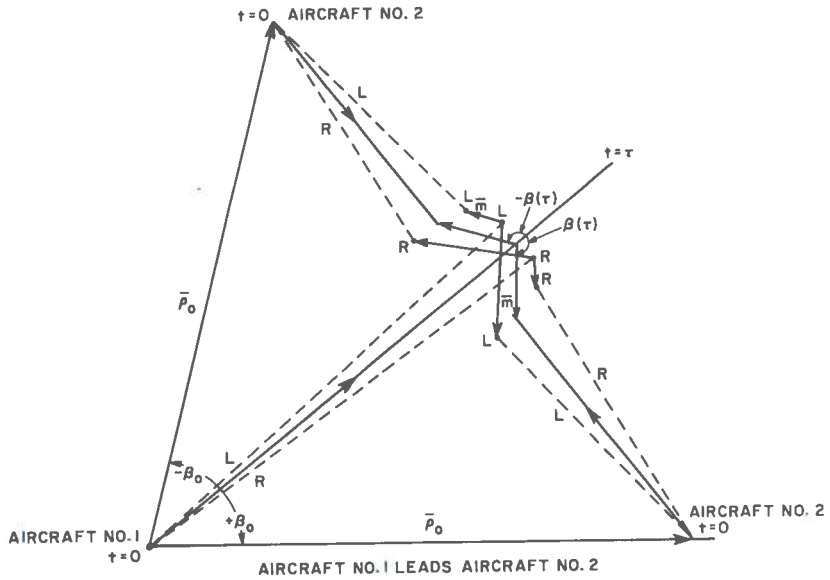

Figure C.6b- Turn from a near miss

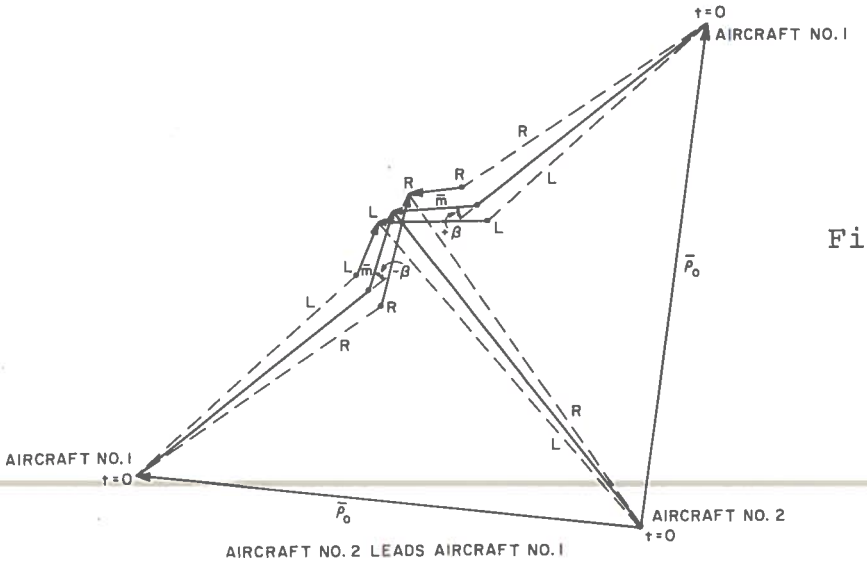

Figure C.6c- Turn from a near miss

so that the sign of δ_o and of ω must be the same for a collision to occur. If however, the rules for turning cited above are followed, no collision is possible. The positive command computation flow is presented in Figure C.7.

Potential Threat Detection and Negative Commands

This section considers the detection of potential threats and the associated negative commands required to prevent these threats from becoming actual conflicts. The prediction of potential threats requires that one know the present state of both vehicles and then perturb these states with the possible turn and dive maneuvers to predict the potential relative positions of the two aircraft at a future time. In the event that a possible maneuver combination exists which would violate the separation criteria, a potential threat is declared and a negative command to prohibit those maneuvers is issued.

The details of potential threat prediction are illustrated in Figures C.8a and C.8b. In this prediction, 99 values of the range vector are computed and tagged with a subscript K. (See figure C.9.) The test for a potential threat consists of comparing all 99 values of range against the separation criteria used for actual threat detection. If none of these values of range vector violate the criteria, a Level 1 control command limiting further maneuvers to standard maneuvers is issued. If however, certain values of the range vector violate the criteria, then these maneuvers must be prohibited. Calculation of these negative commands is easily accomplished by ordering the values

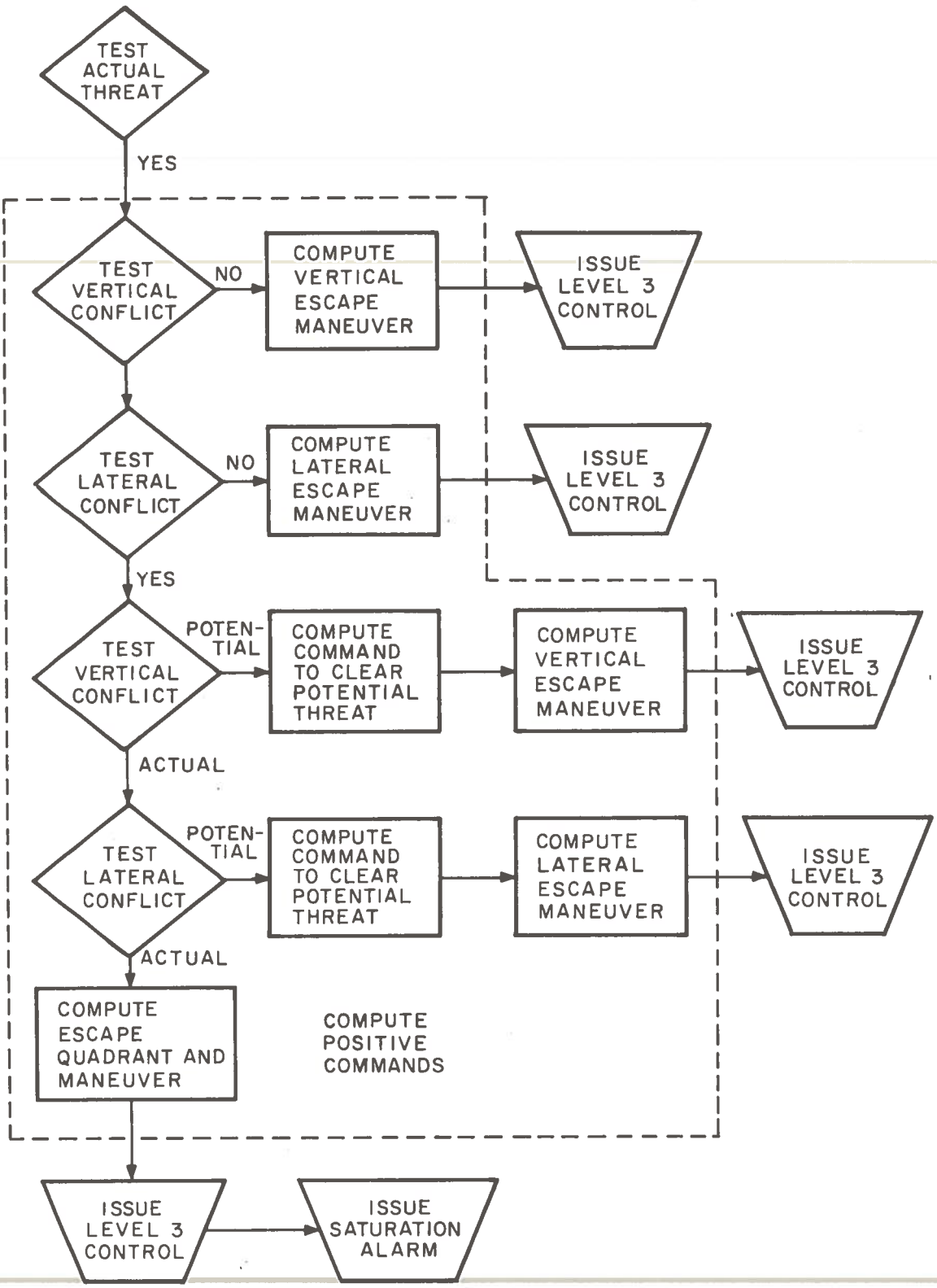

Figure C.7.- Positive command computation flow

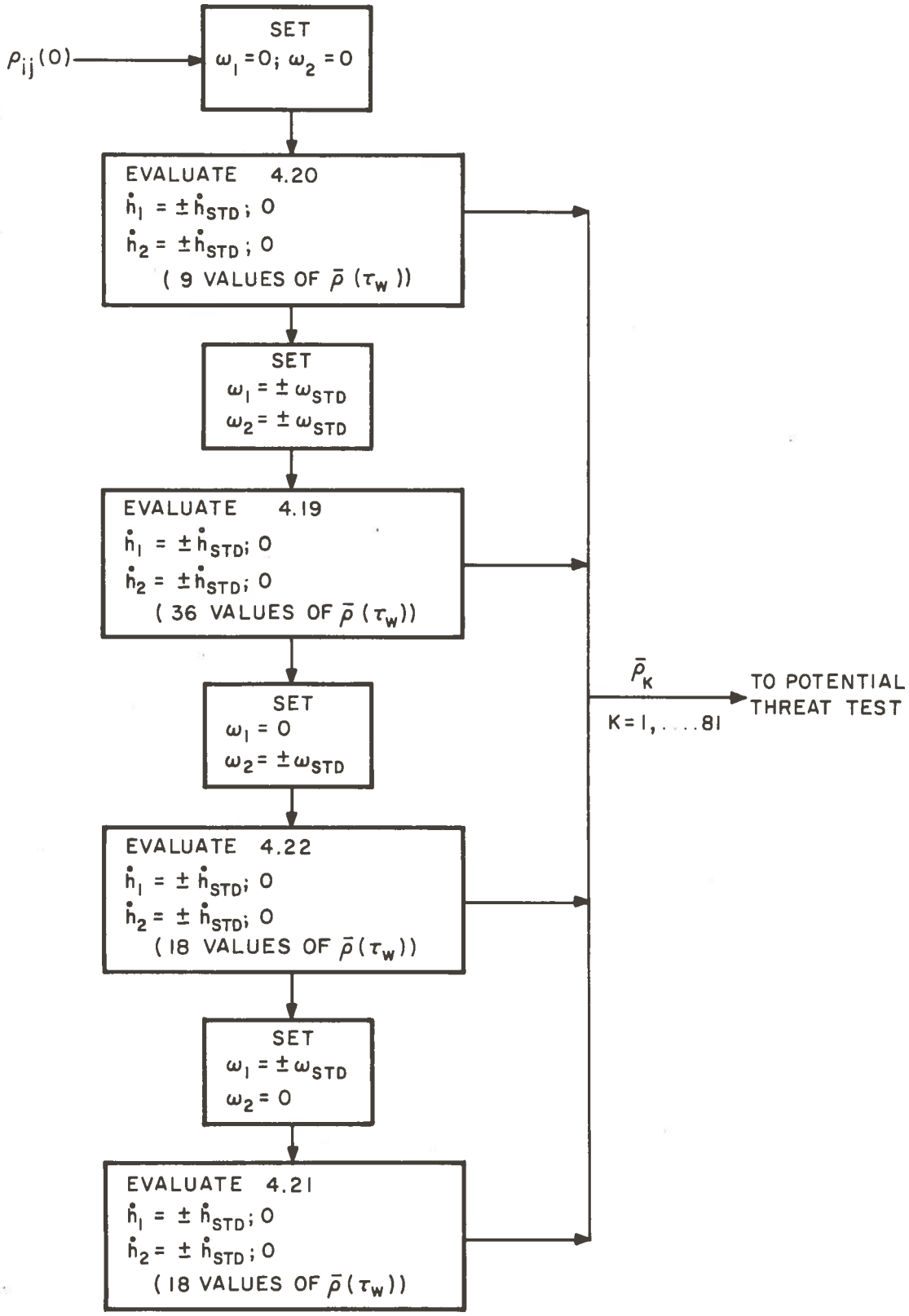

Figure C.8a.- Potential threat prediction both aircraft change state

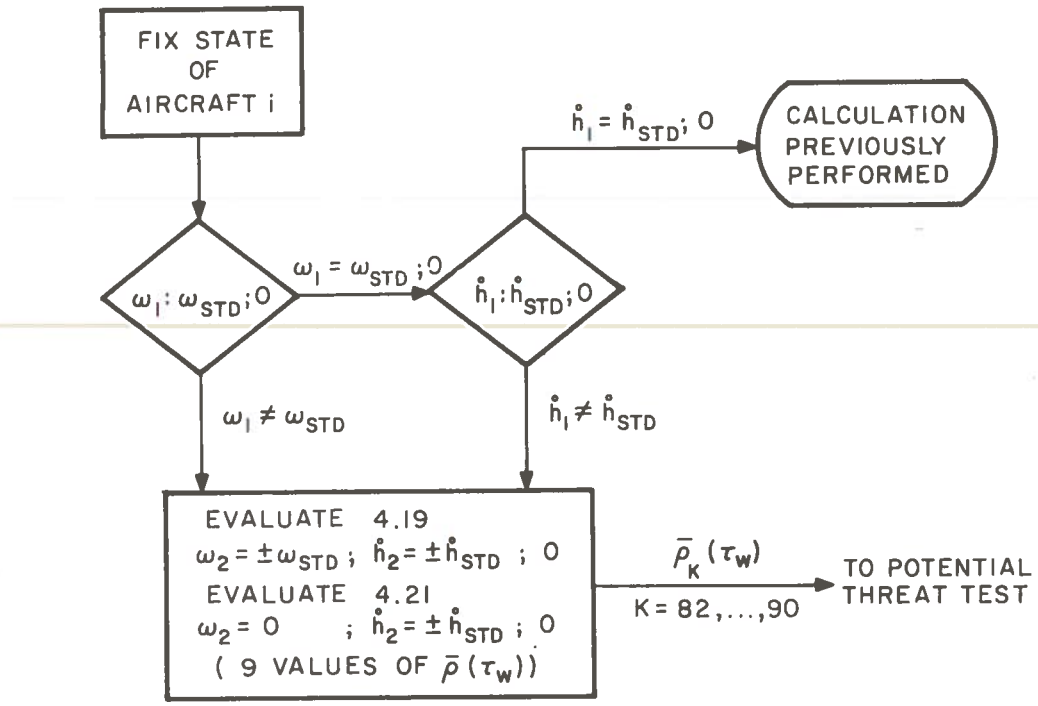

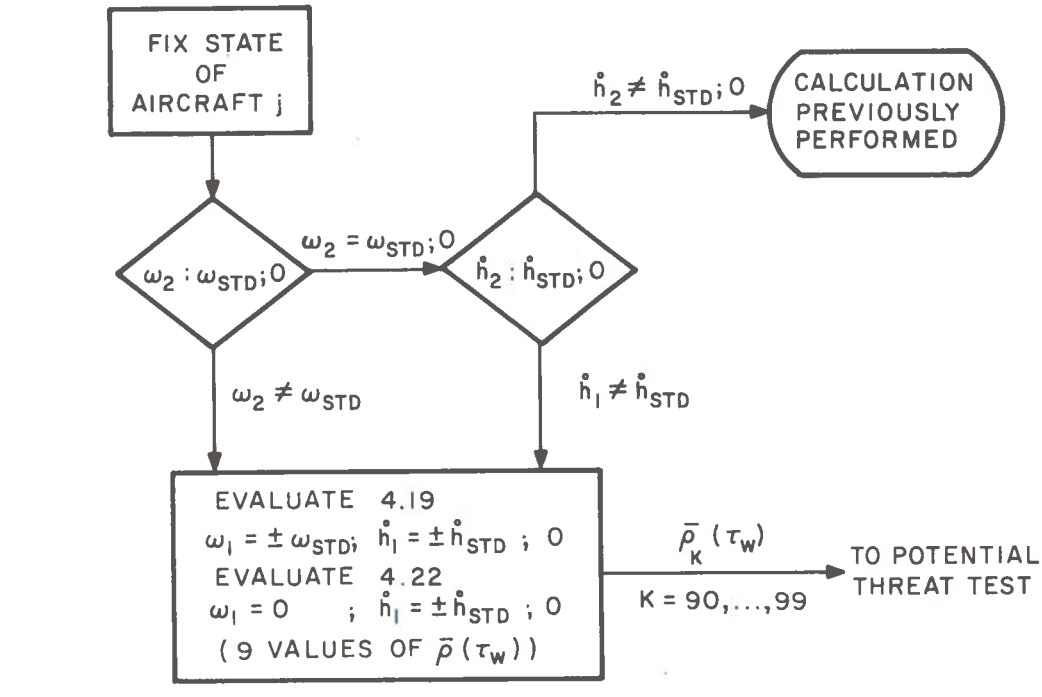

Figure C.8b.- Potential threat prediction one aircraft changes state

of K with specific aircraft states. One method of ordering is presented in Figure C.8b. The computation of negative commands consists of prohibiting those maneuvers associated with a particular value of K. Two basic types of potential threats are possible. The first type results from both aircraft changing state while the second requires that only one aircraft change state to cause a conflict. Both types of potential threats are treated in the illustrative figures. In the event that a single aircraft is capable of causing an actual threat by a maneuver, only that aircraft need be given a negative command providing that the other aircraft cannot cause a threat.

AIRCRAFT NO. 1			AIRCRAFT NO. 2		AIRCRAFT NO. 1			AIRCRAFT NO. 2	
K	ω_1	$\dot{h}_1$	ω_2	$\dot{h}_2$	K	ω_1	$\dot{h}_1$	ω_2	$\dot{h}_2$
1	0	+	0	+	51	0	0	+	-
2	0	+	0	0	52	0	-	+	+
3	0	+	0	-	53	0	-	+	0
4	0	0	0	+	54	0	-	+	-
5	0	0	0	0	55	0	+	-	+
6	0	0	0	-					
7	0	-	0	+	56	0	+	-	0
8	0	-	0	0	57	0	+	-	-
9	0	-	0	-	58	0	0	-	+
					59	0	0	-	0
10	+	+	+	+	60	0	0	-	-
11	+	+	+	0	61	0	-	-	+
12	+	+	+	-	62	0	-	-	0
13	+	0	+	+	63	0	-	-	-
14	+	0	+	0					
15	+	0	+	-	64	+	+	0	+
16	+	-	+	+	65	+	+	0	0
17	+	-	+	0	66	+	+	0	-
18	+	-	+	-	67	+	0	0	+
					68	+	0	0	0
19	+	+	-	+	69	+	0	0	-
20	+	+	-	0	70	+	-	0	+
21	+	+	-	-	71	+	-	0	0
22	+	0	-	+	72	+	-	0	-
23	+	0	-	0					
24	+	0	-	-	73	-	+	0	+
25	+	-	-	+	74	-	+	0	0
26	+	-	-	0	75	-	+	0	-
27	+	-	-	-	76	-	0	0	+
					77	-	0	0	0
28	-	+	+	+	78	-	0	0	-
29	-	+	+	0	79	-	-	0	+
30	-	+	+	-	80	-	-	0	0
31	-	0	+	+	81	-	-	0	-
32	-	0	+	0					
33	-	0	+	-	82	NON	NON	+	+
34	-	-	+	+	83			+	0
35	-	-	+	0	84			+	-
36	-	-	+	-	85	STA	STA	0	+
					86			0	0
37	-	+	-	+	87	NDA	NDA	0	-
38	-	+	-	0	88			-	+
39	-	+	-	-	89	RD	RD	-	0
40	-	0	-	+	90			-	-
41	-	0	-	0					
42	-	0	-	-	91	+	+	NON	NON
43	-	-	-	+	92	+	0		
44	-	-	-	0	93	+	-	STA	STA
45	-	-	-	-	94	0	+		
					95	0	0	NDA	NDA
46	0	+	+	+	96	0	-		
47	0	+	+	0	97	-	+	RD	RD
48	0	+	+	-	98	-	0		
49	0	0	+	+	99	-	-		
50	0	0	+	0					

$\omega_{1,2} = \pm \omega_{STD}; 0$

$\dot{h}_{1,2} = \pm \dot{h}_{STD}; 0$

Figure C.9.- Ordering of potential threat conditions